PERMEABILITY OF BIOLOGICAL MEMBRANES TO MODEL SOLUTES

SAKCHAI AUYCHAIPORNLERT

A THESIS SUBMITTED IN PARTIAL FULFILLMENT
OF THE REQUIREMENTS FOR
THE DEGREE OF MASTER OF SCIENCE IN PHARMACY
(PHARMACEUTICS)
FACULTY OF GRADUATE STUDIES
MAHIDOL UNIVERSITY
2004

ISBN 974-04-4782-1

Thesis

entitled

PERMEABILITY OF BIOLOGICAL MEMBRANES TO MODEL SOLUTES

Sakchai Auychaipornlert

Mr. Sakchai Auychaipornlert

Candidate

Pojawon Lawanprasert

Assoc. Prof. Pojawon Lawanprasert, Ph.D.

Major-Advisor

Narong Sarisuta

Prof. Narong Sarisuta, Ph.D.

Co-Advisor

Rassmidara Hoonsawat

Assoc. Prof. Rassmidara Hoonsawat, Ph.D.

Dean

Faculty of Graduate Studies

Weena

Assoc. Prof. Weena Jirachariyakul, Dr.rer.nat.

Chair

Master of Science in Pharmacy

Programme in Pharmaceutics

Faculty of Pharmacy

Thesis

entitled

PERMEABILITY OF BIOLOGICAL MEMBRANES TO MODEL SOLUTES

was submitted to the Faculty of Graduate Studies, Mahidol University

for the degree of Master of Science in Pharmacy (Pharmaceutics)

on 1 June, 2004

Sakchai Auychaipornlert

Mr. Sakchai Auychaipornlert

Candidate

Pojawon Lawanprasert

Assoc. Prof. Pojawon Lawanprasert, Ph.D.

Chair

Narong Sarisuta

Prof. Narong Sarisuta, Ph.D.

Member

Panida Asavapichayont

Ms. Panida Asavapichayont, Ph.D.

Member

Rassmidara Hoonsawat

Assoc. Prof. Rassmidara Hoonsawat,

Ph.D.

Dean

Faculty of Graduate Studies

Mahidol University

Weena Jirachariyakul

Assoc. Prof. Weena Jirachariyakul,

Dr.rer.nat.

Acting Dean

Faculty of Pharmacy

Mahidol University

ACKNOWLEDGEMENT

The success of my study would never have happened without support and valuable advice from many people. I will memorize every moment and every person who contributed to my valuable experience.

I would like to express my sincere gratitude and great appreciation to my advisor, Associate Professor Dr. Pojawon Lawanprasert for her invaluable suggestion, extensively support, guidance, care, and enthusiastic encouragement throughout my study.

I am equally grateful to Professor Dr. Narong Sarisuta, my co-advisor, for his helpful criticism, consultation, support, warmth, and comment for this thesis.

I am very grateful to Dr. Panida Asavapichayont for her esteem criticism, meaningful advice, correction of this thesis, and also for being member of my examining committee.

I would like to thank Dr. Phongkitti Thisuphakorn, staff of pathology department of the National Cancer Institute for providing me the human skin samples, and the National Cancer Institute.

I would like to thank Associate Professor Dr. Suwan Theeraworapan and Assistant Professor Dr. Roongtawan Suparbpol for providing me the rat skin samples.

A special acknowledgement is extended to the Faculty of Pharmacy, Mahidol University for giving the best opportunity to study the Master Degree of Science in Pharmacy and providing research facilities and to Mr. Kawewut Kanokkaew for his best assistance.

I would like to extend my special appreciation for the kind assistance, encouragement and sincere friendship, to my fellow graduate students and other persons who have not been mentioned here.

Finally, I would like to express my infinite gratitude to my dearest parents for their endless encouragement, love, care, and continuous support throughout my life.

Sakchai Auychaipornlert

PERMEABILITY OF BIOLOGICAL MEMBRANES TO MODEL SOLUTES

SAKCHAI AUYCHAIPORNLERT 4436823 PYPT/M

M.Sc. in Pharm. (PHARMACEUTICS)

THESIS ADVISOR : POJAWON LAWANPRASERT, Ph.D.,
NARONG SARISUTA, Ph.D.

ABSTRACT

An *in vitro* permeation experiment was performed instead of an *in vivo* experiment which has limitations. Various types of membranes have been investigated. In this study, the permeability properties of the biological membrane, i.e., human epidermis, full-thickness rat skin, and egg shell membrane, were studied. Acyclovir, acetophenone, 4-methylacetophenone, nitrobenzene, 3,4-xylenol, chlorocresol, phenol, 4-bromophenol, and 4-chlorophenol were used as model solutes. It was found that the regression equation between log k_p and some physicochemical parameters of solutes could be used to explain the permeation process of model solutes through these membranes when phenol, 4-bromophenol, and 4-chlorophenol were excluded. Lipophilic solute could permeate through human epidermis (stratum corneum), which is composed mainly of lipid, more than hydrophilic solutes, while, this relationship was observed conversely in full-thickness rat skin which is more aqueous than stratum corneum. As egg shell membrane is not composed of lipid and its pore size is larger than the molecular size of model solutes, permeation of these solutes depends mainly on solvatochromic parameters and is not affected by molecular volume. Rat skin was usually used in most of the *in vitro* experiments. This practice is inconvenient so the effect of treatment and storage conditions on barrier functions of rat skin was studied. The Kruskal-Wallis statistical analysis showed that k_p of acyclovir and acetophenone diffusing through three rat skin groups pretreated differently, at -20ºC for 13-15 days, were not different from control groups and no difference was found between sex (p-value > 0.05). The effect of enhancers and vehicles on percutaneous absorption of acyclovir was also studied. It was found that 50%v/v ethanol/water could enhance permeation of acyclovir through human epidermis. 4% w/v *L*-menthol in 50%v/v ethanol/water showed superior permeability enhancement over the other four enhancers, i.e., 0.075%w/v capsaicin, 0.075%w/v nonivamide, 4%w/v methyl salicylate, and 10%w/v tween 80.

KEY WORDS : BIOLOGICAL MEMBRANE/ PERMEABILITY/ ACYCLOVIR/ ACTOPHENONE/ METHYLACETOPHENONE/ NITROBENZENE/ XYLENOL/ CHLOROCRESOL/ PHENOL/ BROMOPHENOL/ CHLOROPHENOL/ CAPSAICIN/ NONIVAMIDE/ MENTHOL/ TWEEN 80/ METHYL SALICYLATE/ PHOSPHATE BUFFER/ NORMAL SALINE/ GLYCERINE

147 pp. ISBN 974-04-4782-1

การซึมผ่านเมมเบรนชีวภาพของสารต้นแบบ (PERMEABILITY OF BIOLOGICAL MEMBRANES TO MODEL SOLUTES)

ศักดิ์ชัย อวยชัยพรเลิศ 4436823 PYPT/M
ภ.ม. (เภสัชการ)
คณะกรรมการควบคุมวิทยานิพนธ์ : พจวรรณ ลาวัณย์ประเสริฐ, Ph.D., ณรงค์ สาริสุต, Ph.D.

บทคัดย่อ

การทดสอบการซึมผ่านของสารเคมีทางผิวหนังโดยวิธีหลอดทดลองมักใช้แทนการศึกษาในมนุษย์ เนื่องจากข้อจำกัดในการทดลองในมนุษย์ เมมเบรนหลายชนิดจึงถูกเลือกนำมาศึกษาคุณสมบัติการซึมผ่าน สำหรับการศึกษานี้เมมเบรนชีวภาพ 3 ชนิด คือ ชั้นหนังกำพร้าของคน ผิวหนังหนู และ เยื่อเปลือกไข่ ถูกนำมาศึกษาคุณสมบัติต่างๆ ในการซึมผ่าน โดยใช้สารเคมีทั้ง 9 ชนิด คือ อะไซโคลเวีย อะซีโตฟีโนน เมทธิลอะซีโตฟีโนน ไนโตรเบนซีน ไซลีนอล คลอโรครีซอล ฟีนอล โบรโมฟีนอล และ คลอโรฟีนอล เป็นสารต้นแบบ จากการศึกษาพบว่าสมการความสัมพันธ์ระหว่างค่าล็อกการิทึมของค่าคงที่การซึมผ่านกับค่าทางฟิสิกส์เคมีของสารต้นแบบ สามารถนำมาอธิบายขบวนการซึมผ่านของสารต้นแบบผ่านเมมเบรนชีวภาพทั้งสามชนิดได้ดี เมื่อค่าต่างๆ ของ ฟีนอล โบรโมฟีนอล และคลอโรฟีนอล ไม่ถูกนำมารวม พบว่าสารต้นแบบที่มีคุณสมบัติไม่ชอบน้ำสามารถซึมผ่านชั้นหนังกำพร้าของคนได้ดีกว่าสารต้นแบบที่มีคุณสมบัติชอบน้ำ ในขณะที่พบผลตรงข้ามในการซึมผ่านผิวหนังหนู เนื่องจากชั้นหนังกำพร้าของคนประกอบด้วยไขมันเป็นส่วนใหญ่ ส่วนผิวหนังหนูมีส่วนประกอบของน้ำมากกว่า สำหรับเยื่อเปลือกไข่ไม่มีส่วนประกอบของไขมันและรูพรุนของเยื่อเปลือกไข่มีขนาดใหญ่กว่าโมเลกุลของสารต้นแบบ ดังนั้นการซึมผ่านของสารต้นแบบจึงขึ้นอยู่กับค่าโซลวาโตโครมิคของสาร แต่ไม่ขึ้นกับขนาดโมเลกุล การศึกษาการซึมผ่านโดยวิธีหลอดทดลองมักใช้ผิวหนังหนูที่ถูกตัดจากตัวหนูใหม่ๆ ซึ่งวิธีนี้อาจไม่สะดวกในการปฏิบัติ ดังนั้นจึงศึกษาผลของสภาวะต่างๆ ในการเก็บรักษาผิวหนังหนู จากการวิเคราะห์ทางสถิติด้วยวิธีครัสคาล-วาลลิส พบว่าการซึมผ่านของอะซัยโครเวียและอะซีโตฟีโนน ในแต่ละกลุ่มของผิวหนังหนูที่จุ่มในสารละลายสามชนิด และเก็บไว้ที่อุณหภูมิ -20 องศาเซลเซียส เป็นเวลา 13-15 วัน พบว่าไม่มีความแตกต่างอย่างมีนัยสำคัญกับกลุ่มควบคุม ทั้งสภาวะที่เก็บรักษาและระหว่างเพศ ที่ระดับความเชื่อมั่นร้อยละ 95 นอกจากนี้การศึกษาผลของสารช่วยเพิ่มการซึมผ่านและตัวทำละลายต่อการซึมผ่านของอะไซโคลเวียผ่านชั้นหนังกำพร้าของคน พบว่า 50%v/v เอธานอล/น้ำ สามารถเพิ่มการซึมผ่านอะซัยโครเวียได้ และพบว่า 4%w/v เมนทอลใน 50%v/v เอธานอล/น้ำ สามารถเพิ่มการซึมผ่านอะไซโครเวียได้สูงสุด มากกว่าสารเพิ่มการซึมผ่านทั้งสี่ชนิดคือ 0.075%w/v แคปซัยซิน 0.075%w/v โนนิวามายด์ 4%w/v เมทธิลซาลิไซเลท และ10%w/v ทวีน 80

147 หน้า ISBN 974-04-4782-1

LIST OF CONTENTS

LIST OF CONTENTS (continued)

LIST OF TABLES

LIST OF TABLES (continued)

LIST OF TABLES (continued)

LIST OF FIGURES

LIST OF FIGURES (continued)

LIST OF FIGURES (continued)

LIST OF ABBREVIATIONS

α	alpha
&	and
β	beta
ºC	degree Celsius (centigrade)
cm^2	square centimeter
cm^3	cubic centimeter
DMSO	dimethyl sulfoxide
e.g.	exempli gratia, for example
et al.	et alli, and other
FTIR	fourier transformed infrared spectrometer
g	gram
h	hour
HCL	hydrochloric acid
i.e.	id est, that is
$K_{o/PB}$	octanol-phosphate partition coefficient
$K_{o/w}$	octanol-water partition coefficient
k_p	permeability coefficient
log	logarithm
M	molarity
µL	microliter
µm	micrometer
mg	milligram
min	minute
mL	milliliter
mm	millimeter
mPa	millipascal
N	normality

LIST OF ABBREVIATIONS (continued)

nm	nanometer
%	percent
pH	the negative logarithm of the hydrogen ion concentration
pKa	the negative logarithm of acid dissociation constant
QSAR	quantitative structure activity relationship
s	second
S.D.	standard deviation
SMPB	Sörensen modified phosphate buffer
TQSAR	theoretical quantitative structure activity relationship
UV	ultra violet
v/v	volume by volume
w/v	weight by volume
w/w	weight by weight

CHAPTER 1
INTRODUCTION

In recent years, it has been shown that the skin became popular as a potential site for systemic drug delivery because it was thought (a) to avoid the problem of stomach emptying, pH effect, and enzyme deactivation associated with gastrointestinal passage; (b) to avoid hepatic first-pass metabolism; and (c) to enable control of input, as exemplified by termination of delivery through removal of the device. However, delivery of drug through the skin is associated with various difficulties because skin is an effective, selective barrier to chemical permeation. Human skin comprises three tissue layers, i.e., epidermis, dermis, and subcutaneous tissue. The stratum corneum is the outermost layer of skin, provides the main barrier for chemical permeation. For producing the therapeutic effect, transdermal drug delivery requires that suitable amount of drug be permeated through the skin. The literature reports have documented different methodologies for increasing drug permeation through skin such as drug and vehicle interaction, drug modification, liposomes, chemical enhancers, iontophoresis or ultrasound, etc (1-3).

Acyclovir, a synthetic analogue of 2′-deoxiguanosine, is one of the most effecttive and selective agents against Herpes simplex virus type 1 and 2 (HSV-1 and HSV-2), Varicella zoster virus, and to lesser extent against Epstein-Barr virus and cytomegalovirus. According to histopathologic investigations, HSV-1 replication initially takes place in the cells of the basal layer of the epidermis and later extends to the rest of the epidermis. Therefore, the basal layer of the epidermis is considered to be the primary site of antiviral drug activity. Additionally, acyclovir is slowly and poorly absorbed from gastrointestinal tract. Only 13-21% of drug is absorbed and time to reach peak concentration is 1.5-2 hours. Thus, transdermal drug delivery may be useful for delivery of acyclovir to the site of action (4-7). Recently, there is a research group that developed novel method involving the use of transdermal drug delivery system (i.e., acyclovir transdermal patch) to describe quantitatively the

relationship between the antiviral efficacy and the acyclovir skin flux. The results revealed that this method can be used to evaluate the topical efficacy and systemic efficacy of the drug in hairless mice. Additionally, results showed that some acyclovir patch formulation can achieve 100% topical efficacy by using azone as skin permeation enhancer (7-11).

A number of substances were reported to be skin permeation enhancer. For example, capsaicin, the pungent principle of red pepper, has a variety of therapeutic advantage such as antinociceptive activity. Nonivamide is one of synthetic analogues of capsaicin which has the similar chemical structure and pharmacological profiles to those of capsaicin. Both of them were reported to be a skin permeation enhancer for each other and for ketoprofen, indomethacin, and naproxen. The concentration used either by incorporation in formulation or pretreatment on skin before application of the formulation was between 0.025-5% (12-16). It was found that menthol could enhance permeation of some solutes through skin, e.g., isosorbide dinitrate, ketoprofen, leuprolide acetate, propranolol, morphine hydrochloride, tamioxifen, and paraben group. The concentration used was between 0.5-10% (17-24). Surfactant could also be used as skin permeation enhancer. Tween 80, a nonionic surfactant, could enhance lorazepam permeation through rat skin. Tweens are widely used in cosmetic, food products and oral, parenteral, and topical formulations. They are generally regarded as nontoxic nonirritant materials (25,26). Methyl salicylate was used in topical products for muscular pain relief. Concentrations of methyl salicylate in available topical products are between 5-50%. It was found that methyl salicylate could enhance leuprolide acetate permeation through nude mouse skin (17,27).

Optimally, the testing of transdermal delivery system should be performed *in vivo*. This is often impossible, especially in the development stages when the toxicity or irritancy of new drugs, excipients or devices may not be documented. Therefore, *in vitro* experimental procedures have become important in this field. Laboratory test systems require a membrane to mimic the barrier function of the human stratum corneum. Many different types of membrane, both biological and synthetic membranes such as rat skin, pig skin, cobra skin, excised human skin, egg shell membrane and silicone membrane have been investigated (28-30).

In this study, the barrier properties of full-thickness rat skin, egg shell membrane, and human epidermis to model solutes were investigated. Effects of treatment and storage condition on permeability properties of full-thickness rat skin of both sexes to model solutes were studied. Finally, effect of enhancers and vehicles on percutaneous absorption of acyclovir through human skin was studied by varying type and concentration of enhancers and vehicles. The objectives of this study were:

1. To study the permeability properties of human epidermis, full-thickness rat skin, and egg shell membrane by using model solutes.

2. To study the effect of enhancers and vehicles on percutaneous absorption of acyclovir.

3. To study the effect of treatment and storage conditions on barrier functions of rat skin to model solutes.

CHAPTER 2
LITERATURE REVIEW

1. The structure and function of skin

The skin is the largest organ of the body, accounting for more than 10% of body mass, and the one that enables the body to interact most intimately with its environment. In essence, the skin consists of four layers that is the stratum corneum (nonviable epidermis), the remaining layers of the epidermis (viable epidermis), dermis, and subcutaneous tissue. There are also several associated appendages that are hair follicles, sweat ducts, apocrine glands, and nails. Many of the functions of the skin can be classified as essential to survival of the body bulk of mammals and humans in a relatively hostile environment. In a general context, these functions may be classified as protective, maintaining homeostasis, or sensing. The importance of the protective and homeostasis role of the skin is illustrated in one context by its barrier property. This allow the survival of humans in an environment of variable temperature, water content (humidity and bathing), and the presence of environmental dangers, such as chemicals, bacteria, allergens, fungi, and radiation. In a second context, the skin is a major organ for maintaining the homeostasis of the body, especially in terms of its composition, heat regulation, blood pressure control, and excretory roles. Third, the skin is a major sensory organ in terms of sensing environmental influence, such as heat, pressure, pain, allergen, and microorganism entry. Finally, the skin is an organ that is in a continual state of regeneration and repair (1).

2. Anatomy and physiology of human skin

From a functional point of view as seen in Figure 1, the skin is a flat and thin organ. The human skin comprises mainly three tissue layers as described above (i.e., epidermis layer, dermis layer, and subcutaneous tissue). Beside that, the skin also comprises several associated appendages such as hair follicle, sweat ducts, apocrine gland, and nail.

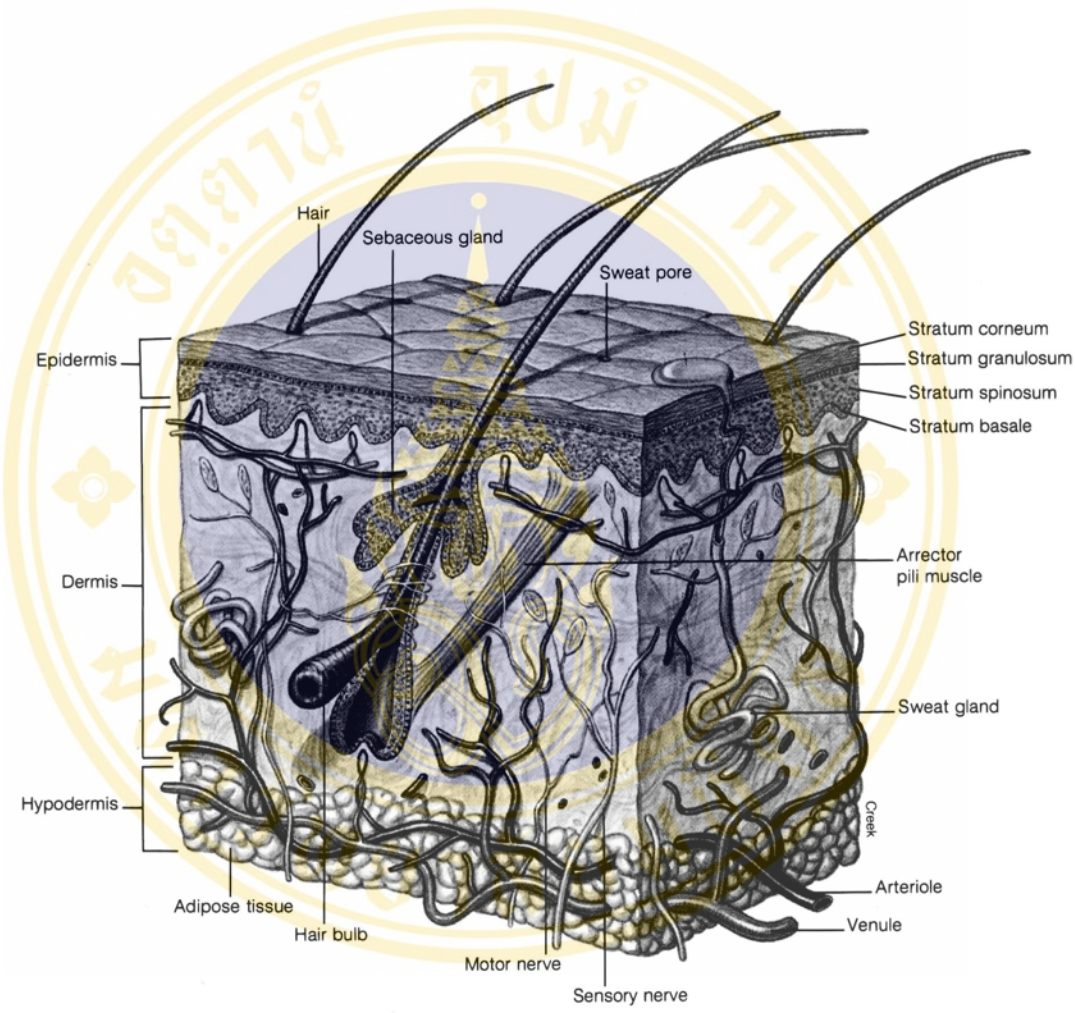

Figure 1 Three-dimensional view of the skin (31).

2.1 The epidermis

The epidermis layer performs a number of functions, one of the most important being the generation of the stratum corneum. The stratum corneum is the heterogeneous outermost layer of the epidermis and is approximately 10-20 μm thick. It is nonviable epidermis and consists, in a given cross-section, of 15-25 flattened, stacked, hexagonal, and conified cells embedded in a mortar of intercellular lipid. Each cell is approximately 40 μm in diameter and 0.5 μm thick. The thickness of stratum corneum varies and may be a magnitude of order larger in areas such as the palms of the hand and soles of the feet, areas of the body associated with frequent direct and substantial physical interaction with the physical environment. It is not surprising that the absorption of solutes, such as methyl salicylate, is slower through these regions than through the skin of other parts of the body. The stratum corneum barrier proper-ties may be partly related to its very high density (1.4 g/cm^3 in dry state), its low hydration of 15-20%, compared with the usual 70% for the body, and its low surface area for solute transport. Each stratum corneum cell or corneocyte is composed mainly of insoluble bundled keratin (~70%) and lipid (~20%) encased in a cell envelope, accounting for about 5% of the stratum corneum weight. The intercellular region consists mainly of lipids and desmosome for corneocyte cohesion. The composition of the stratum corneum intercellular lipids is unique in biological system (Table 1). These lipids exist as a continuous lipid phase, occupying about 20% of the stratum corneum volume, and arranged in multiple lamellar structures. The barrier function is further facilitated by the continuous desquamation of this horny layer with a total turnover of the stratum corneum occurring once every 2-3 weeks. Disorders of epithelization, such as psoriasis, lead to a faster skin turnover, sometimes being reduced to 2-4 days, with improper stratum corneum barrier function formation (1,2).

2.2 The dermis

The dermis, a critical component of the body, not only provides the nutritive, immune, and other support systems for the epidermis, through a thin papillary layer adjacent to the epidermis, but also plays a role in temperature, pressure, and pain regulation. The main structural component of the dermis is referred to as a coarse reticular layer. The dermis is about 0.1-0.5 cm thick and consists of collagenous fibers

Table 1 Lipid content of the stratum corneum intercellular space (1)

Lipid	% (w/w)	mol %
Cholesterol esters	10.0	7.5[a]
Cholesterol	26.9	33.4
Cholesterol sulfate	1.9	2.0
Total cholesterol derivatives	38.8	42.9
Ceramide 1	3.2	1.6
Ceramide 2	8.9	6.6
Ceramide 3	4.9	3.5
Ceramide 4	6.1	4.2
Ceramide 5	5.7	5.0
Ceramide 6	12.3	8.6
Total ceramides	41.1	29.5
Fatty acids	9.1	17.0[a]
Others	11.1	10.6[b]

[a] Based on C_{16} alkyl chain.

[b] Based on MW of 500.

(70%), providing a scaffold of support and cushioning, and elastic connective tissue, providing elasticity, in a semigel matrix of mucopolysaccharides. In general, the dermis has a parse cell population. The main cells present are the fibroblasts, which produce the connective tissue components of collagen, laminin, fibronectin, and vitronectin, i.e., mast cell, which are involved in the immune and inflammatory responses, and melanocytes involved in the production of the pigment melanin. Contained within the dermis is an extensive vascular network providing for the skin nutrition, repair, and immune responses, and for the rest of the body, heat exchange, immune response, and thermal regulation. The blood flow rate to the skin is about 0.05 mL min^{-1} cm^{-3} of skin, providing a vascular exchange area equivalent to that of the skin surface area. Skin blood vessels derive from those in the subcutaneous tissues, with an arterial network supplying the papillary layer, the hair follicles, the sweat and apocrine glands, the subcutaneous area, as well as the dermis itself. These arteries feed into arterioles, capillaries, venues, and then into veins. This blood supply reaches to within 0.2 mm of the skin surface, thus, it quickly absorbs and systematically dilutes most compounds passing the epidermis. The generous blood volume in the skin usually acts as a sink for diffusing molecules reaching the capillaries, keeping penetrant concentrations in the dermis very low, maximizing epidermal concentration gradients, and thus promoting percutaneous absorption (1).

2.3 The subcutaneous tissue

The deepest layer of the skin is the subcutaneous tissue of hypodermis. The hypodermis acts as a heat insulator, a shock absorber, and an energy storage region. This layer is a network of fat cells arranged in lobules and linked to the dermis by inter-connecting collagen and elastin fibers. As well as fat cells, possibly 50% of the body's fat, the other main cells in the hypodermis are fibroblasts and macrophages. One of the major roles of the hypodermis is to carry the vascular and neural systems for the skin. It also anchors the skin to underlying muscle. Fibroblasts and adipocytes can be stimulated by the accumulation of interstitial and lymphatic fluid within the skin and subcutaneous tissue (1).

2.4 Skin appendages

There are four skin appendages that are the hair follicles with their associated sebaceous glands, eccrine sweat glands, apocrine sweat glands, and the nails. Each appendage has a different function as outlined in Table 2. The hair follicles are distributed across the entire skin surface with the exception of the soles of the feet, the palms of the hand and the lips. A smooth muscle, the erector pilorum, attaches the follicle to the dermal tissue and enables hair to stand up in response to fear. Each follicle is associated with a sebaceous gland that varies in size from 200 to 2000 μm in diameter. The sebum secreted by this gland, consisting of triglycerides, free fatty acids, and waxes, protects and lubricates the skin as well as maintaining a pH of about 5. The fractional area for these is slightly more than 1/1000 of the total skin surface (Table 2). Also described in Table 2 are the eccrine of sweat glands and apocrine glands, accounting for about two-third and one-third of all glands, respectively. The eccrine glands are epidermal structure that are simple, coiled tubes arising from a coiled ball, of approximately 100 μm in diameter, located in the lower dermis. It secretes a dilute salt solution with a pH of about 5, this secretion being stimulated by temperature, as well as emotional stress through the autonomic nervous system. These glands have a total surface area of about 1/10,000 of the total body surface. The apocrine glands are limited to specific body regions and are also coiled tubes. These glands are about ten times the size of the eccrine ducts, extend as low as the subcutaneous tissues and are paired with hair follicles (1,2).

In many respects the nail may be considered as vestigial in human. However, some manipulative and protection function can be ascribed. Certainly nail plate composition, layers of flattened keratinized cell fused into a dense, but somewhat elastic mass, will afford some protection to the highly sensitive terminal phalanx. The cells of the nail plate originate in the nail matrix and grow distally at a rate of about 0.1 mm/day. In the keratinization process the cells undergo shape and other changes, similar to those experienced by the epidermis cells forming the stratum corneum. This is not surprising because the nail matrix basement membrane shows many biochemical similarities to the epidermal basement membrane. Thus, the expression of integrin $\alpha_2\beta_1$ and $\alpha_3\beta_1$ within the nail matrix basement membrane zone is indicative of a highly proliferated tissue. The structure of the keratinized layer is very tightly knit

Table 2 Appendages associated with the skin (1)

Parameter	Appendage			
	Hair follicle	Eccrine gland	Apocrine gland	Nails
Function	Protection (hair) and lubrication (sebum)	Cooling	Vestigal secondary sex gland?	Protection
Distribution	Most of the body	Most of the body	Axillae, nipples, anogenital	Ends of fingers and toes
Average/cm^2	57-100	100-200	Variable	-
Fractional area	2.7×10^{-3}	10^{-4}	Variable	-
Secretion	Sebum	Sweat (dilute saline)	"Milk" protein, lipoproteins, lipid	Nil
Secretions stimulated by	Heat (minor)	Heat, cholinergic	Heat	-
Biochemical innervations of gland response	-	Cholinergic	Cholinergic (?)	-
Control	Hormonal	Sympathetic nerves	Sympathetic nerves	-

but unlike the stratum corneum, no exfoliation of cells occurs. Given that it is a cornified epithelial structure, the chemical composition of the nail plate is not remarkable, and there are many similarities to that of the hair. Thus, the major components are highly folded keratin protein (containing many disulfide linkages) with small amounts (0.1-1.0%) of lipid, the latter presumably located in the intercellular spaces. The principal plasticizer of the nail plate is water, which is normally present at a concentration of 7-12% (1).

3. Drug transport through the skin

The skin is a tissue that separates the internal living organism from the external environment. It has a complex structure and performs many physiological functions such as metabolism, synthesis, temperature regulation, and excretion. The outermost layer of this organ, the stratum corneum, is considered to be the main barrier to the percutaneous absorption of exogenous materials.

3.1 Sebum as a barrier

The surface of the skin is the first point of contact for a topically applied formulation. Under normal circumstances, this is covered by a 0.4 to 10 μm irregular and discontinuous layer of sebum, sweat, bacteria, and dead cells. The presence of this layer is considered to have a negligible effect on percutaneous absorption, as it allows polar and nonpolar materials to penetration. Furthermore, no correlation has been found between the hydration state of the stratum corneum and the removal of the sebum layer by swabbing with solvents, the total amount of seborrhea lipids, or their composition. Therefore, the contribution of these endogenous surface materials to skin transport processes is effectively discounted (1,2).

3.2 The stratum corneum barrier

The barrier properties of the stratum corneum as the major rate-limiting step in the diffusion process of a drug permeating across skin. However, some researcher suggested that other skin components can contribute to the overall barrier resistance, especially for lipophilic solutes. The structure of the stratum corneum, as described in an earlier section, has been liked to “bricks and mortar”, where the bricks are the

component cells or corneocytes, and the mortar is the intercellular lipids (Figure 2). The membrane is interrupted only by appendages such as hair follicles and sweat gland. However, it is still considered to be a predominantly dual-compartment system composed of a matrix of corneocytes tightly packed with keratin, surrounded by a complex array of lipids arranged in bilayers. Transport across the stratum corneum is largely a passive process, and thus the physicochemical properties of a permeant are an important determinant of its ability to penetrate and diffuse across the membrane. There are generally considered to be three routes by which compounds can diffuse across the stratum corneum that are intercellular, trancellular, and transappendageal (Figure 2) as described further section. Once it has penetrated through the epidermis, a compound may be carried away by the dermal blood supply or be transported to deeper tissue. Therefore, owning to the structure of the skin the desired physico-chemical properties of a permeant are dependent on the route taken to transverse the stratum corneum (1,2).

3.2.1 Transcellular pathway

It was originally believed that transcellular diffusion mechanisms dominated over the intercellular and transappendageal routes during the passage of solutes through the stratum corneum. However, transport by the transcellular route would involve the repeated partitioning of the molecule between lipophilic and hydrophilic compartments, including the almost impenetrable corneocyte intracellular matrix of keratin and kerato-hyaline. Scheuplein further suggested that polar and nonpolar solutes permeate the stratum corneum by different mechanisms. The polar solutes were thought to diffuse through a high-energy pathway involving immobilized water near the outer surface of keratin filaments. In contrast, the lipid-soluble solutes diffused through a nonpolar lipid pathway. Roberts et al, analysed the Scheuplein's data and their phenol data, suggested that all solutes were transported through a lipid pathway and ameliorated through the effects of and unstirred water (viable epidermis) layer, as evidenced by a decrease in the energy of activation for permeation. Although the lipid route was thought to be transcellular, evidence for its location was not defined. Scheuplein also recognized that the dermis contributed to the resistance of the more lipophilic solutes. Most experimental evidence now suggests that transport through

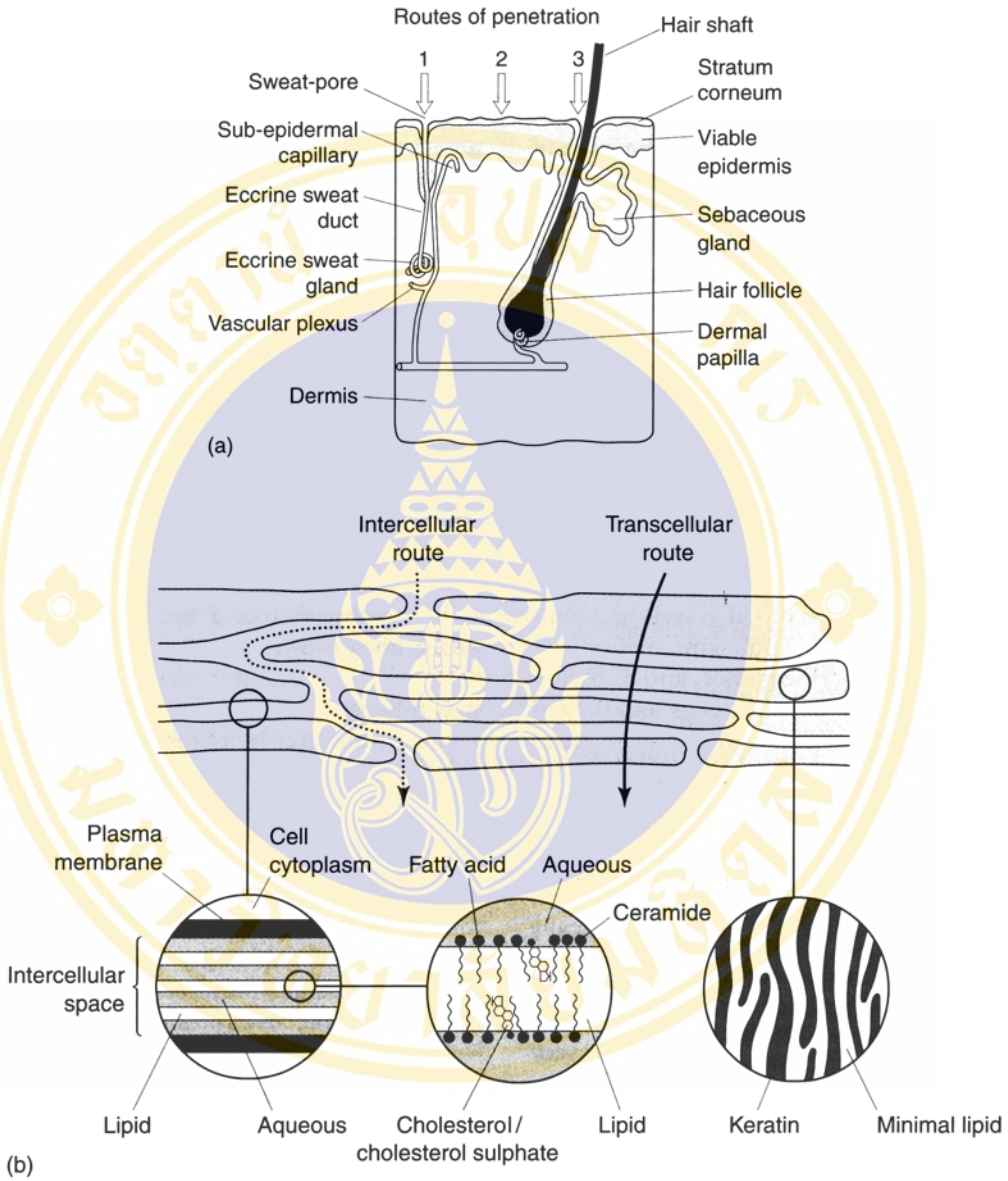

Figure 2 Simplified diagram of skin structure and routes of drug penetration.

(a) Macroroutes: (i) via the sweat ducts, (ii) across the continuous stratum cor-neum, or (iii) through the hair follicles with their associated sebaceous glands. (b) Representation of the stratum corneum membrane, illutrating two micro-routes for permeation (2).

the stratum corneum is by the intercellular route (1).

3.2.2 Intercellular pathway

The intercellular stratum corneum spaces were initially dismissed as a potentially significant diffusion pathway because of the small volume they occupy. However, the physical structure of the intercellular lipids was thought to be a significant factor in the barrier properties of the skin. Theoretical evidence, presented by Albery and Hadgraft in 1979, suggested that the tortuous intercellular diffusion pathway around keratinocytes was the preferred route of penetration through the stratum corneum, rather than the permeant diffusing through the keratinized cells (transcellular route). However, it should be recognized that although theoretical considerations favor this route, there are difficulties in designing appropriate diffusion studies to confirm that this route is the predominant pathway. In 1991, Boddé et al., vistualized the diffusion of mercuric chloride through dermatomed human skin samples by using ammonium sulfide vapor to precipitate the compound within the sample and subsequent transmission electron microscopy. Their results indicated that the intercellular route of transport through the stratum corneum predominate, however, after longer transport times, the apical corneocytes tended to take up the compound, leading to and apparent bimodal distribution. There was mercury both inside and outside the cells in the apical region of the stratum corneum, whereas in the medial and proximal region the mercury was located intercellular (1).

3.2.3 Skin appendages

Fractional area of skin appendages available for absorption is small about 0.1% and this route usually does not contribute appreciably to the steady-state flux of a drug. However, the route may be important for ions and large polar molecules that cross intact stratum corneum with difficulty. Skin appendages may also act as shunts, important at short times prior to steady state diffusion such as in bioassays that use pharmacological reactions. Thus, minute concentrations of nicotinates or cortico-steroids penetrating rapidly down the shunt route may quickly trigger erythema or blanching, respectively (2).

4. Basic principles of diffusion through membranes

A useful way to study percutaneous absorption is first to consider how molecules penetrate inert (artificial) membranes, and then move on to the special situation of skin transport. An understanding of the basic principles of permeation through membrane is also valuable in all other areas of biopharmaceutics such as oral, baccal, rectal, lung, vaginal, uterine, injection or eye. The underlying mathematics is also relevant to dosage form design, particularly sustained controlled release formulations and drug targeting.

4.1 The diffusion process

Passive diffusion is matter by moving of molecule from one region of a system to another, which is a random molecular motion. The basic hypothesis underlying the mathematical theory for isotropic materials, which have identical structural and diffusional properties in all directions, is that the rate of transfer of diffusing substance per unit area of a section is proportional to the concentration gradient measured normal to the section. This following is expressed as Fick's first law of diffusion.

$$J = -D\frac{\partial C}{\partial x} \qquad (1)$$

where J = the rate of transfer per unit area of surface (the flux)

C = the concentration of diffusing substance

x = the space coordinate measured normal to the section

D = the diffusion coefficient

The negative sign indicates that the flux is in the direction of decreasing concentration. In many situations D is constant, but in more complex materials D depends markedly on concentration; its dimensions are $(\text{length})^2(\text{time})^{-1}$, often specified as $\text{cm}^2\ \text{s}^{-1}$.

Fick's first law contains three variables, J, C, and x of which J is additionally a multiple variable, dm/dt, where m is amount and t is time. Fick's second law has been usually employed, which reduces the number of variables by one. For the commonly

experimental situation in which diffusion is unidirectional that is the concentration gradient is only along the *x*-axis. Equation 2 expresses Fick's second law as follows:

$$\frac{\partial C}{\partial t} = D\frac{\partial^2 C}{\partial x^2} \qquad (2)$$

A number of experimental designs employ a membrane separating two compartments, with a concentration gradient operating during a run and 'sink' conditions prevailling in the receptor compartment. If measuring the cumulative mass of diffusant, *m*, which passes per unit area through the membrane as a function of time, the plot, shown in Figure 3, is obtained. At long time the plot approaches a straight line and from its slope, the steady state flux is obtained, as expressed in equation 3.

$$\frac{dm}{dt} = \frac{DC_0K}{h} \qquad (3)$$

where C_0 = the constant concentration of drug in the donor solution

K = the partition coefficient of the solute between the membrane and the bathing solution

h = the thickness of the membrane

If a steady-state plot is extrapolated to the time axis, the intercept so obtained at $m = 0$ is the lag time, L:

$$L = \frac{h^2}{6D} \qquad (4)$$

For biological membrane, sometimes the *D*, *K*, and *h* value may be difficult or impossible to measure. A composite parameter of permeability which includes *D*, *K*, and *h* value are defined as permeability coefficient (i.e., $P = KD/h$) for explaining the permeability of various solute through those biological membrane (2).

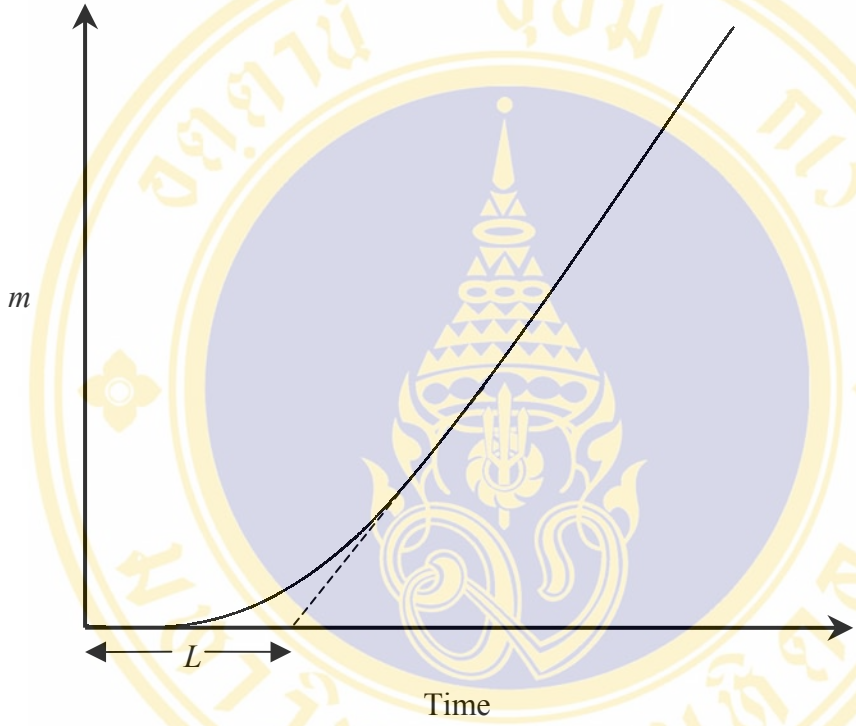

Figure 3 The time course for absorption for the simple zero-order flux case obtained by plotting the cumulative amount of diffusant crossing unit area of membrane (*m*) as a function of time. Steady state is achieved when the plot becomes linear, and extrapolation of the linear portion to the time axis yields the lag time (*L*) (2).

4.2 Complex diffusional barrier

4.2.1 Barrier in series

The treatment above deals only with the simple situation which diffusion occurs in a single isotropic medium. In fact that, the skin is a heterogeneous multi-layer tissue and in percutaneous absorption the concentration gradient develops over several strata. The skin can be treated in term of a laminate, each layer of which contributes a diffusional resistance (R) which is directly proportional to the layer thickness (h) and indirectly proportional to the product of the layer diffusivity (D) and the partition coefficient (K) with respect to the external phase. The total diffusional resistance of all layers in the skin, that is stratum corneum, viable epidermis, and dermis, is given by the following expression:

$$R_T = \frac{1}{P_T} = \frac{h_1}{D_1 K_1} + \frac{h_2}{D_2 K_2} + \frac{h_3}{D_3 K_3} \qquad (5)$$

where R_T = the total resistance to permeation

P_T = the thickness-weighted permeability coefficient

The numbered refer to the separate skin layer

If one segment has a greater resistance than the other layers, then that single high resistance phase determines those composite barrier properties. As to known that the stratum corneum is the main barrier for most solutes permeate through skin, thus, the equation 5 is reduced to this following simple equation; $P_T = K_1 D_1 / h_1$, where the subscript 1 refers to the stratum corneum resistance phase (2).

4.2.2 Barrier in parallel

Human skin is pierced by shunts and pores, such as hair follicle and sweat glands. Investigators often idealize this complex structure and consider the simple situation in which the diffusional medium consists of two or more diffusional pathways linked in parallel. Then the total diffusional flux per unit area of composites (J_T) is the sum of the individual flux through the separate routes.

$$J_T = f_1 J_1 + f_2 J_2 + \ldots \quad (6)$$

where $f_1, f_2, \ldots$ = the fractional areas for each diffusional route

$J_1, J_2, \ldots$ = the fluxes per unit area of each separate route

In general, for independent linear parallel pathways during steady state diffusion, the equation is given by following.

$$J_T = C_0 (f_1 P_1 + f_2 P_2 + \ldots) \quad (7)$$

where $P_1, P_2, \ldots$ = the thickness weighted permeability coefficients

C_0 = the constant concentration of drug in the donor solution

If only one route allow diffusant to pass, while the other routes are impermeable, then the solution reduces to the simple membrane model with the steady state flux determined by the fractional area and the permeation rate through the open channel (2).

5. Methods for studying percutaneous absorption

5.1 *In vitro* methodology

In vitro techniques to assess skin penetration and permeation are used extensively, although, *in vivo* data should be performed and required for topical or trandermal drug delivery formulation registration. However, the *in vitro* techniques have advantages over *in vivo* testing. For example, permeation through the skin can be measured directly by *in vitro*, for which sampling is carried out immediately below the skin surface. This contrasts with most *in vivo* methods, which rely on the measurement of systemic levels of permeant. For *in vitro* technique, it is essential to consider the ultimate use of gene-rated data when developing experimental protocols. Routinely, simple mathematical model, which is based on certain assumptions of boundary conditions, is applied to experimental data. The most commonly used solutions to diffusion equations that are applied to the *in vitro* situation make the following assumptions. The receptor phase is a perfect sink, depletion of the donor phase is negligible, and the membrane is a homogenous slab. None of these assumptions

is wholly true in practice, and the potential significant of these imperfections must not be overlooked. Careful experimental design can be used to achieve a close approximation to reality. The following section is discussion about materials and equipments that often used *in vitro* permeation experiment (1).

5.1.1 Diffusion cell design

In vitro systems range in complexity from a simple two-compartment "static" diffusion cell to multi-jacketed "flow-through" cells (Figure 4). Construction materials must be inert, and glass is most common, although Teflon and stainless steel are also used. Excised skin is always mounted as a barrier between a donor chamber and a receptor chamber, and the amount of compound permeating from the donor to the receptor side is determined as a function of time. Efficient mixing of the receptor phase (sometimes the donor phase also required) is essential, and sample removal should be simple. Neither of these processes should interfere with diffusion of the permeant. Continuous agitation of the receptor medium, sampling from the bulk liquid rather than the side arm of cell, and accurate replenishment after sampling, are important practical considerations. It is essential that air bubbles are not introduced below the membrane during sampling.

Static diffusion cells are usually of the upright (Franz type) or side-by-side type, with receptor volume of about 2-10 mL and surface areas of exposed membranes of near 0.2-2 cm^2. The dimensions of diffusion cell should be accurately measured, and precise values should be used in subsequent calculation, with due attention to analyse dilution resulting from sampling and replenishment. The main difference in the application of these two static cell types is that side-by-side cells can be used for the measurement of permeation from one stirred solution, through a membrane, and into another stirred solution. This is of particular advantage when examining flux from saturated solutions in the presence of excess solid if accumulation of solid on the membrane surface must be prevented. This type of cell can also be modified to allow the absorption of permeants in the vapor phase. Upright cells are particularly useful for studying absorption from semisolid formulations spread on the membrane surface and are optimal for simulating *in vivo* performance. The donor compartments can be

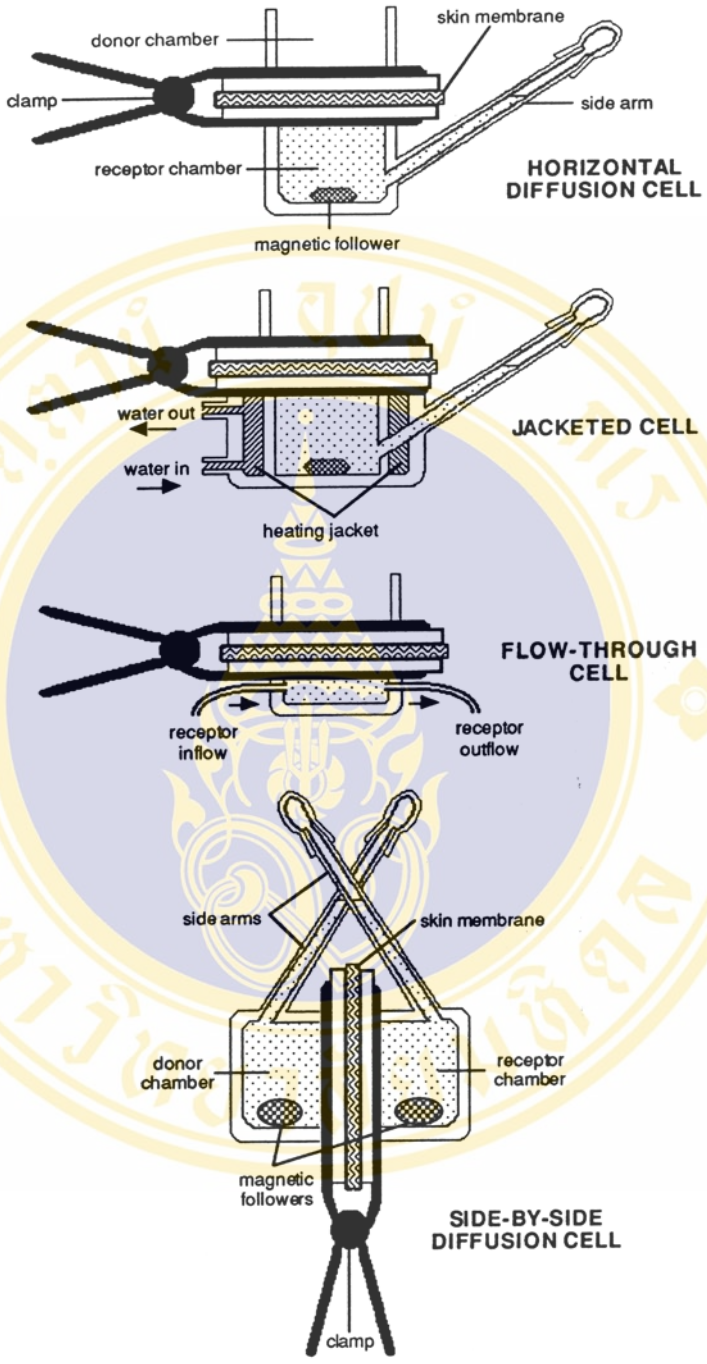

Figure 4 Basic diffusion cell designs: static horizontal cells may be jacketed (as in Franz-type) or unjacketed (and temperature-controlled using a water bath or heating block). Flow-through cells usually have a small chamber to maximize mixing. Side-by-side cells are used mainly for solution vehicles (1).

capped to provide occlusive conditions, or left open, according to the objectives of the particular study

Flow-through cells can be useful when the permeant has a very low solubility in the receptor medium, and designs are continuously improving. Sink conditions are maximized as the fluid is continuously replaced using a suitable pump (at a rate of about 1.5 mL/h). However, the dilution produced by the continuous flow and raise problems with analytical sensitivity, particularly if the permeation is low. Flow-through and static system have produced equivalent results (1).

5.1.2 Receptor chamber and medium

Receptor chamber dimensions are constrained by the conflicting requirements of guaranteeing that the receptor phase can act as a sink, while ensuring that sample dilution does not preclude analysis. A large receptor volume may ensure sink conditions, but will reduce analytical sensitivity unless large samples can be taken and subsequently concentrated. The ideal receptor phase provides an accurate simulation of the conditions pertaining to *in vivo* permeation of the test compound. As a general rule the concentration of the permeant in the receptor fluid should not be allowed to exceed approximately 10% of saturated solubility. Excessive receptor phase concentration can lead to a decrease in the rate of absorption, which may result in an underestimate of bioavailability. The most commonly used receptor fluid is pH 7.4 phosphate buffered saline, although this is not always the most appropriate materials. It has been postulated that if a compound has water solubility less than about 10 μg/mL, then a wholly aqueous receptor phase is unsuitable, and the addition of solubilizers becomes necessary. It is important to recognize the possibility that solubilizers may interfere with the barrier function of the skin itself. Bronaugh examined several commonly used receptor phases and made several recommendations. One of the most useful receptor phases was and an aqueous solution containing 6% Volpo N20, a nonionic polyethylene glycol-20-oleyl ether surfactant. This did not influence the flux of either water or urea across rat skin, when compared with normal saline, suggesting that Volpo N20 did not disrupt the barrier function of rat skin to hydrophilic compounds. Rat skin usually responds to penetration enhancers to a greater degree than human skin and thus one would predict that Volpo N20 should have a negligible

effect on the flux of hydrophilic compounds across human skin. The problem of very lipophilic permeants has been addressed by the used of nonaqueous and nonliquid receptor media. Sheets of silicone rubber (0.02 inches thick) were used to collect pesticides with low solubilities, which were then desorbed from the rubber with an appropriate solvent and subsequently analysed. Other solutions have included the use of flowing gaseous receptor phase for volatile permeants (1).

5.1.3 Selection, variation, and preparation of skin membrane

a. Intrasubject and intersubject variability

Few studies have addressed the issues of intra and intersample variability in human skin permeability, because of the few sufficiently large datasets available for accurate statistical evaluation. There are at least two issues in this area that need to be addressed. The first is the degree and nature of the distribution patterns of skin permeability *in vitro*. This was addressed to some extent by Southwell et al, who investigated both *in vitro* and *in vivo* variation in the permeability of human skin between different specimens and the same specimens. From the permeation characteristics for a series of compounds, they concluded that *in vitro* interspecimen variation was 66 $\pm$ 25% and intraspecimen variation was 43 $\pm$ 25%. The pattern *in vivo* was similar, although the overall level of variation was somewhat smaller. Kastings et al and Cornwell and Barry concluded that there was evidence that the permeability of human skin *in vitro* is log-normally rather than normally distributed. Williams et al examined the permeation of 5-fluorouracil (644 determinations from 71 specimens) and estradiol (211 determinations from 28 specimens) through human abdominal skin. Here, where site variability was excluded, the data were lognormal distribution. A lognormal distribution implies that the use of normal gaussian statistics is inappropriate, and the use of geometric means should be considered (1).

b. Age and sex differences

The questions of how age and sex affect the permeability of human skin have been rather poorly addressed to date. Some studies have concluded that, *in vitro* in human, there was no discernible dependence of skin permeability on age, sex, or storage conditions. The effect of age on percutaneous absorption has been examined

in vivo in humans, with variable results. It was postulated that reduced hydration levels and lipid content of older skin may be responsible for a demonstrated reduction in skin permeability if the permeants were hydrophilic (no reduction was seen for model hydrophobic compounds). The reduced absorption of benzoic acid (log $K_{o/w}$ = 1.83) demonstrated in the elderly was in line with this suggestion, but not the reduction in absorption of testosterone (log $K_{o/w}$ = 3.32) with age. A number of potential physiological changes the may be responsible for age related alterations in skin permeability have been suggested. These include a noted increase in the size of individual stratum corneum corneocytes throughout life, increased dehydration of the outer layers of the stratum corneum with age, decreased epidermal turnover, and decreased microvascular clearance (1,2)

.

c. Racial differences

Several authors have documented differences between the permeability of skin base on its racial origin. White skin is slightly more permeable the black skin, which correlates with observations that black skin has both more cell layers within the stratum corneum and higher lipid content. A recent study of white, Hispanic, black, and Asian skin ranked them in order of permeability to methyl nicotinate as black < Asian < white < Hispanic. It has been reported that the corneocytes of black, white, and oriental skin are of a similar size, but that there are differences in spontaneous desquamation. It has also been reported that there may be differences between black and white skins in micro-vascular reactivity, following dermal application of vasoactive agents, but this is possibly due to subjective, rather than objective measurement. No differences in the permeation of water through black or white skin *in vitro* were observed and similarly, there was no racial difference in the *in vivo* percutaneous absorption of diflorasone diacetate. Lotte et al, have determined the penetration and permeation of several compounds into skin stripping and through (24 h urinary excretion) Asian, black, and white skin. There were no statistical differences in penetration of permeation of benzoic acid, caffeine, or acetyl-salicylic acid among the races (1).

d. Storage conditions

It is unclear whether the proposed lognormal distribution *in vitro* is an experimental artifact caused by excision and isolation from the body, or by storage conditions before use that is by freezing storage. Some authors concluded that freezing had no measurable effect on permeability. Yazdanian reported an effect for cattle, although there was no general pattern of differences between frozen and fresh skin. Wester et al, have cautioned against the use of frozen, stored human skin for studies in which cutaneous metabolism may be a contributing factor. However, it is important to appreciate that the state of hydration of the tissue before freezing may influence subsequent permeation characteristics. As a general rule tissues should not be hydrated when placed into frozen storage (1). Additionally, Hadzija BW et al, and Kasting GB et al, found that both length of time in the frozen stage and the temperature maintained throughout the storage process of hairless rat skin and excised human skin respectively, may affect iontophoretic transport (32-34).

e. Anatomical site variations

Site-to-site variation of skin permeability has been examined using the tape-stripping method and correlated with corneocyte diameter and, hence, diffusional path-length. Although, in practice, skin permeation of compounds follows a different pattern in different skin regions, it is generally agreed that some body site (the head and genital region) are uniformly more permeable than others (extremities). For example, transepidermal water loss and skin permeation of benzoic acid, caffeine, and acetyl-salicylic acid decreased in the order forehead > postauricular > abdomen > arm. Similarly, the per-meation of hydrocortisone decreased in the order scrotum > jaw > forehead > scalp > back > forearm > palm, and abdomen was more permeable to methyl salicylate than either the arms or feet (1). Additionally, Harada K et al, reported the permeation of salicylic acid through difference human skin region. They found that greater permeability of the scrotum and negligible permeability of the sole to salicylic acid was apparent. The face, neck, and inguinal skin seem more permeable than the breast, back, thigh (inner aspect), lower leg (pretibial), and foot (dorsal) (35).

f. Membrane preparation

Different methods can be used to prepare human skin. The membrane is one of the following; (a) Full-thickness skin, incorporating the stratum corneum, viable epidermis, and dermis, (b) Dermatomed skin, in which the lower dermis has been removed, (c) Epidermal membrane, comprising the viable epidermis and the stratum corneum (prepared by heat separation), and (d) The stratum corneum alone (prepared from step (c) by enzyme treatment) (1).

The most suitable type of tissue is dependent on the nature of the permeant. The environment of skin *in vivo* differs somewhat from that *in vitro*. *In vivo* the continuously perfused subcutaneous vasculature, which penetrates the dermis to significant degree, can rapidly remove permeants reaching the epidermal-dermal junction. These vessels, if still present, are not perfused in simple *in vitro* models. *In vitro* the relatively aqueous environment of the dermis will inhibit the penetration of lipophilic compounds, whereas *in vivo* this barrier is circumvented by the capillary bed. Hence, the use of dermatomed, epidermis, or the stratum corneum membranes is more appropriate for particularly lipophilic permeant. Other considerations may justify the use of epidermal membranes, even where the dermis does not present an artificial barrier to a permeant. For example, if a study involves an assessment of the skin content of permeant, it is much easier to extract of solubilize epidermal membrane, or the stratum corneum, than full-thickness skin. Conversely, if an experiment includes tape-stripping, it may be easier to perform on full-thickness skin, rather than epidermal membranes (1).

The preparation of epidermal membranes and the stratum corneum is time-comsuming, and the necessary processing increase the possibility of damage to the skin membrane. Careful consideration of the most appropriate type of skin preparation is required, and this should address the physicochemical nature of the penetrating species, the data required, tissue availability, and the time scales involved. With animal skin, full-thickness membranes are usually used, because it is difficult to isolate intact epidermis or the stratum corneum owing to the presence of numerous hair follicles, which may also compromise dermatomed tissue (1).

5.1.4 Application technique

The manner in which a substance is applied to the skin surface can be a major determinant of its subsequent absorption. Several factors must be considered in selecting a suitable application procedure, including the nature of the vehicle, the permeant concentration, the amount of vehicle applied, the mechanism of application, the exposure time, and the method for removing an applied vehicle (if required). There are two basic approaches to applying substance to the skin. One is infinite-dose techniques, which involve application of sufficient permeant to make any changes in donor concentration during the experimental timeframe, caused by diffusion or evaporation negligible (i.e., the dose is effectively infinite). This is desirable if the experimental objectives include calculation of diffusional parameters, such as permeability coefficients, or for investigation of mechanisms of penetration enhancement. Another one is finite dose techniques, which is designed to model in-use conditions, involve application of a dose that may show marked depletion during an experiment. Depletion occurs where the proportion of permeant entering the membrane is large, relative to the amount applied. Alternatively, the permeant may be removed from the skin surface during, for example, the simulation of a rinsing or washing procedure. With finite dosing the permeation profile may exhibit the characteristic plateau effect that accompanies donor depletion. The finite dose technique may involve application of permeants or enhancers in small volume of volatile solvent, such as, acetone or ethanol. This allows assessment of the gross effects of enhancers, but results are more difficult to interpret mechanism. Direct comparison of finite and infinite-dose applications is relatively rare, but the predicted effects have been investigated (1).

5.1.5 The permeation experiment

a. Duration

The duration experimental time is recommended that be restricted to 24 or 48 hours. The ECVAM report suggests experiments may be extended to 72 hours, in the presence of antimicrobial agents, in such instances. From electrical resistance measurements and permeation parameters, human epidermal membranes were shown to retain integrity for up to 5 days, provided they were supported on suitable non-rate

limiting membranes (e.g., Millipore GSWP filters). In the absence of the filter membrane support, tissue integrity was compromised by the physical stress accompany sample withdrawal and skin washing. However, investigators should be aware of possible barrier degradation over extended time frames (1).

b. Sample interval

Sample interval should be appropriate frequencies to allow realistic assessment of such parameters, such as, lag time and steady state or pseudo steady state. For a compound with unknown permeation characteristics, samples should ideally be taken at 2 h intervals for the duration of the experiment. Early samples (1-4 h) may be important in identifying compromised cells showing anomalously high early permeability (1).

c. Number of replication

Given the high intrasubject and intersubject variability in human skin permeability, a large number of replication for each dosage regimen is recommended. The most widely quoted recommendation for number of replication in *in vitro* studies on human skin is twelve, and comparison should be matched. Fewer replications may be employed, if cost, time, or skin availability is problem, provided that the limitations of replicate reduction are recognized. The permeability characteristics of laboratory animal skin are, in general, more uniform than those of human skin, and fewer replicates may be successfully employed (1).

d. Temperature

In vitro skin diffusion experiments are normally conducted with a skin temperature of 32ºC (the *in vivo* value). This is achieved by maintaining the receptor solution at 37ºC, either by immersing cells in a water bath or by using cell jacket perfused at the correct temperature (1).

e. Skin integrity

Skin integrity can be addressed in a qualitative manner by simple visual examination of specimens, or more quantitatively by measurement of transepidermal

water loss or by the flux of marker compounds, such as tritiated water or sucrose. The generally accepted permeability coefficient for water diffusion through human skin is 1.5 x 10^{-3} cm/h or less, although an upper limit of 2.5 x 10^{-3} cm/h has also been used (1).

f. Permeant analysis

The quality of the data derived from any experiment is ultimately dependent on the integrity of the analytical method employed, and all aspects of the analytical procedure should be included in the overall experimental design. The ideal analytical procedure provides accurate assessment of both the quantity and nature of the material present at a given time, and the detection limit of the method must be capable of producing data of practical significance (1).

5.2 Other *in vitro* methods for studying percutaneous absorption

5.2.1 Skin stripping

Skin stripping with adhesive tape is commonly used *in vivo*, and also *in vitro*. Tape stripping experiments are performed as follows; (a) a permeant is applied to the skin surface for a fixed time period, (b) permeant remaining on the skin surface is removed by wiping or washing, (c) a succession of the stratum corneum layers are removed by sequential tape strips, and (d) the permeant contents of the tape strips are determined. These experiments evaluate how the concentration of a permeant applied to the skin surface changes with depth into the stratum corneum. The shape of this concentration depth profile will be time dependent and vary with permeant, according to the rapidity, degree, and nature of uptake by the stratum corneum. If steady state diffusion is achieved, then the distribution of a permeant across a homogeneous membrane should be represented by a linear decline from the outside to the inside. Before steady state, the distribution of a permeant across a homogeneous membrane will be represented by a series of concave curves converging to a straight line as time progresses. Hence, in a tape stripping experiment, assuming that the stratum corneum is homogeneous and that the depth profiled with each tape strip is the same, a linear concentration-strip number profile in the steady state region of any diffusion experiment would be expected. In practice, neither of these assumptions generally

appears to be correct, resulting in nonlinear profiles (Figure 5). If the membrane is not homogeneous, then distribution of a permeant with the skin at steady state will not be a linear function of depth. The majority of both *in vivo* and *in vitro* reports show the distribution of compounds within the skin to be related to strip number in a nonlinear fashion. There is usually an approximate exponential decay in the amount of permeant from the outside to the inside of the stratum corneum (e.g., erythromycin, lanolin, fentanyl, alniditan, and hair dyes). However, steady state may not have been attained or the nonlinear dependence of concentration on strip number may be a result of nonlinear removal of the stratum corneum (1).

5.2.2 Attenuated total reflectance fourier transform infrared (ATR-FTIR) spectroscopy

ATR-FTIR technique is fairly straightforward; (a) a membrane is placed in direct contact with the surface of a ZnSe ATR crystal, mounted on a spectrometer, (b) a shallow trough is placed on top of the membrane, (c) trough is sealed to the membrane (e.g., with petroleum jelly), (d) the solvent-solute system under study is placed in the trough, and (e) the spectrometer is linked to a computer equipped with the appropriate soft-ware and FTIR spectra taken at the crystal-membrane interface over a time period. The IR beam penetrates the membrane to a depth of only about 2-3 μm, therefore, only the interfacial region is probed. As permeant enters the interfacial region there is an increase in the IR peak areas associated with the penetrating species. The major limitation is that the permeant must have an IR absorption in the transparent region of the membrane, such as compounds containing cyano and azido groups or deuterated compounds. The data obtained is the concentration-time profile at the crystal-membrane interface, which builds up at a rate related to the diffusion coefficient and gradually plateaus at a level related to the solubility of the permeant in the membrane under study. These two parameters can be estimated by a nonlinear curve fit to the data by using a solution to Fick's laws of diffusion (1).

ATR-FTIR spectroscopy was originally used to study diffusion through simple homogeneous synthetic systems, such as silicone membranes. The technique was applied to examination of diffusion into semisolids and to the investigation of ethanol diffusion in glycerogelatin films. In conjunction with bulk transport techniques, it was

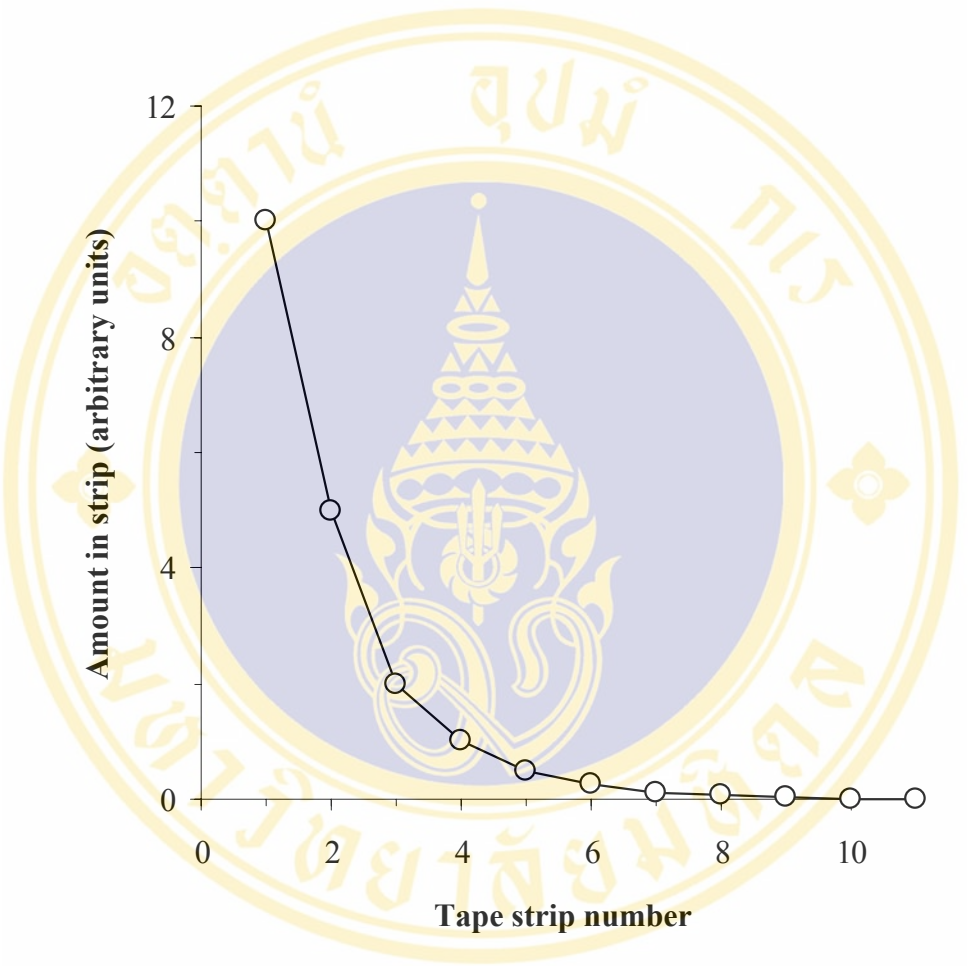

Figure 5 Typical pattern of permeant content in tape strips removed from the stratum corneum following a fixed period of exposure (1).

used to show that values of diffusion coefficients methodology has been specifically refined to permit its use with human stratum corneum, and it has also been applied to the investigation of morphological differences between the upper and lower layers of the stratum corneum. Data from regular diffusion cells and ATR-FTIR spectroscopy showed a high correlation and has been used to predict diffusional path-lengths in the stratum corneum (1).

5.2.3 Isolated perfused tissue models

Perfused tissue model use excised region of skin, complete with their associated microvasculature, immediately after sacrifice and with continuous solution perfusion, such as Krebs-Ringer buffer, glucose, and albumin aerated with oxygen and carbon dioxide. Several variations on the theme involve both different species and area of skin. Isolated perfused porcine skin flaps, bovine udders, and rabbit ears have been used. The perfused pig ear model uses an isolated ear perfused with oxygenated blood from the same pig. These techniques permit the investigation of the effect of local blood circulation on the accumulation and removal to topically applied materials (1).

5.2.4 Artificial cultured skin

The technology behind the construction of human skin equivalent (artificial skin) is derived predominantly from research into the treatment of burns. A classification and evaluation of the numerous different types of human skin equivalents concluded that the technique is limited to the reconstitution of the epidermis with a stratum corneum. Such models have been used to investigate both cutaneous metabolic events and dermal irritation, with varying degree of success. The use of artificially cultured skin in permeation experiments is still of limited application because the methodology is both expensive and not clearly predictive of *in vivo* results. *In vitro* skin equivalents are generally approximately ten times more permeable than human skin. On the other hand, reconstructed epidermis transplanted onto a nude athymic mouse had permeability similar to normal human skin after one month (1).

5.2.5 Animal and synthetic membrane as model membranes

A range of animal and synthetic membranes have been evaluated as models for percutaneous penetration. These may offer the possibility of providing a less variable system for formulation evaluation and for investigation of permeation phenomena.

5.2.5.1 Animal models

Given the limited availability of human tissue and the fact that a number of percutaneous investigations may be too toxic to be carried out on living subjects, a number of animal models have been investigated for their usefulness in predicting percutaneous absorption kinetics.

a. Hairless mouse

These laboratory animals have been used extensively in transdermal absorption research, probably because of the perceived similarity between their skin structure and that of humans. Homozygous animals carrying the hairless, recessive genes develop a normal coat of hair up to the age of about 10 days after which the complete hair shaft is lost from the follicle. Sparse thin hairs grow at intervals during the life of the animal but are soon lost. Hyperkeratosis of the stratum corneum and upper part of the hair canals begins about two weeks post partum and cysts may develop in the hair follicles or sebaceous glands with subsequent keratinization. While the number and diameter of the hair follicles in hairless mouse skin approaches that of human skin more closely than most other laboratory animals, the stratum corneum of these animals is less than half as thick as that of human tissue with commensurately lower barrier properties. Reports from the literature tend to suggest that the observed permeability of hairless mouse skin highly dependent on the characteristics of the permeant, being equivalent to human tissue for some compounds and vastly different for other compounds. The skin of the hairless mousse is experimentally useful from a sampling viewpoint in that it is loose and does not adhere to the underlying viscera. The facile removal of large pieces of membrane of uniform thickness with little clinging peritoneal tissue is therefore possible. In most cases full thickness hairless mouse skin has been used, as separation of the relatively thin stratum corneum-

epidermis from underlying tissue by chemical or dermatome means is fairly difficult. Histologically, hairless mouse skin does not exhibit the rete ridges of human tissue and hence the thickness of the stratum corneum-epidermis is fairly uniform in whole skin samples. Valia and Chien studied the rates of uptake, binding, cutaneous metabolism and permeation of oestradiol in the abdominal epidermis and dermis of hairless mouse skin. No sex dependent difference was observed in the mechanism and rate of metabolism to oestrone, however, the uptake and binding of oestradiol by female skin was greater than that by male skin. Furthermore, their results imply that there may be a sex linked difference in the partition coefficient of this diffusant between donor solution and skin. While, the bioconversion and binding of corticosteroids may not be as prolific as that of the sex steroids in these animals, the potential for preferential metabolism or preferential partitioning of the diffusant into the skin with regard to the sex of the animal requires consideration. It is generally assumed that animals of the same sex should be used for comparative investigations to overcome the variance introduced by sex related idiosyncrasies (28).

b. Rat

The rat is a common laboratory animal which has been used extensively in the study of transdermal drug absorption. Excised rat skin has generally been considered more permeable than human or pig skin, however, in the diffusion of certain compounds rat skin appears to be as good as pig skin in modeling absorption through human tissue. Studies using the hairless rat, the nude rat, and the fuzzy rat have also demonstrated these animals to be useful in certain circumstances. While, split-thickness skin (350 μm), prepared by dermatome, has been used in diffusion experiments, clipped, full thickness skin is more commonly employed. The dermatomed sections contain only a portion of the epidermis and demonstrate enhanced absorption of hydrophobic compounds in comparison to full thickness tissue. Although, adequate correlation of *in vitro* with *in vivo* data has been shown possible, extensive sex and anatomical region-related variations in permeability have been noted for rat skin by other researchers. In spite of these observations, the convenience and availability of these animals, and the reasonable similarity between rat and human

skin, indicate that this species could play an important role in transdermal absorption research (28).

c. Pig

In several *in vitro* studies the skin of the pig of miniature pig has proved to be a good animal model for human skin. Galey and coworkers observed the permeation rate of tritiated water through dermatomed, full thickness pig skin to be very slightly greater than that through human tissue. Hawkins and Reifenrath reported a statistically significant correlation between the percutaneous penetration of ten compounds through whole pig skin *in vitro* and values reported for human skin *in vivo*. They further reported that better agreement between *in vitro* and *in vivo* results is obtained if sectioned pig skin is used instead of full thickness membrane, presumably because the barrier thickness of the pig skin would then approach that of human skin. Although, the stratum corneum of the pig is almost twice the thickness of the human layer, Bronaugh et al, reported that pig skin is very similar to human tissue in the density of hair follicles (average 11 follicles /cm^2 of both skins) and that this is the lowest density found in any laboratory animal. However, pig skin follicles, incorporating coarse hair shafts, are almost twice the diameter of their human counterparts. The thickness of the porcine dermis makes the use of full thickness skin impractical; however, Bronaugh et al. indicated that they were unable to separate the epidermis from full skin samples by the methods of heat, trypsin, or ammonia because of the presence of the coarse hair follicles. They therefore concluded that the best method of pig skin preparation is to section the sample using a dermatome (28).

d. Shed snake skin

Although, shed snake skin is not a mammalian integument, many compounds penetrate snake skin and human stratum corneum at similar rates. Since, snakes moult periodically, a single animal can provide repeated sheds, thus, eliminating interindividual variability. Skins can be obtained without injury to the animal and do not have to be subjected to chemical or heat stress prior to used (Figure 6,7). The epidermis is shed as a large, intact sheet, thus a single snake skin can provide multiple samples. Shed snake skin is not a living tissue, can be stored a room temperature for

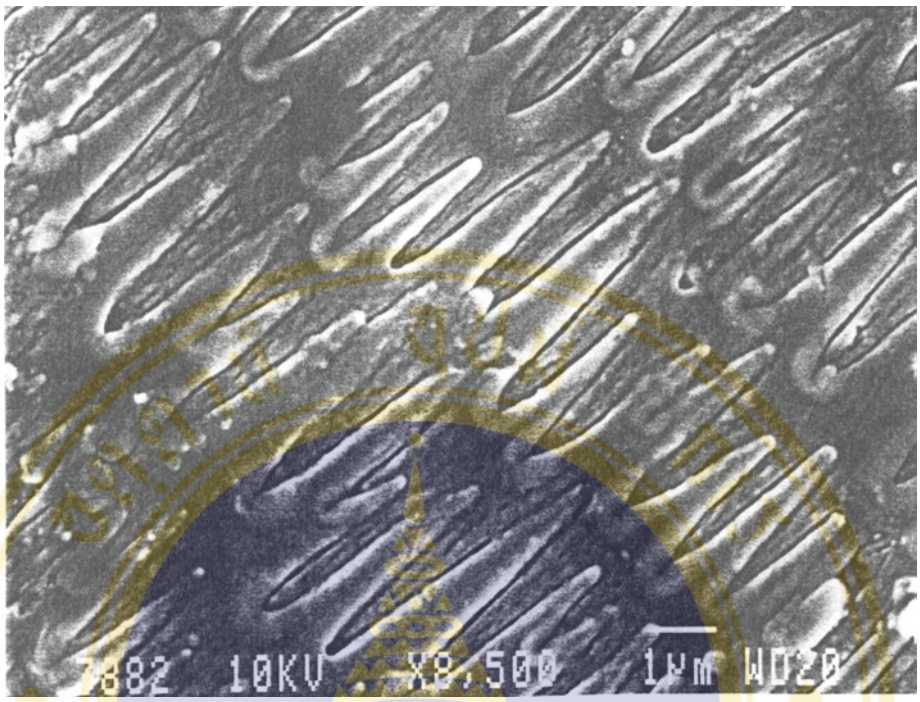

Figure 6 Dorsal lipophilic surface of shed forest cobra (*Naja melanoleuca*) skin (28).

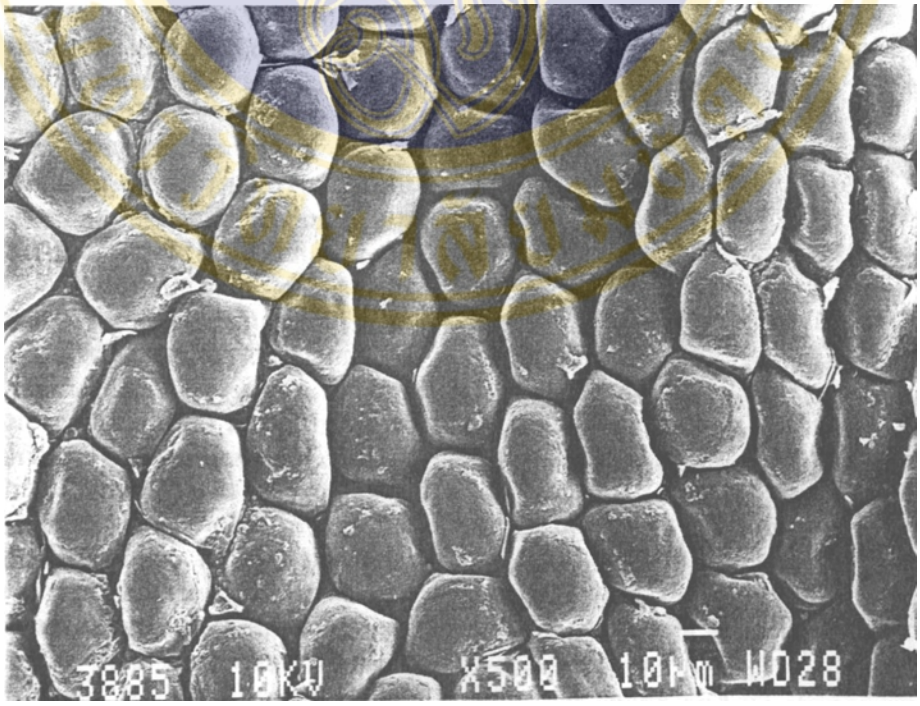

Figure 7 Ventral lipophilic surface of shed forest cobra (*Naja melanoleuca*) skin (28).

relatively long periods and is easily transported. Stored or fresh skins appear to show no differences in permeability. Since snake skin lacks hair follicles, the problems associated with transfollicular routes of penetration, which may be significant in mammalian skins, can be avoided (28).

f. Egg shell membrane

An interesting investigation (Washitake et al., 1980) used egg shell membrane (Figure 8), which like human stratum corneum, consists mainly of keratin. The membrane is prepared by immersing the whole egg in 0.5 M hydrochloric acid which dissolves the outer shell. Thereafter, the contents of the egg may be removed and the membrane washed and refrigerated or soaked in isopropyl myristate under vacuum to impregnate the keratin matrix. The replacement of water in the membrane with this lipid is assumed to increase its likeness to stratum corneum biochemistry. It was found that the egg shell membrane was more permeable than cellulose media and exhibited approximately equivalent permeability to a polysamide lipoid membrane for the passage of β-methasone 17-valerate. Although its relatively low resistivity would tend to suggest that egg shell membrane has limited usefulness in the design of *in vitro* diffusion systems, it may be worthwhile considering given the ease of obtaining the membrane (28,30).

5.2.5.2 Synthetic membranes

It may, theoretically, be possible to adequately simulate the *in vivo* permeation of a drug using a specific diffusion system and synthetic membrane. The commercial availability, stability, interbatch uniformity and ease of usage make the use of synthetic media highly desirable. The barrier potential of porous membranes is dictated by the probability of diffusant molecule entering and diffusing through the pores, and the factors governing selectivity to diffusion would be the relative molecular size, molecular shape and its electrostatic interactions with the membrane. Conversely, aporous media appear to offer some rate-limiting factor to permeation and may, therefore, more closely simulate diffusion through biological tissue. The barrier properties here generally relate to the solubility of the diffusant in the polymer matrix (partition coefficient between donor vehicle and membrane) and the ease of diffusant

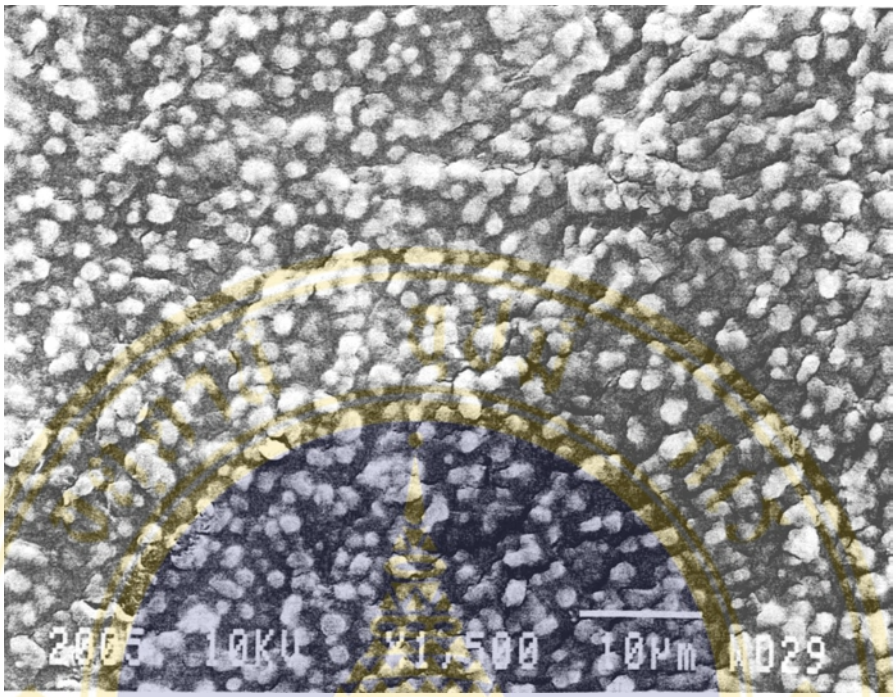

Figure 8 Surface topography of egg shell membrane (sample obtained by blunt dissection) (28).

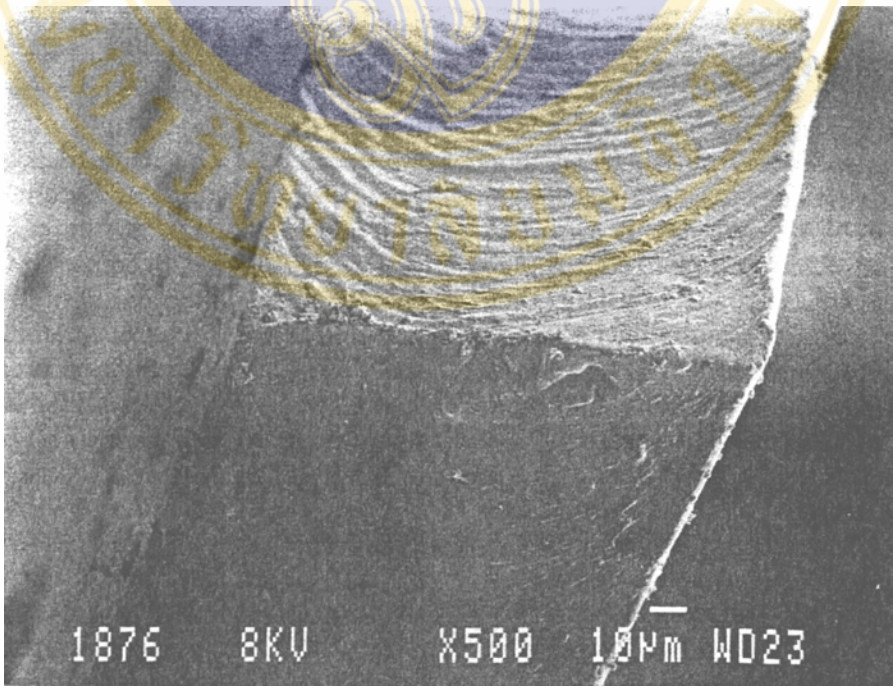

Figure 9 Section through aporous silicone membrane (Silastic 500-1, Dow Corning, USA) (28).

passage through the polymer (28).

a. Cellulose media

Cellulose is a relatively rigid structure consisting of glucopyranose rings joined by β-1,4-linkages. This conformation allows only two types of movement in the chains: inversion of the pyranose ring or rotation around the glycosidic linkage. In addition, the cellulose chains exist in a partially crystallized form due to interchain hydrogen bonding. Commercial cellulose membranes have a cut off of 8000-15000 daltons for molecular dialysis and on purchase normally contain a number of softener, preservative, and plasticizer additives which may affect drug permeation depending on the membrane pretreatment prior to experimentation. These plasticizer and preservative additives are usually ultraviolet radiation absorbing substances that may leach into the receptor chamber solution and interfere with the subsequent analysis procedure. The removal of these substances is therefore imperative and since they are mainly water soluble compounds. They may be removed by soaking the membrane in water, or as recommended by some manufacturers, boiling the membrane. Cellulose acetate (dialysis) media have been used extensively in diffusion cell systems, while cellulose nitrate has been used as a model for the gastric barrier. Generally, cellulose membranes are reported to be more permeable than biological membranes or aporous synthetic media and are nondiscriminatory to the characteristics of the diffusant molecule. These membranes have been used for quality control release studies (28).

b. Filter membranes

Porous filter membranes have seen relatively little usage in diffusion systems in comparison to the synthetic polymers. Preparation of this medium is fairly facile and only involves soaking the membrane in purified water at the temperature and for the time recommended by the manufacturer. Thereafter, the membrane should be rinsed with fresh water and blotted dry before use. The soaking procedure is conducted simply to maintain uniformity in membrane preparation as the filter material is reported to be non-hygroscopic and has a very low adsorptive potential. The degree of hydration which the medium undergoes during immersion is, therefore, thought to be minimal. Generally, porous filter media appear to be most useful as a support

medium where the release rate of drug from the delivery system is under investigation, and not the actual transdermal kinetics of the permeant. In these cases the filter medium does not simulate the skin and provides no significant barrier to diffusant passage (28).

c. Synthetic polymers

Diffusion of a molecule through continuous synthetic polymer is analogous in many ways to diffusion through unstirred liquids. Mass transfer through the matrix is dependent on the frequency of void formation of sufficient size to accommodate the diffusant. Voids are formed by the random oscillation of polymer chains and the larger the diffusant species the greater the number of neighboring polymer units which would have to move in a specific manner in order to generate a void of sufficient volume to accommodate the diffusant. The degree of bonding interaction between the polymer chains will determine the rigidity of the matrix and, thus, the propensity for hole formation and resultant permeability. Furthermore, crystallinity within the matrix generates regions of low diffusivity and the presence of solvents facilitates the oscillation of polymeric segments, both situations altering the overall permeability of the membrane.

Silicone polymers such as polydimethylsiloxane (Figure 9) have received attention because they are lipophilic in nature and highly permeable to many non-ionic drugs which dissolve in the barrier matrix and diffuse across it. Commercial products may contain additive filler, such as 20-30% silica or graphite, to improve the membrane strength and their presence may increase the barrier potential to permeation. This filler is randomly oriented, nonuniform in size and is impervious to permeants but readily enters into adsorption interactions. Permeation rates are, therefore, generally lower through filled media and lag time are increased. Generally, it can be concluded that these fillers simply reduce the volume of polymer which is available for the steady state passage of permeating molecules and makes their diffusive path longer and more tortuous. Silicone membranes without additives are currently available and their choice for diffusion cell research is obviously advantageous. Silicone membranes may be shipped from the manufacturer covered with a film of dusting powder, to facilitate handing and packing of the synthetic sheets,

which must be removed prior to use. Removal of water soluble powder is easily accomplished by rinsing with water. Therefore, the most important parameters with regard to permeation appear to be polymer chain mobility (rigidity) and the solubility of the diffusant in the matrix, which influences the partition coefficient. Generally, it is assumed that silicone membrane is the most useful of the synthetic media for use in diffusion cell systems. Its relatively inert, lipophilic nature makes it an ideal environment for partitioning and permeation of lipophilic drugs, while its aporosity provides some rate limiting function to this process (28).

6. Pharmacological and physicochemical properties of acyclovir

Acyclovir is a synthetic analogue of 2′-deoxiguanosine or purine nucleoside analog derived from quanine. The drug differs structurally from guanine by the presence of an acyclic side chain (Figure 10). Acyclovir, has molecular weight 225, occurs as a white, crystalline powder and has solubilities of 1.3 mg/mL in water at 25º C and 0.2 mg/mL in alcohol. The drug has pK_a of 2.27 and 9.25 and partition coefficient in octanol/0.2 M phosphate buffer of 0.018. The sodium salt (acyclovir sodium), which has a molecular weight of 247 and water solubility exceeding 100 mg/mL, is used for intravenous infusion. At physiological pH, acyclovir exists as the unionized form and maximum solubility of 2.5 mg/mL. Acyclovir is one of the most effective and selective agents against Herpes simplex virus type 1 and 2 (HSV-1 and HSV-2), Varicella zoster virus, and to lesser extent against Epstein-Barr virus and cytomegalovirus. According to histopathologic investigations, HSV-1 replication initially takes place in the cells of the basal layer of the epidermis and later extends to the rest of the epidermis. Therefore, the basal layer of the epidermis is considered to be the primary site of antiviral drug activity. Acyclovir is slowly and poorly absorbed from gastrointestinal tract. Only 13-21% of drug is absorbed and time to reach peak concentration is 1.5-2 hours. A number of researchers attempted to develop the drug delivery system for delivery acyclovir to the site of action via skin which thought that it may useful for treatment these skin diseases (4-7). Recently, there is a research group that developed novel method involving the use of transdermal drug delivery system (i.e., acyclovir transdermal patch) to describe quantitatively the relationship between the antiviral efficacy and the acyclovir skin flux. The results revealed that

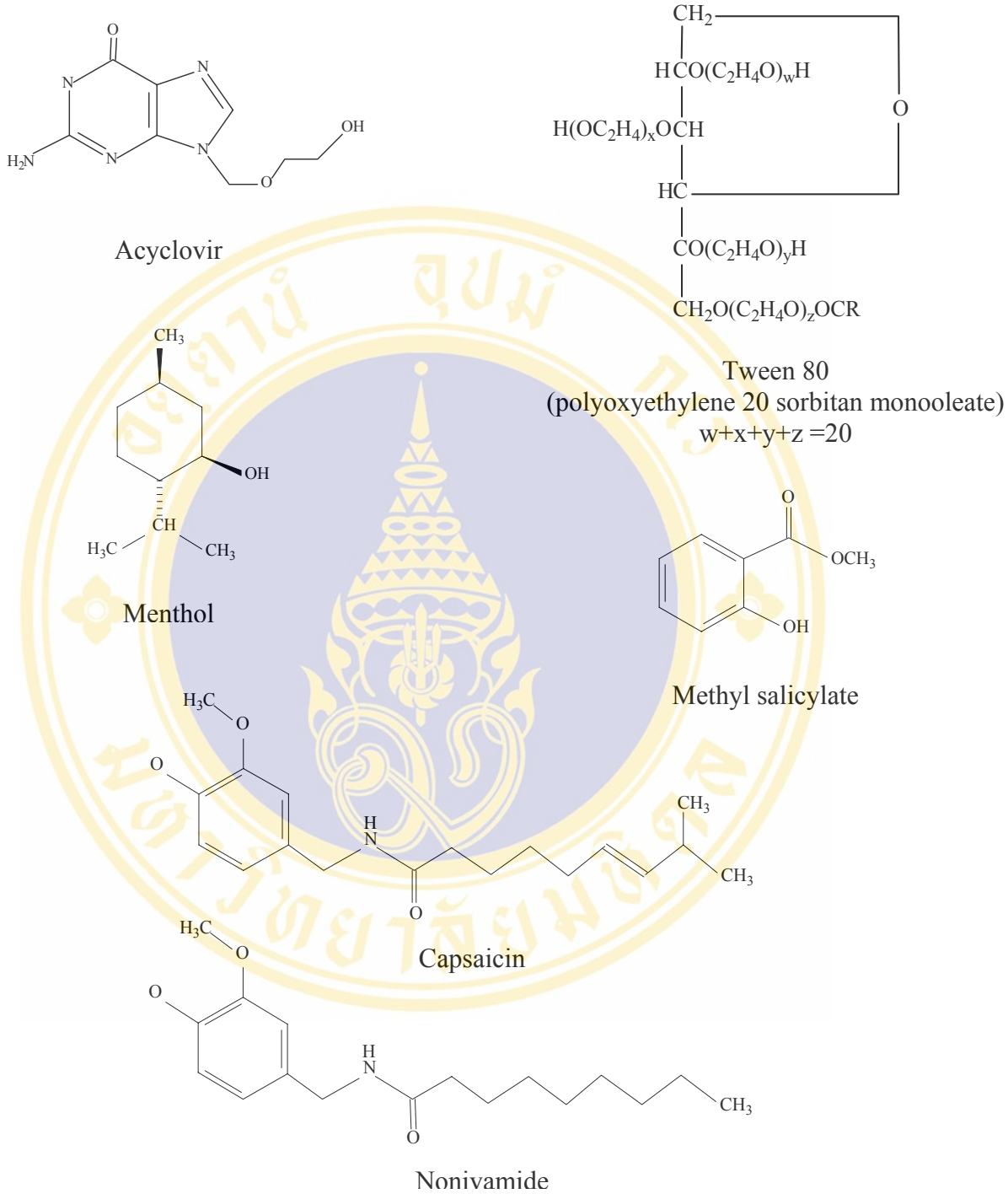

Figure 10 Chemical structure of acyclovir and five chemical enhancers that are tween 80, menthol, capsaicin, nonivamide, and methyl salicylate

this method can be used to evaluate the topical efficacy and systemic efficacy of the drug in hairless mice. Additionally, results showed that some acyclovir patch formulation can achieve 100% topical efficacy by using azone as skin permeation enhancer (7-11). Other research groups found synergic effect between chemical enhancers and vehicles to increase acyclovir permeation through skin, such as 5% oleic acid or oleyl alcohol in propylene glycol (36). Additionally, Okamoto H et al. observed maximal enhancing effect to acyclovir through rat skin by using the combination system of propylene glycol as vehicle and azone as enhancer, and they suggested that the combination of hydrophilic vehicle and hydrophobic enhancer resulted in a large enhancing effect (37). Other techniques were also used to increase skin permeation of acyclovir. For example, Volpato NM et al, (38,39) could observe the increasing permeation of acyclovir through nude mice skin by using iontophoresis technique. Jalón EG et al, (40) prepared topical acyclovir-loaded microparticle, they found higher accumulative drug concentration than acyclovir suspension (control) in the first layers of the porcine ear dermatomed skin, located of basal epidermis, after application of microparticles preparation for 88 hours.

7. Physicochemical and enhancing effect of some chemical enhancer

Using chemical enhancers is one of the most strategies to improve the skin drug permeation for formulating topical or transdermal delivery system. A number of sub-stances have been reported to be skin enhancer. Ideally, the goal of skin penetration enhancement is for the enhancer to reversibly reduce the barrier resistance of the stratum corneum without damaging viable cells, including nontoxic, nonirritant, no allergenic, and should be pharmacologically inert (41). The skin enhancing mechanism of reported enhancers are differently, Barry BW classified those skin enhancers into three groups that are lipid action, protein modification, and partition promotion. Lipid action group, these enhancers disrupt stratum corneum lipid organization, making it permeable. The essential action increases the drug's diffusion coefficient. The enhancer molecules jump into the bilayer, rotating, vibrating and translocating, forming microcavities, and increasing the free volume available for drug diffusion. Several enhancers operate mainly in this way, such as azone, terpenes, fatty acid, DMSO, and alcohols, etc. Protein modification group, these enhancers

interact well with keratin in corneocytes, opening up the dense protein structure, making it more permeable, thus, increasing drug's diffusion coefficient. Ionic surfactant, decylmethylsulphoxide, and DMSO are example for this enhancement group. Finally, partition promotion group, many solvents enter stratum corneum, change its solution properties by altering the chemical environment, and thus, increase partitioning of second molecule into the stratum corneum layer. Ethanol and propylene glycol, for example, were classified into this enhancement group (3)

7.1 Tween 80

Polysorbate 80 or tween 80 ($C_{64}H_{124}O_{26}$), molecular weight of 1310, is one of the group polysorbates that is a nonionic surfactant (Figure 10). It is prepared from sorbitol in a three step process. Water is initially removed from the sorbitol to form a sorbitan (a cyclic sorbitol anhydride). The sorbitan is then partially esterified with a fatty acid that is oleic acid, to yield a hexitan ester. Finally, ethylene oxide is then chemically added in the presence of a catalyst to yield the polysorbate. Tween 80 soluble in ethanol and water and insoluble in solvent mineral oil and vegetable oil. It has typical properties as following, hydrophilic-lipophilic balance (HLB) of 15.0, specific gravity at 25ºC of 1.08, viscosity of 425 mPa s, saponification value of 45-55, moisture content of 3.0%, acid value of 2.0, and hydroxyl value of 65-80. Tween 80 is stable to electrolytes and weak acids and bases, gradual saponification occur with strong acids and bases, and sensitive to oxidation. Discoloration or precipitation occurs with various substances, especially phenols, tannins, tars, or tar-like materials. The antimicrobial activity of paraben preservatives is reduced in the presence of polysorbates. Tween 80 is widely used in cosmetics, food products, and oral, parenteral and topical pharmaceutical formulations. It is generally regarded as nontoxic and nonirritant materials. However, there have been occasional reports of hypersensitivity to polysorbates following their topical use. Polysorbates have also been associated with serious adverse effects, including some deaths; in low-birthweight infants administered intravenously a vitamin E preparation containing a mixture of polysorbate 20 and 80. The WHO has set an estimated acceptable daily intake for polysorbates 20, 40, 60, 65, and 80 calculated as total polysorbate ester at up to 25 mg/kg body weight. Polysorbates are hydrophilic nonionic surfactants used widely as emulsifying

agents (1-15%) in the preparation of stable oil-in-water pharmaceutical emulsions. They may also be used as solubilizing agents (1-10%) for a variety of substances including essential oils and oil soluble vitamins, and as wetting agents (0.1-3%) in the formulation of oral and parenteral suspensions (26). From literature, there are reports the skin enhancing effect of tween 80 to some drug as showed in Table 3.

7.2 Menthol

Menthol ($C_{10}H_{20}O$), molecular weight 156.27 (Figure 10), occurs widely in nature as *l*-menthol and is the principal component of peppermint and cornmint oils obtained from the *Mentha piperita* and *Mentha arvensis* species. Commercially, *l*-menthol is mainly produced by extraction from these volatile oils. It may also be prepared by partial or total synthetic methods. Racemic menthol is prepared synthetically via a number of routes, such as, by hydrogenation of thymol. Typical properties of menthol, it is very soluble in 95% ethanol, chloroform, and ether, very slightly soluble in glycerin, and practically insoluble in water. It has melting point of 34-36ºC, boiling point of 212ºC. Appearance of *l*-menthol is colorless, primatic or acicular, shiny crystals, with a strong, characteristic odor, taste, and cooling effect. The crystalline form may change with time due to sublimation within a closed vessel. While, *d*-menthol has appearance as same as *l*-menthol, but it is without the characteristic odor, taste, and cooling effect. *l*-Menthol has melting point of 41-44ºC, flash point of >100ºC, and specific rotation of -50º (10%w/v alcoholic solution). For *d*-menthol has melting point of 43-44ºC, flash point of 91ºC, and specific rotation of +48º (10%w/v alcoholic solution). Menthol is incompatible with β-naphthol, butylchloral hydrate, camphor, chlorohydrate, chromium trioxide, phenol, potassium permanganate, pyrogallol, resorcinol, and thymol. Menthol is widely used in pharmaceutical confectionery and toiletry products as a flavoring agent or odor enhancer. In addition to its characteristic peppermint flavor, *l*-menthol, which occurs naturally, also exerts a cooling of refreshing sensation which is exploited in many topical preparations. Unlike mannitol which exerts a similar effect due to a negative heat of solution. *l*-Menthol interacts directly with the body's coldness receptors. *d*-Menthol has no cooling effect, while racemic menthol imparts an effect approximately

Table 3 The skin enhancing effect of tween 80

Drug	Composition		Barrier membrane	Diffusion cell type	Temp. (ºC)	Enhancing ratio	Ref.
	Donor compartment	Receptor compartment					
Lorazepam	Lorazepam 100mg Eudragit RL PM 900mg 2-Propanol 50mL Triethyl citrate 300mg Tween 80 1 or 5% Transdermal patch	Phosphate buffer pH 7.0	Hairless rat skin	Keshary-Chien type	37 ± 0.5	~2	(25)
Chloramphenicol	Chloramphenicol 1mg/mL Tween 80 0.2-1.0 % Ringer's solution NF	Ringer's solutioin NF	Hairless mouse skin	Vertical type	37	0.9-1.5	(42)
Hydrocortisone	Hydrocortisone 0.2% Tween 80 0.51% 2-Propanol 40% with/without hydroxyethylcellulose (gelling agent)	Normal saline solution containing 0.25% chlorobutanol	Albido mice skin	Vertical type	24.5 ± 0.1	1.8 (solution) 1.5 (gel)	(43)

half that of *l*-menthol. When used to flavor tablets menthol is generally dissolved in 95% ethanol and sprayed on tablet granules and not used as a solid excipient. Menthol is also used in perfumery, tobacco products and as a therapeutic agent (44). Beside that, a number of researchers have used menthol as chemical skin enhancer to many drugs as presented in Table 4.

7.3 Capsaicin and nonivamide

Capsaicin (trans-8-methyl-N-vanillyl-6-nonenamide) has an empirical formula of $C_{18}H_{27}NO_3$, a molecular weight of 305.4, and a chemical structure as shown in Figure 10. It is the primary pungent principle in the fruit of capsicum plants such as hot pepper. Capsaicin is a crystalline neutral principle, with melting point of 65ºC, and is practically insoluble in cold water, although it is freely soluble in ethanol, ether, benzene, or chloroform. Capsaicin produces a persistent burning of the tongue in a dilution of 1:100,000, whereas in a solution of 1:1,000,000 it imparts a sensation of warmth. As proved for over-the-counter (OTC) monograph use, capsicum oleoresin is a concentrate containing all of the active ingredients of capsicum extracts, including capsaicin. All of the identified actives are vanillylamides of fatty acids, of which five closely related primary pungent priciples have been identified as responsible for the overall pungent of the material. Capsaicin produces marked alterations in the function of a defined subpopulation of unmyelinated sensory afferents, termed C-poly-modal nociceptor. Following an initial period of intense irritation marked by localized erythema, stinging and burning, thermal and mechanical hyperalgesia, and generalized axon-reflex vasodilatation, topical capsaicin application renders human and other animals insensitive to further irritation by a variety of noxious chemical stimuli. The well-known ability of capsaicin to deplete neuropeptides, such as sub-stance P, from sensory nerve terminals in skin has served as the rationale for its use in the treatment of cutaneous pain states, such as postherpetic neuralgia (herpes zoster), postmastectomy pain syndrome, painful diabetic neuropathy, and vulvar vestibulitis. Likewise, following this reasoning, the dermatologic use of capsaicin for treatment of intractable pruritus associated with hemodialysis (49). Moreover, Degim et al. pointed out that the capsaicin has the enhancement effect for naproxen because of a similar chemical structure to azone which

Table 4 The skin enhancing effect of menthol

Drug	Composition		Barrier membrane	Diffusion cell type	Temp. (ºC)	Enhancing ratio	Ref.
	Donor compartment	Receptor compartment					
Ketoprofen	Ketoprofen 3% Menthol 1-10% Hydroxypropyl cellulose, propylene glycol, water	Phosphate buffer pH 7.4, 10% PEG 400	Rat skin	Vertical type	37 ± 0.5	39.7-61.3	(15)
Leuprolide acetate	Leuprolide acetate 40mg/mL Menthol 0.5-2% Klucel 2% Ethanol/water 4/1 v/v	PEG 400 40% 0.1M N-2-hydro- 60% xyethylpiperazine N'-2-ethanesulfonic acid	Nude mouse skin	Franz type	37	91-1522	(17)
Methyl paraben	Suspension of methyl paraben in 15% ethanol/water 1% *l*-Menthol	Phosphate buffer pH 7.4	Guinea pig skin	Side-by-side	37	~16	(20)
Testosterone	Eutectic mixture of menthol:testosterone (4:1) in 50% ethanol/water	50% ethanol/water	Nude mouse skin	Side-by-side	37	2.6	(21)

Table 4 (continued) The skin enhancing effect of menthol

Drug	Composition		Barrier membrane	Diffusion cell type	Temp. (ºC)	Enhancing ratio	Ref.
	Donor compartment	Receptor compartment					
S-Propanolol HCl (SPL) RS-propanolol HCl (RSPL)	S, RS-propanolol 10mg *l*-Menthol 20mg Propylene glycol	30% v/v PEG 400 in water	Guinea pig skin	Side-by-side	37	SPL 2.12 RSPL 0.85	(23)
Propanolol HCl	Propanolo HCl 0.01M *l*-Menthol 1-10% w/v 40% v/v ethanol/water	Distilled water	Hairless rat skin	Side-by-side	37	852-904	(22)
Morphine HCl	Morphone HCl 1% w/w *l*-Menthol 5% w/w in D_2O or 40% EtOD	Distilled water	Hairless rat skin	Side-by-side	37	30 (in D_2O) 145 (in 40%EtOD)	(18)
Tamoxifen	Tamoxifen 2.35×10^{-3} nmol/mL Menthol 5% 50% Ethanol/water	Phosphate buffer pH 7.4	Porcine ear epidermis	Franz type	37 ± 0.5	36.22	(24)

Table 4 (continued) The skin enhancing effect of menthol

Drug	Composition		Barrier membrane	Diffusion cell type	Temp. (ºC)	Enhancing ratio	Ref.
	Donor compartment	Receptor compartment					
Nicardipine HCl	Nicardipine HCl 1%w/w Menthol 1-12%w/w Hydroxypropylcellulose 2%w/w Ethanol 70%v/v	70% v/v ethanol/water	Albino rat skin	Keshary-Chien type	37 ± 0.5	2.30-7.01	(45)
Indomethacin (IM), Antipyrin (ANP)	Indomethacin 0.5% or Antipyrine 2% *l*-Menthol 3% 40% ethanol/water	Phosphate buffer pH 7.4	Yucatan micropig skin (full-thickness and epidermis)	Franz type	37	whole-skin 12.7, IM 11.5, ANP epidermis 11.5, IM	(46)
Insulin	**a.** Pretreatment with 500 µL of 5% Menthol in ethanol for 2 h **b.** Insulin 3mg/mL 500 µL	Phosphate buffer pH 7.4	Female Sprague-Dawley rat skin	Franz type	37 ± 0.2	2.6	(47)
Zidovudine	Zidovudine 50mg/mL Menthol 5%w/v 66.6% ethanol/water	Phosphate buffer pH 7.4 and 0.02%w/v sodium azide	Male Sprague-Dawley rat skin	Franz type	37 ± 0.5	53.0	(48)

is the chemical skin enhancer. Nonivamide is a synthetic analogue of capsaicin. The pharmacological and pungent profiles of nonivamide were found to be similar to those of capsaicin, and it has been used as a substitute for capsaicin in neuro-physiological studies. The skin enhancing effect of capsaicin and nonivamide is showed in table 5.

7.4 Methyl salicylate

Methyl salicylate (2-hydroxybenzoic acid methyl ester) has an empirical formula of $C_8H_8O_3$, a molecular weight of 152.15, and a chemical structure as shown in Figure 10. It occurs in leaves of *Gaultheria procumbens* L., *Ericaceae*, and in the bark of *Betula lenta* L., *Betulaceae*, but mostly prepared by esterification of salicylic acid with methanol. The product of commerce is about 99% pure. An appearance of methyl salicylate is colorless, yellowish or reddish, oily liquid, odor and taste of gaultheria. It has melting point of -8.6ºC, boiling point of 220-224ºC. It is slightly soluble in water, soluble in chloroform and ether, miscible with alcohol and glacial acetic acid. Methyl salicylate or namely oil of wintergreen is an active ingredient in various over-the-counter topical preparations (e.g., gels, creams, ointments, spray, lotions, and liniments) indicated for the relief of musculoskeletal pains and aches. The content of this drug in topical preparations are about <1 to 55%. Ingestion of relatively small amounts may cause severe poisoning and death (average lethal dose is 10 mL in children, and 30 mL in adults). Additionally, the medical literature has warned practitioners of the possible dangers of these topical preparations, including the potential for salicylate poisoning and the risk of excessive anticoagulation in patients taking warfarin (50,51). For skin enhancing effect of methyl salicylate, there is a report that revealed the skin enhancing effect to nanopeptide that is leuprolide as presented in table 6.

Table 5 The skin enhancing effect of capsaicin (CS) and nonivamide (NVA)

Drug	Composition		Barrier membrane	Diffusion cell type	Temp. (ºC)	Enhancing ratio	Ref.
	Donor compartment	Receptor compartment					
Indomethacin	**a.** Pretreatment with capsaicin or nonivamide 1-5% in 50%ethanol/warter for 2 h **b.** Indomethacin 1%w/v in 50% ethanol/pH 7.4 buffer	50% ethanol/pH 7.4 buffer	Female nude mouse skin	Franz type	37	1.16-2.23 (CS) 1.28-2.04 (NVA)	(16)
Naproxen	**a.** Pretreatment with 50µl/cm^2 of 3% capsaicin in ethanol for 2 h **b.** Suspension of naproxen in pH 5 buffer	Phosphate buffer pH 7.4	**a.** Female abdominal human skin **b.** Isolated perfuse rabbit ear (ex vivo)	Franz type	37	1.9 (*in vitro*) 3.8 (*ex vivo*)	(14)
Ketoprofen	Ketoprofen 3% Nonivamide 0.025-0.1% Hydroxypropyl cellulose, propylene glycol, water	Phosphate buffer pH 7.4, 10% PEG 400	Rat skin	Vertical type	37 $\pm$ 0.5	2.4-5.0	(15)
Nonivamide, sodium nonivamide acetate (SNA)	NVA:SNA 20-80% in buffer	50% ethanol/pH 7.4 buffer	Rat skin	Franz type	37 $\pm$ 0.5	Flux 9.23-17.97 µg/cm^2/h	(12)

Table 6 The skin enhancing effect of methyl salicylate

Drug	Composition		Barrier membrane	Diffusion cell type	Temp. (ºC)	Enhancing ratio	Ref.
	Donor compartment	Receptor compartment					
Leuprolide acetate	Leuprolide acetate 40mg/mL Methyl salicylate 2% Klucel 2% Ethanol/water 4/1 v/v	PEG 400 40% 0.1M N-2-hydro- 60% xyethylpiperazine N'-2- ethanesulfonic acid	Nude mouse skin	Franz type	37	65	(17)

CHAPTER 3
MATERIALS AND METHODS

Materials

1. Acyclovir (Lot number BL 0324MU3, Biolab, Thailand)
2. Chlorocresol (Lot number M6K 9159, Nacalai Tesque, Inc., Japan)
3. 4-Bromophenol (Lot number M6P 4398, Nacalai Tesque, Inc., Japan)
4. 4- Chlorophenol (Lot number FHE01, Nacalai Tesque, Inc., Japan)
5. 3,4-Xylenol (Lot number M6K 8477, Nacalai Tesque, Inc., Japan)
6. 4-Methylacetophenone (Lot number M6A 9201,Nacalai Tesque, Inc., Japan)
7. Acetophenone (Batch number 340647/1 1194, Fluka, Switzerland)
8. Nitrobenzene (Lot number 22812, May & Baker Ltd., England)
9. Phenol (Lot number 8F248288H, Carlo Erba Reagenti, Italy)
10. Glycerine USP
11. Di-sodium hydrogen phosphate anhydrous (Lot number A791086, Merck, Germany)
12. Sodium dihydrogen orthophosphate (Batch number Z9G017A, APS Finechem, Australia)
13. Sodium chloride (Lot number 01262281B, Carlo Erba Reagenti, Italy)
14. Capsaicin >60% (Lot number GI 01, Tokyo Kasei Kogyo Co., Ltd., Japan)
15. Nonivamide (Lot number GG02, Tokyo Kasei Kogyo Co., Ltd., Japan)
16. *l*-Menthol (Lot number F37727, J.T. Baker Inc., USA)
17. Tween 80 (Lot number 1147A, S. Tong Chemical Co., Ltd., Thailand)
18. Methyl salicylate (Lot number 2001010237, S. Tong Chemical Co., Ltd., Thailand)

Equipment

1. Side-by-side diffusion cells (Japan)
2. Magnetic stirrer (Multistirrer™ MS-101, Iuchi, Japan)

3. Magnetic controller (Multistirrer™ M-1, Iuchi, Japan)
4. UV-spectrophotometer (Model S1000, Secomam, France)
5. UV-spectrophotometer (Model Lambda 35, Perkin Elmer, USA)
6. Precision electronic balance (Model AA-200 DC, Denver Instrument, USA)
7. Water bath with thermostat (Type W760, Memmert, Germany)
8. Centrifuge (Model Universal 30F, Hettich, Germany)
9. pH meter (Model CG842/14 pH, Scott, Germany)
10. Ultrasonic bath (Tru-Sweeper™ Model 950 D, New York, USA)

Methods

1. Calibration curve for determination of model solutes

Calibration curve of nine model solutes (i.e., acyclovir, acetophenone, 4-methyl-acetophenone, phenol, 4-bromophenol, 4-chlorophenol, nitrobenzene, 3,4-xylenol, and chlorocresol) in Sörensen modified phosphate buffer pH 7.4 (SMPB pH 7.4) (52) and calibration curve of acyclovir in 50% v/v ethanol/water were prepared. Each calibration curve was performed by dissolving the accurately weighed solute in medium solution and then adjusting to volume in volumetric flask. This solution was subsequently used as stock solution. Stock solution of each solute was accurately pipetted and adjusted to volume with medium solution in each volumetric flask to obtain serial solute concentrations. The UV-spectrophotometer was used to determine the absorbance of model solutes at the maximum wavelength of each solute. For all cases, triplicate sample were run.

2. Solubility of model solutes

The solubility of model solutes in Sörensen modified phosphate buffer pH 7.4 were determined by dissolving excess solute in Sörensen modified phosphate buffer pH 7.4 in glass tube with plastic screw cap. Each tube was shaken in water bath at 37$\pm$1ºC until equilibrium was obtained. Amount of dissolved solute was determined by UV-spectrophotometry technique. For all cases, triplicate sample were run.

3. Preparation of barrier membrane

3.1 Human epidermis

The breast skin of Thai female aged between 35-70 years was obtained from the National Cancer Institute, within a few hours after operation. The human epidermis is taken after the whole skin has been soaked in water at 60ºC for 2 minutes (1,28, 29). The human epidermis wrapped in aluminum foil was put in a plastic bag and then stored at –20ºC until use. Prior to use, the human epidermis was hydrated by immerging in Sörensen modified phosphate buffer pH 7.4, for 30 minutes (1,28,29).

3.2 Egg shell membrane

A whole duck egg was soaked in 0.5 N HCL solution. The outer calcareous shell was dissolved, then a part of the egg shell membrane was cut off and the inner contents were removed. The egg shell membrane, thoroughly washed in distilled water, was stored in a plastic bag and kept for no more than one week in a refrigerator until use (30).

3.3 Full-thickness rat skin

After anesthetizing the Wistar male and female rats, weighing about 200-500 grams, the abdominal hair of rat was removed using hand razors. The abdominal skin was surgically separated from the animal, and adhering subcutaneous fat was then carefully cleaned. Full-thickness abdominal rat skin was subsequently used in the study.

4. Permeability of barrier membranes to model solutes

The permeation studies of nine model solutes (i.e., acyclovir, acetophenone, 4-methylacetophenone, phenol, 4-bromophenol, 4-chlorophenol, nitrobenzene, 3,4-xylenol and chlorocresol) through barrier membrane were measured using the side-by-side diffusion cell (Figure 11). The barrier membranes used were human epidermis, full-thickness rat skin, and egg shell membrane. The exposed area of membrane was 0.89 cm^2. The rat skin and human skin was set in place with the stratum corneum facing the donor compartment and opposite side facing the receptor compartment. For egg

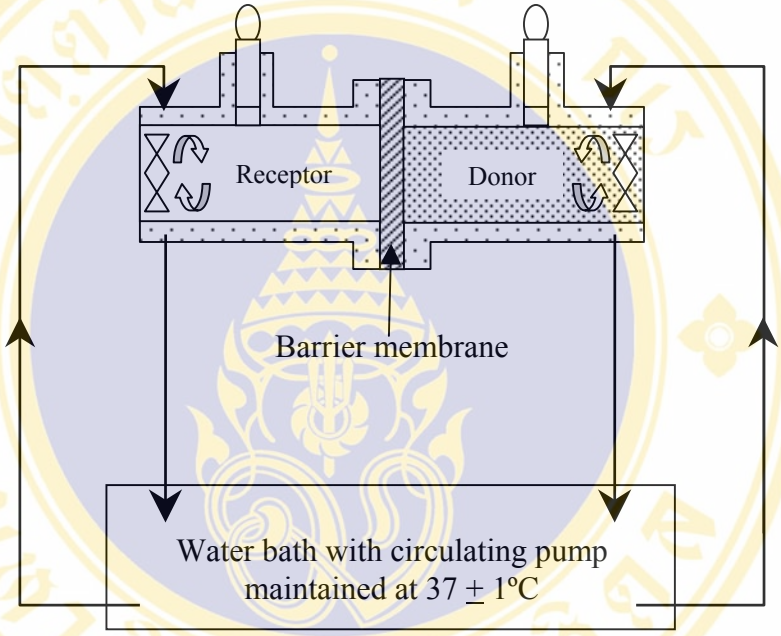

.

Figure 11 Scheme of permeation experiment using side-by-side diffusion cell.

shell membrane, the membrane was set in place with the outer side facing the donor compartment and inner side facing the receptor compartment. The donor compartment was filled with 2.5 mL solution of excess solute to reserve the saturated solution throughout experimental period, and the receptor compartment was filled with 2.5 mL Sörensen modified phosphate buffer pH 7.4. During the experiments, the solution in both diffusion compartments was maintained at 37 $\pm$ 1ºC by circulating the water from water bath with thermostat through diffusion jacket and stirred with teflon-coated magnetic stirrer bars. At designated time intervals, 500 µL aliquots were collected from the receptor compartment and 500 µL of Sörensen modified phosphate buffer pH 7.4 was added into the receptor compartment immediately after each sample collection. The sample solution was diluted and an absorbance at maximum wavelength of each solute was measured. Flux, permeability coefficient, and lag time of each solute was calculated form the plot of cumulative amount of solute per unit area of permeation against time when the steady state was obtained. These permeation parameters were calculated by following Fick's first law (2,53).

The steady state flux:

$$\text{Flux} = \text{Slope of the plot at linear portion} \quad (8)$$

Permeability coefficient (k_p) (cm/min):

$$k_p = \frac{\text{Flux}}{C_0} \quad (9)$$

where C_0 = the solubility of solute in the donor solution

Lag time:

$$\text{Lag time} = \text{Extrapolation of the linear portion to the time axis} \quad (10)$$

5. Effect of treatment and storage conditions on barrier functions of rat skin

Effect of treatment and storage conditions on barrier functions of rat skin was studied by using four different conditions. The rat skin was prepared by using the method described previously (section 3.3). For the first group (control), the skin pretreated with Sörensen modified phosphate buffer pH 7.4 was stored in a plastic bag and kept in refrigerator overnight before use. For the other three groups, the skin pretreated with Sörensen modified phosphate buffer pH 7.4, 0.9%w/v normal saline, or 10%v/v glycerine respectively, was stored in a plastic bag and kept at -20ºC for 13-15 days before use. Prior to use, the rat skin was hydrated by immerging in Sörensen modified phosphate buffer pH 7.4, for 30 minutes. The permeation experiment was the same as that described above. The model solutes chosen for these experiments were acetophenone and acyclovir.

6. Effect of enhancers and vehicles on percutaneous absorption of acyclovir

Effect of enhancers and vehicles on percutaneous absorption of acyclovir was studied by varying type and concentration of enhancers and vehicles. These permeation experiments were performed by using human epidermis as barrier membrane. Type and concentrations of enhancers were listed in Table 7. Donor compartment was filled with 2.5 mL of 0.1%w/v acyclovir Sörensen modified phosphate buffer pH 7.4 or 50%v/v ethanol/water with or without enhancer. Receptor compartment was filled with 2.5 mL Sörensen modified phosphate buffer pH 7.4. Other conditions of permeation experiment were the same as that described above.

Table 7 Chemical enhancers and its concentration used in percutaneous absorption study of acyclovir.

Enhancer	Concentration (%w/v)
Capsaicin	0.075
Nonivamide	0.075
l-Menthol	4
Methyl salicylate	4
Tween 80	10

CHAPTER 4
RESULTS AND DISCUSSION

1. Calibration curve for determination of model solutes

The UV-spectrophotometric procedure was employed for determination of all model solutes concentration (i.e., acyclovir, acetophenone, 4-methylacetophenone, phenol, 4-bromophenol, 4-chlorophenol, nitrobenzene, 3,4-xylenol and chlorocresol). The calibration curve of each model solutes in Sörensen modified phosphate buffer pH 7.4 and calibration curve of acyclovir in 50% v/v ethanol/water at the maximum wavelength are shown in Tables 8-17 and Figures 12-21, respectively.

2. Solubility of model solutes

The solubility of each model solute was determined when the equilibrium was obtained. It was found that the time (72 hours) was sufficient for equilibration of all solutes. Table 18 shows the solubility of each model solutes in Sörensen modified phosphate buffer pH 7.4 at 37 $\pm$ 1ºC.

3. Permeability of barrier membranes to model solutes

The cumulative amount per unit area of nine model solutes permeated through each biological membrane (i.e., human epidermis, full-thickness rat skin, and egg shell membrane) during 6 hours at 37 $\pm$ 1ºC are shown in Tables 19-21 and Figures 22-24, respectively. The model solutes used herein were also used in permeation studies carried out by other researchers (54,55). Preliminary study has been carried out in order to confirm that the solute concentration in the receptor was less than saturated solubility value of the solute in Sörensen modified phosphate buffer pH 7.4 system. The calculation of flux, permeability coefficient, and lag time values of all model solutes in this experiment are presented in Tables 22-24. It was assumed that, for all membranes, the steady state flux and permeability coefficient values could be obtained within 6 hours (30,38,54,56). The lag time of all model solutes showed that

Table 8 Calibration curve of acyclovir in Sörensen modified phosphate buffer pH 7.4 at λ_{max} 251 nm

Concentraion (µg/mL)	Absorbance (n=3)
4.03	0.244 ± 0.003
6.04	0.369 ± 0.006
8.06	0.493 ± 0.009
10.07	0.623 ± 0.012
12.09	0.746 ± 0.012

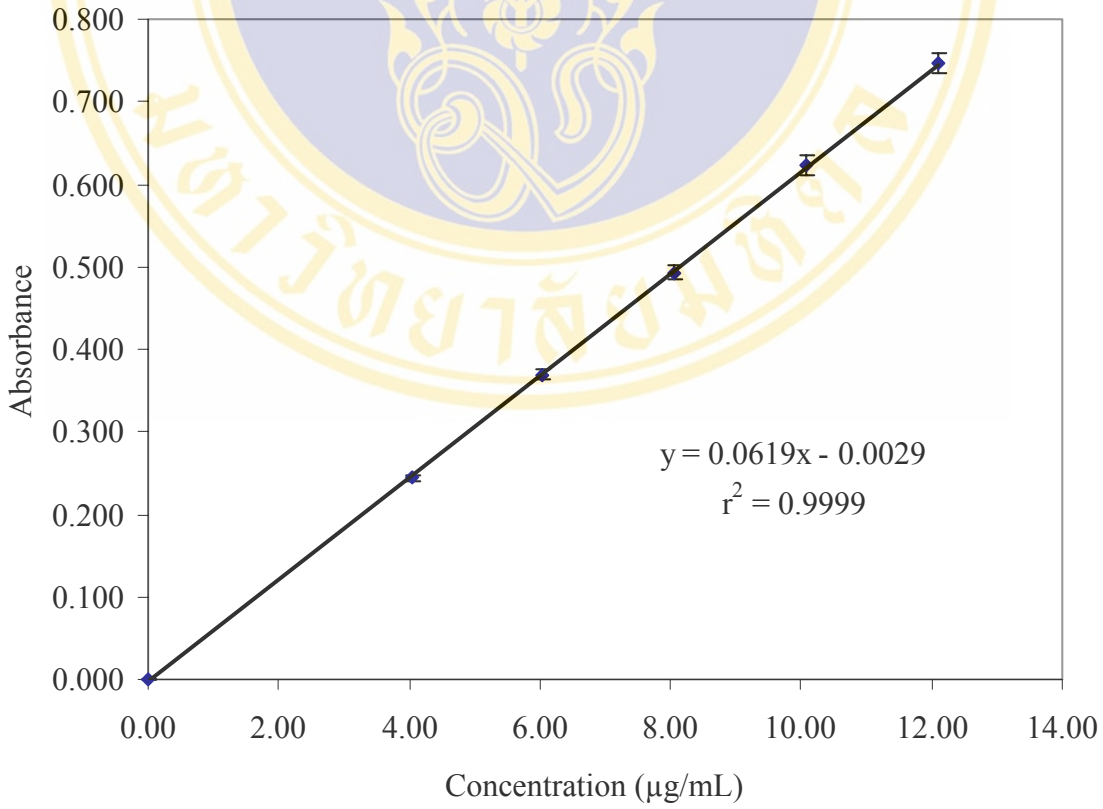

Figure 12 Calibration curve of acyclovir in Sörensen modified phosphate buffer pH 7.4 at λ_{max} 251 nm (n=3)

Table 9 Calibration curve of acyclovir in 50%v/v ethanol in water at λ_{max} 251 nm

Concentraion (µg/mL)	Absorbance (n=3)
4.03	0.259 ± 0.005
6.05	0.379 ± 0.007
8.06	0.505 ± 0.007
10.08	0.626 ± 0.014
12.09	0.743 ± 0.008

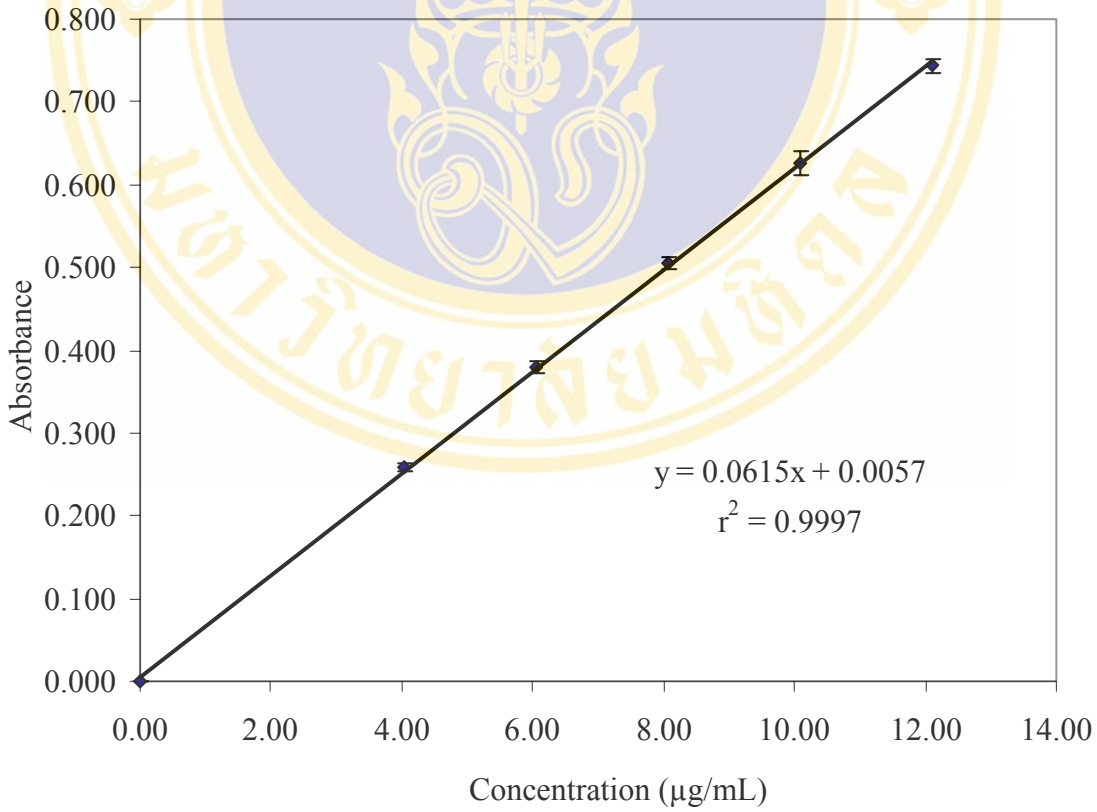

Figure 13 Calibration curve of acyclovir in 50%v/v ethanol in water at λ_{max} 251 nm (n=3)

Table 10 Calibration curve of acetophenone in Sörensen modified phosphate buffer pH 7.4 at λ_{max} 245 nm

Concentraion (µg/mL)	Absorbance (n=3)
2.02	0.200 ± 0.007
4.04	0.410 ± 0.015
5.05	0.515 ± 0.010
6.06	0.617 ± 0.012
8.08	0.820 ± 0.011

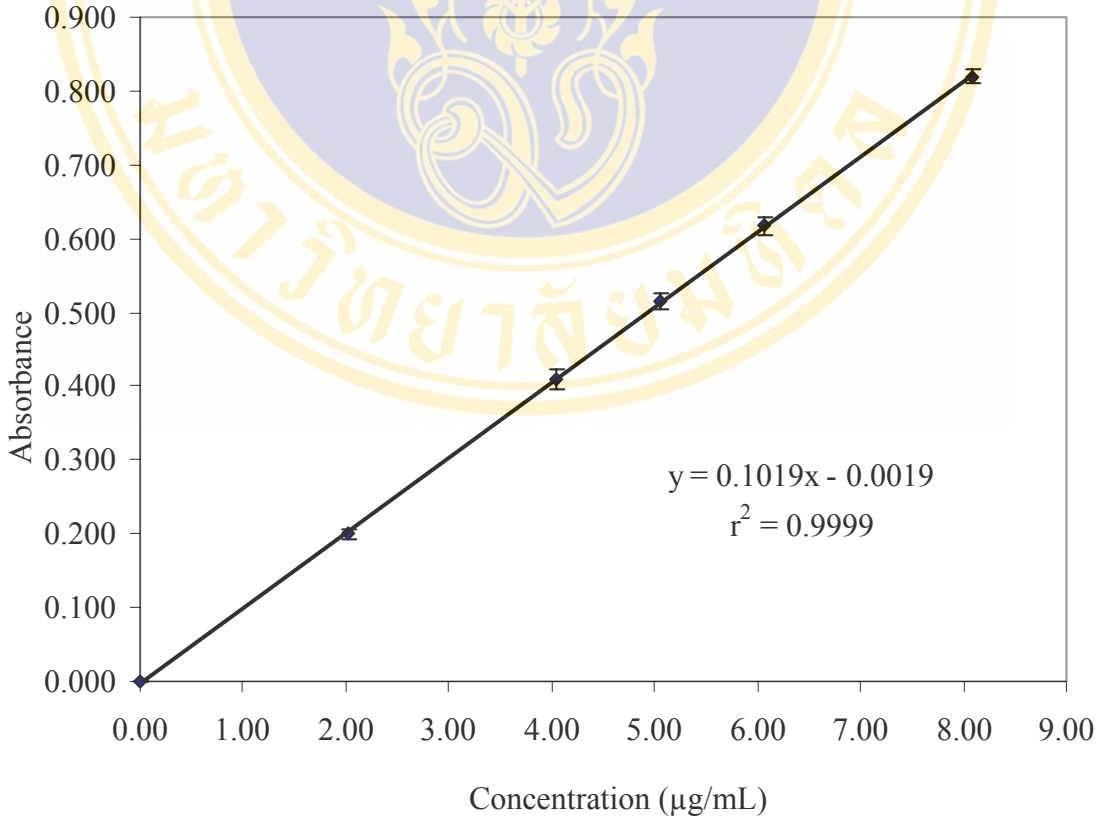

Figure 14 Calibration curve of acetophenone in Sörensen modified phosphate buffer pH 7.4 at λ_{max} 245 nm (n=3)

Table 11 Calibration curve of 4-methylacetophenone in Sörensen modified phosphate buffer pH 7.4 at λ_{max} 256 nm

Concentraion (µg/mL)	Absorbance (n=3)
2.13	0.205 ± 0.010
3.19	0.320 ± 0.010
4.26	0.438 ± 0.002
5.32	0.550 ± 0.007
6.38	0.671 ± 0.008

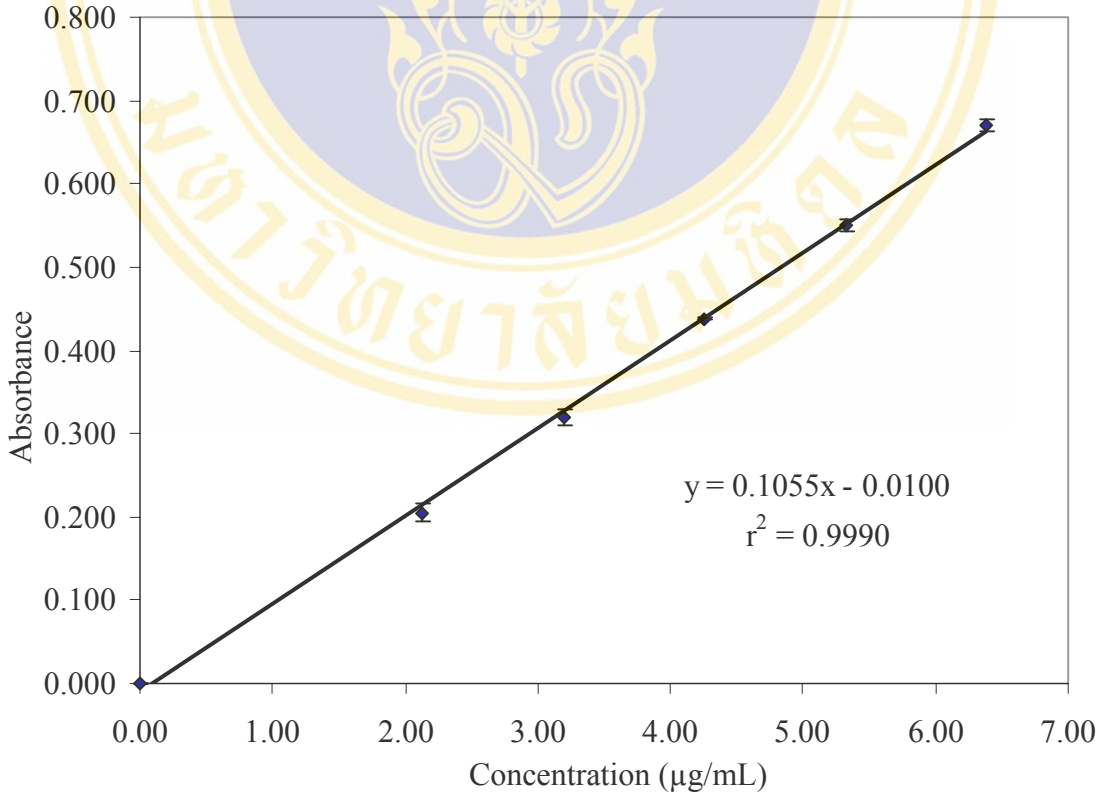

Figure 15 Calibration curve of 4-methylacetophenone in Sörensen modified phosphate buffer pH 7.4 at λ_{max} 256 nm (n=3)

Table 12 Calibration curve of phenol in Sörensen modified phosphate buffer pH 7.4 at λ_{max} 269 nm

Concentraion (µg/mL)	Absorbance (n=3)
15.97	0.237 ± 0.006
21.29	0.320 ± 0.010
26.62	0.405 ± 0.009
31.94	0.491 ± 0.011
37.26	0.579 ± 0.014
42.59	0.656 ± 0.020

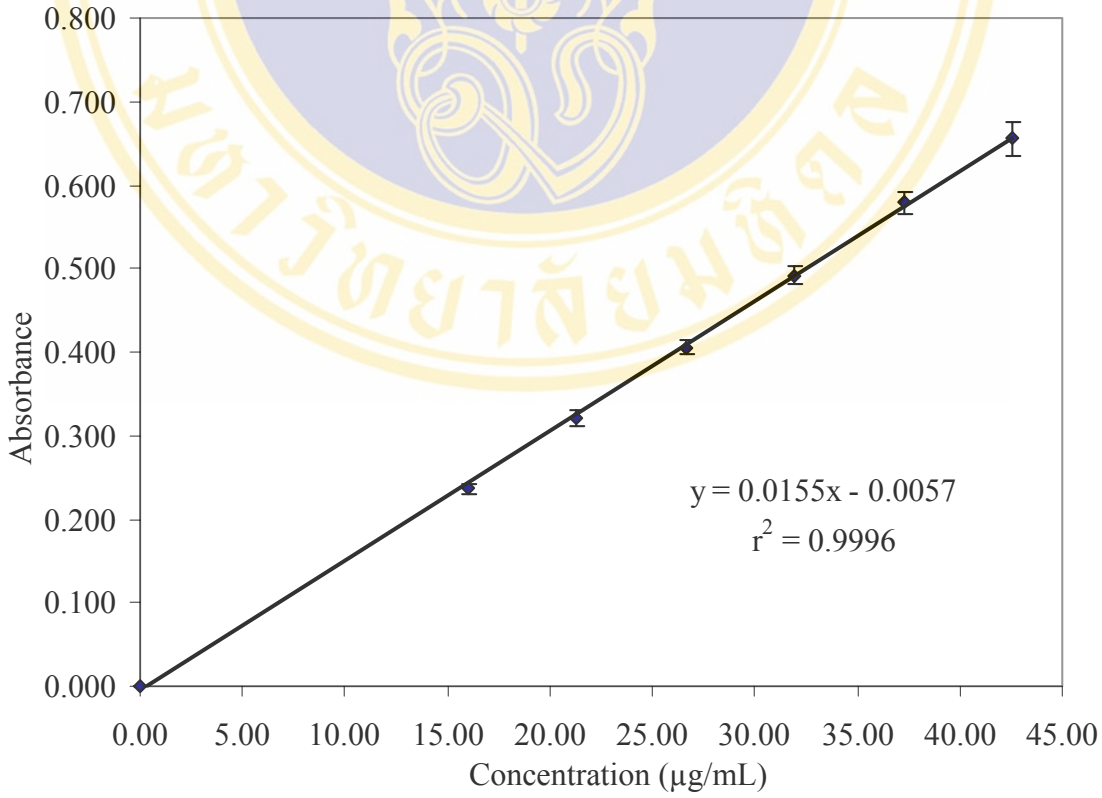

Figure 16 Calibration curve of phenol in Sörensen modified phosphate buffer pH 7.4 at λ_{max} 269 nm (n=3)

Table 13 Calibration curve of 4-bromophenol in Sörensen modified phosphate buffer pH 7.4 at λ_{max} 279 nm

Concentraion (µg/mL)	Absorbance (n=3)
16.20	0.129 ± 0.004
32.40	0.254 ± 0.010
48.60	0.388 ± 0.012
64.80	0.517 ± 0.014
81.00	0.647 ± 0.023
97.20	0.771 ± 0.034

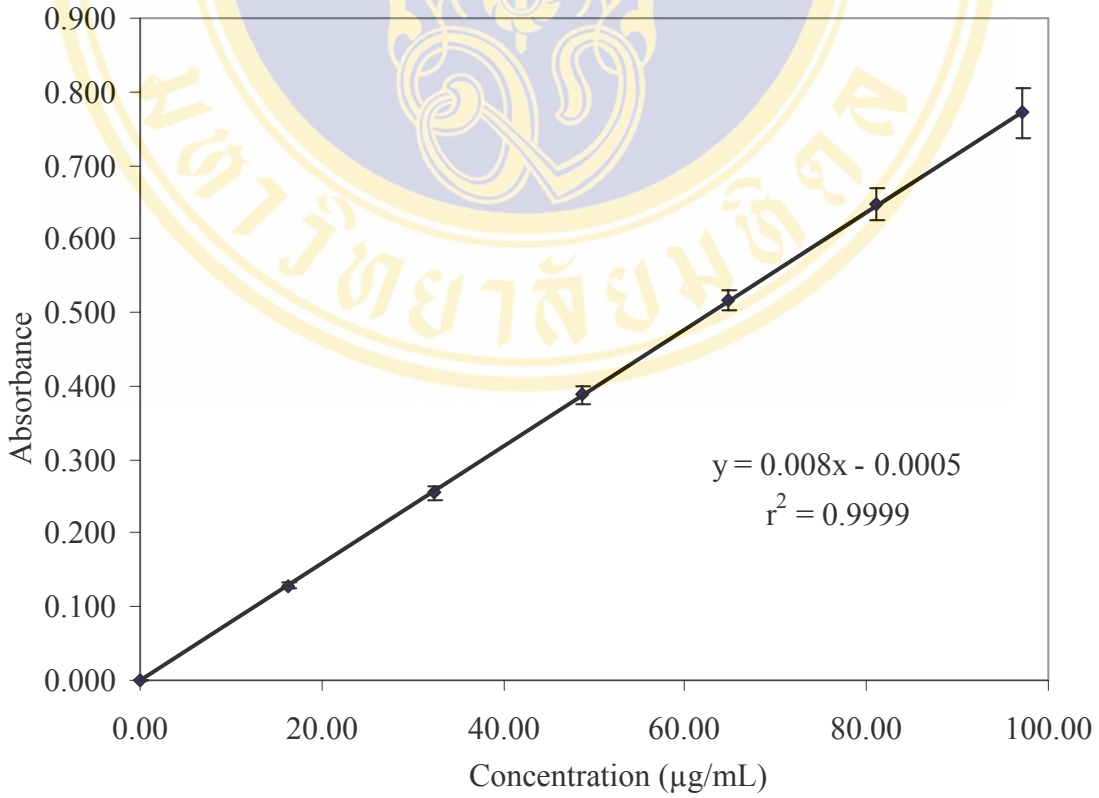

Figure 17 Calibration curve of 4-bromophenol in Sörensen modified phosphate buffer pH 7.4 at λ_{max} 279 nm (n=3)

Table 14 Calibration curve of 4-chlorophenol in Sörensen modified phosphate buffer pH 7.4 at λ_{max} 279 nm

Concentraion (µg/mL)	Absorbance (n=3)
20.82	0.237 ± 0.004
31.23	0.363 ± 0.004
41.64	0.488 ± 0.004
52.05	0.614 ± 0.006
62.46	0.732 ± 0.006

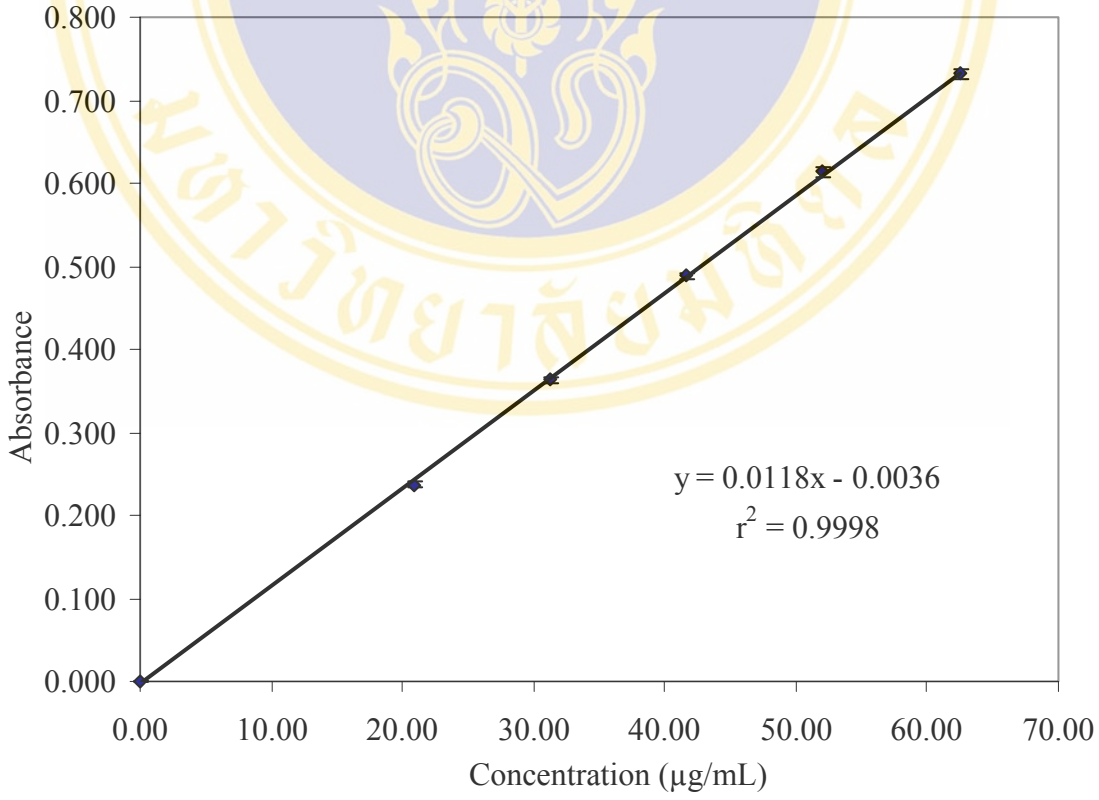

Figure 18 Calibration curve of 4-chlorophenol in Sörensen modified phosphate buffer pH 7.4 at λ_{max} 279 nm (n=3)

Table 15 Calibration curve of nitrobenzene in Sörensen modified phosphate buffer pH 7.4 at λ_{max} 267 nm

Concentraion (µg/mL)	Absorbance (n=3)
4.11	0.260 ± 0.002
6.17	0.393 ± 0.006
8.22	0.525 ± 0.011
10.28	0.659 ± 0.019
12.34	0.789 ± 0.013

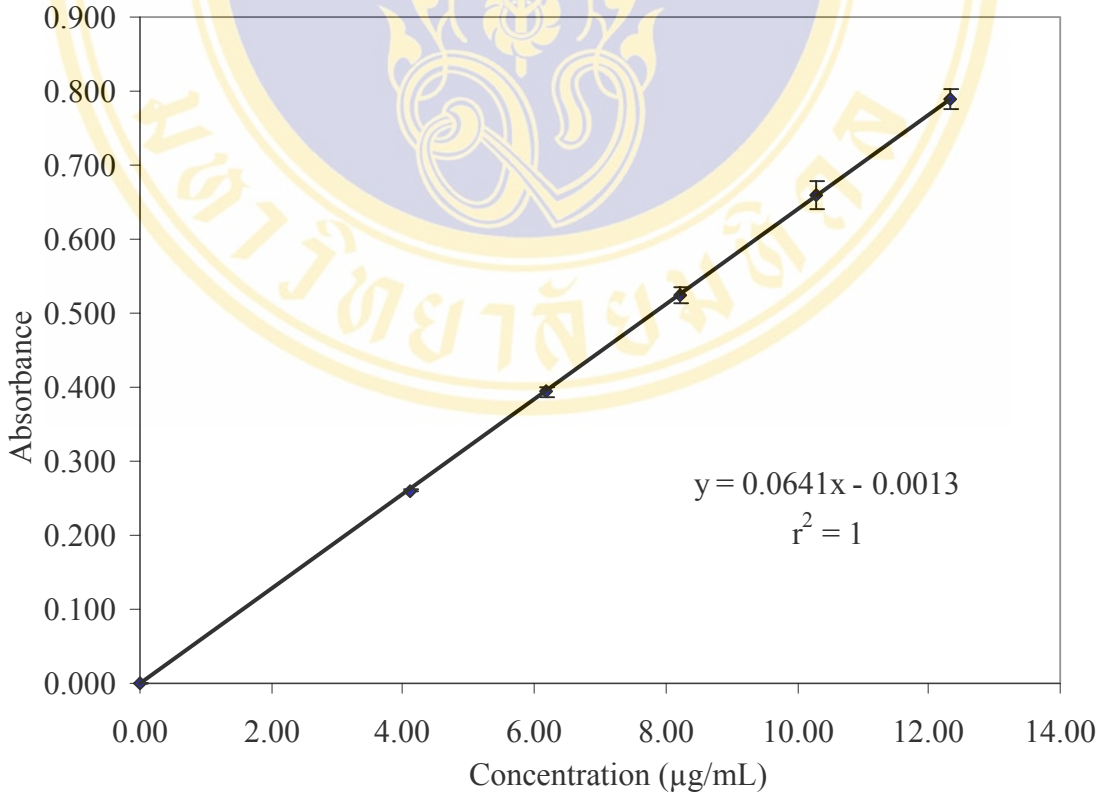

Figure 19 Calibration curve of nitrobenzene in Sörensen modified phosphate buffer pH 7.4 at λ_{max} 267 nm (n=3)

Table 16 Calibration curve of 3,4-xylenol in Sörensen modified phosphate buffer pH 7.4 at λ_{max} 276 nm

Concentraion (µg/mL)	Absorbance (n=3)
10.65	0.161 ± 0.007
21.29	0.319 ± 0.013
31.94	0.477 ± 0.015
42.59	0.634 ± 0.022
53.23	0.794 ± 0.024

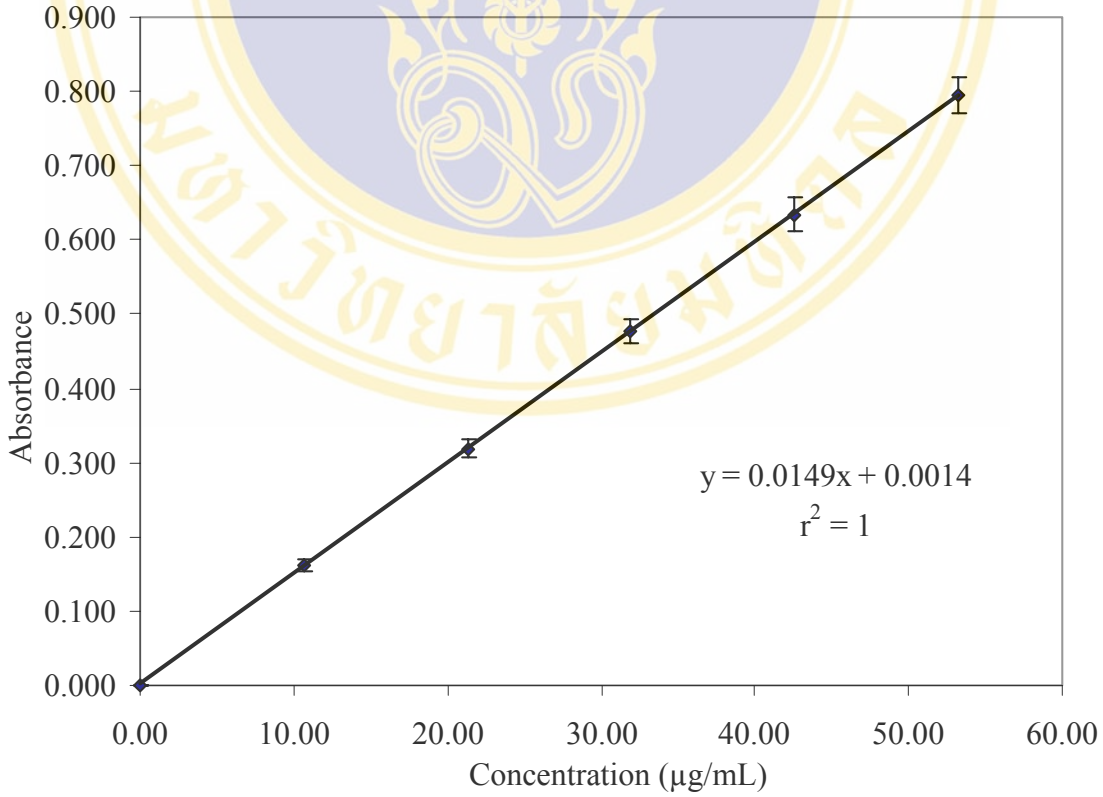

Figure 20 Calibration curve of 3,4-xylenol in Sörensen modified phosphate buffer pH 7.4 at λ_{max} 276 nm (n=3)

Table 17 Calibration curve of chlorocresol in Sörensen modified phosphate buffer pH 7.4 at λ_{max} 225 nm

Concentraion (µg/mL)	Absorbance (n=3)
4.11	0.205 ± 0.015
6.17	0.314 ± 0.006
8.22	0.419 ± 0.014
10.28	0.525 ± 0.021
12.33	0.633 ± 0.016
14.39	0.749 ± 0.025

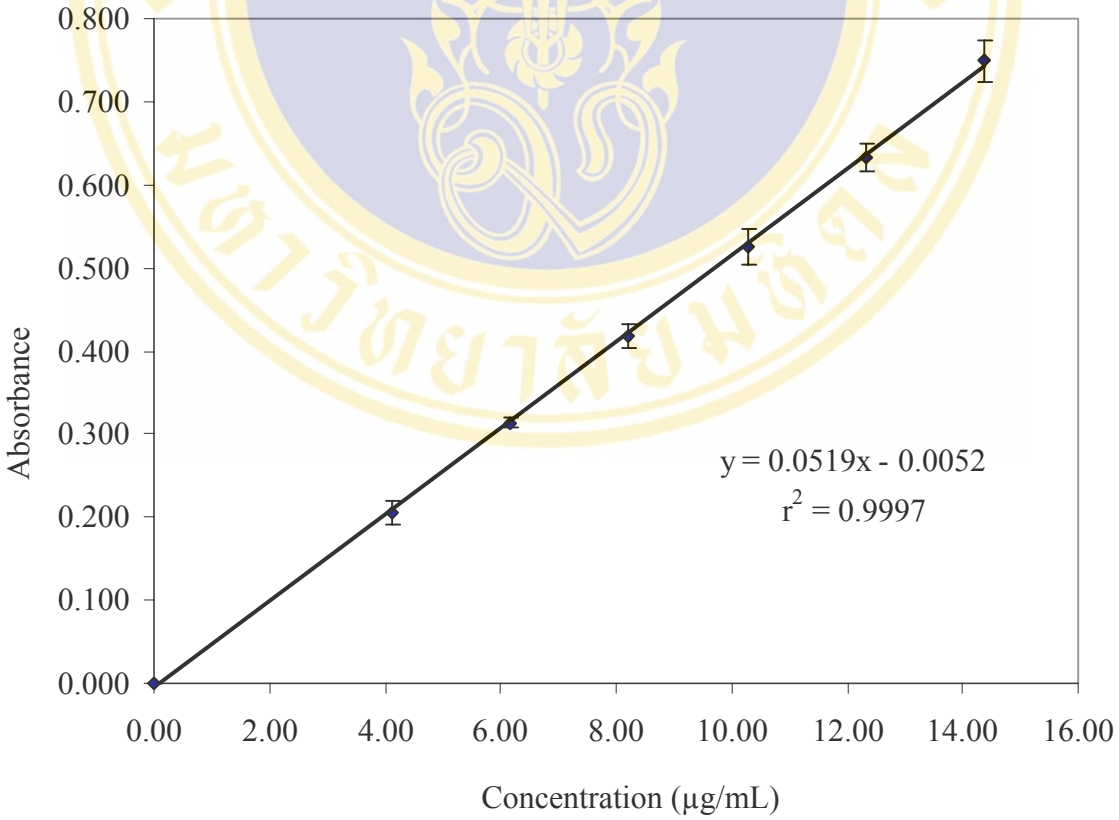

Figure 21 Calibration curve of chlorocresol in Sörensen modified phosphate buffer pH 7.4 at λ_{max} 225 nm (n=3)

Table 18 Solubilities of model solutes in Sörensen modified phosphate buffer pH 7.4 at 37 ± 1ºC

Solute	Solubility (%w/v)			
	Sample 1	Sample 2	Sample 3	Average ± S.D.
Acyclovir	0.26	0.24	0.26	0.25 ± 0.01
Acetophenone	0.51	0.53	0.53	0.52 ± 0.01
4-Methylacetophenone	0.19	0.20	0.19	0.19 ± 0.00
Phenol	7.52	7.47	7.43	7.47 ± 0.05
4-Bromophenol	0.25	0.25	0.25	0.25 ± 0.00
4-Chlorophenol	0.56	0.55	0.54	0.55 ± 0.01
Nitrobenzene	0.18	0.18	0.18	0.18 ± 0.00
3,4-Xylenol	0.54	0.55	0.58	0.55 ± 0.02
Chlorocresol	0.54	0.52	0.52	0.53 ± 0.01

Table 19 Cumulative amount per unit area of model solutes permeated through human epidermis for 6 hours at 37 ± 1ºC

Time	Cumulative amount of solute (μg/cm^2) [a]		
(min)	Acyclovir	Acetophenone	4-Methylacetophenone
0	0.00 ± 0.00	0.00 ± 0.00	0.00 ± 0.00
15	1.14 ± 1.44	183.46 ± 65.18	127.07 ± 16.87
30	1.23 ± 1.50	361.14 ± 115.21	242.19 ± 21.88
45	1.02 ± 1.30	532.44 ± 137.56	378.60 ± 37.22
60	0.95 ± 1.43	692.44 ± 191.88	515.84 ± 64.09
75	0.83 ± 1.19	845.83 ± 233.32	640.91 ± 86.56
90	0.87 ± 1.27	1,001.95 ± 279.01	766.05 ± 120.42
105	0.71 ± 0.97	1,153.72 ± 326.36	893.51 ± 168.29
120	0.71 ± 0.97	1,325.19 ± 358.76	1,008.98 ± 189.52
135	0.71 ± 0.97	1,508.41 ± 352.26	1,132.30 ± 227.28
150	0.71 ± 0.97	1,663.99 ± 388.84	1,241.53 ± 254.23
165	0.71 ± 0.97	1,810.60 ± 446.55	1,362.10 ± 289.73
180	0.71 ± 0.97	2,022.56 ± 397.59	1,476.86 ± 320.56
210	0.71 ± 0.97	2,292.17 ± 449.51	1,698.71 ± 387.61
240	0.71 ± 0.97	2,614.88 ± 514.80	1,915.10 ± 452.63
270	0.71 ± 0.97	2,941.91 ± 582.22	2,131.23 ± 535.39
300	0.71 ± 0.97	3,247.59 ± 600.04	2,343.06 ± 605.39
330	1.11 ± 0.91	3,545.74 ± 679.65	2,554.69 ± 687.71
360	0.79 ± 0.90	3,833.50 ± 726.64	2,792.78 ± 755.26

[a] the values shown are mean ± S.D. from 4 experiments

Table 19 (continued) Cumulative amount per unit area of model solutes permeated through human epidermis for 6 hours at 37 ± 1ºC

Time	Cumulative amount of solute (μg/cm^2) [a]		
(min)	Phenol	4-Bromophenol	4-Chlorophenol
0	0.00 ± 0.00	0.00 ± 0.00	0.00 ± 0.00
15	20,711.92 ± 4,138.81	549.86 ± 321.81	1,596.48 ± 374.85
30	38,333.16 ± 7,552.30	1,085.93 ± 590.97	3,057.61 ± 713.38
45	57,022.57 ± 13,336.07	1,628.43 ± 832.15	4,639.74 ± 787.93
60	75,440.85 ± 18,744.79	2,162.59 ± 1,056.49	6,178.19 ± 795.59
75	94,290.39 ± 24,487.31	2,640.91 ± 1,207.04	7,671.93 ± 896.57
90	112,855.16 ± 28,502.71	3,162.48 ± 1,427.49	9,083.96 ± 985.10
105	131,891.40 ± 31,548.87	3,651.98 ± 1,611.67	10,424.81 ± 1,031.91
120	151,861.49 ± 35,898.07	4,167.78 ± 1,802.15	11,686.62 ± 1,182.50
135	170,213.57 ± 38,714.25	4,650.61 ± 1,949.12	12,958.84 ± 1,272.04
150	188,710.81 ± 42,491.27	5,137.46 ± 2,099.39	14,169.30 ± 1,391.94
165	208,309.91 ± 44,622.31	5,671.37 ± 2,267.84	15,429.54 ± 1,409.56
180	229,354.31 ± 46,021.61	6,190.06 ± 2,440.21	16,667.95 ± 1,477.91
210	265,773.31 ± 50,999.79	7,073.43 ± 2,735.04	18,780.01 ± 1,539.36
240	297,406.18 ± 54,036.92	7,974.86 ± 2,944.32	20,693.80 ± 1,758.20
270	331,376.54 ± 58,469.54	8,800.85 ± 3,165.69	22,459.95 ± 1,923.15
300	361,377.74 ± 57,869.97	9,606.21 ± 3,389.58	24,182.29 ± 2,198.11
330	393,054.40 ± 58,717.80	10,357.19 ± 3,573.01	25,857.57 ± 2,613.62
360	422,429.11 ± 61,915.87	11,185.43 ± 3,827.02	27,554.06 ± 2,800.40

[a] the values shown are mean ± S.D. from 4 experiments

Table 19 (continued) Cumulative amount per unit area of model solutes permeated through human epidermis for 6 hours at 37 ± 1ºC

Time	Cumulative amount of solute (μg/cm^2) [a]		
(min)	Nitrobenzene	3,4-Xylenol	Chlorocresol
0	0.00 ± 0.00	0.00 ± 0.00	0.00 ± 0.00
15	130.14 ± 16.48	234.96 ± 126.06	461.20 ± 112.44
30	250.46 ± 26.97	513.41 ± 263.12	1,241.52 ± 323.93
45	383.78 ± 39.03	817.40 ± 410.96	2,077.55 ± 555.44
60	507.30 ± 51.26	1,143.66 ± 535.62	2,952.97 ± 746.35
75	640.07 ± 58.07	1,474.11 ± 763.61	4,045.27 ± 1,080.57
90	778.52 ± 78.97	1,755.14 ± 842.59	4,821.56 ± 1,230.91
105	919.09 ± 100.12	2,090.18 ± 962.84	5,780.11 ± 1,478.37
120	1,037.03 ± 109.38	2,364.39 ± 1,035.01	6,655.16 ± 1,799.81
135	1,163.28 ± 128.03	2,719.51 ± 1,162.34	7,511.61 ± 2,007.62
150	1,293.73 ± 159.19	3,041.80 ± 1,246.21	8,425.09 ± 2,306.44
165	1,426.68 ± 187.05	3,393.99 ± 1,387.68	9,370.99 ± 2,527.50
180	1,555.35 ± 211.07	3,742.08 ± 1,480.21	10,209.37 ± 2,726.38
210	1,802.03 ± 245.57	4,411.15 ± 1,722.20	11,673.03 ± 3,196.57
240	2,077.13 ± 295.73	5,100.04 ± 1,997.04	13,337.93 ± 3,634.83
270	2,272.02 ± 320.74	5,749.43 ± 2,199.77	14,751.30 ± 4,001.47
300	2,523.86 ± 369.35	6,398.17 ± 2,543.59	16,476.39 ± 4,509.17
330	2,766.22 ± 401.98	7,054.96 ± 2,855.45	17,989.10 ± 4,973.98
360	3,058.77 ± 479.06	7,696.84 ± 3,164.12	19,456.35 ± 5,555.75

[a] the values shown are mean ± S.D. from 4 experiments

Table 20 Cumulative amount per unit area of model solutes permeated through full-thickness rat skin for 6 hours at 37 ± 1ºC

Time	Cumulative amount of solute (μg/cm^2) [a]		
(min)	Acyclovir	Acetophenone	4-Methylacetophenone
0	0.00 ± 0.00	0.00 ± 0.00	0.00 ± 0.00
15	38.19 ± 21.36	52.36 ± 62.27	14.62 ± 3.63
30	51.46 ± 28.27	101.36 ± 146.22	24.68 ± 8.81
45	65.45 ± 36.72	172.17 ± 248.47	39.04 ± 19.12
60	77.12 ± 44.91	252.72 ± 353.42	56.96 ± 31.74
75	89.70 ± 53.27	345.18 ± 466.47	77.00 ± 46.26
90	103.78 ± 64.24	434.45 ± 561.57	99.07 ± 60.39
105	113.65 ± 69.81	547.04 ± 665.49	126.07 ± 80.21
120	124.02 ± 77.65	653.04 ± 771.36	151.91 ± 95.34
135	133.66 ± 84.61	776.95 ± 882.30	180.45 ± 111.88
150	145.58 ± 94.03	889.66 ± 989.89	210.10 ± 128.96
165	156.23 ± 101.99	1,019.35 ± 1,100.65	242.17 ± 149.69
180	169.01 ± 113.52	1,163.34 ± 1,221.41	276.44 ± 169.41
210	184.28 ± 124.02	1,464.47 ± 1,471.58	345.19 ± 207.61
240	203.48 ± 139.27	1,749.61 ± 1,672.68	418.18 ± 250.23
270	225.26 ± 156.21	2,043.24 ± 1,908.79	492.04 ± 290.25
300	243.07 ± 170.91	2,343.22 ± 2,127.58	572.48 ± 328.80
330	262.29 ± 187.58	2,698.16 ± 2,405.06	654.37 ± 371.50
360	280.75 ± 203.03	3,059.36 ± 2,648.92	739.65 ± 411.07

[a] the values shown are mean ± S.D. from 4 experiments

Table 20 (continued) Cumulative amount per unit area of model solutes permeated through full-thickness rat skin for 6 hours at 37 ± 1ºC

Time	Cumulative amount of solute (μg/cm^2) [a]		
(min)	Phenol	4-Bromophenol	4-Chlorophenol
0	0.00 ± 0.00	0.00 ± 0.00	0.00 ± 0.00
15	589.11 ± 530.01	243.72 ± 154.74	56.33 ± 30.23
30	1,842.83 ± 1,026.67	340.25 ± 226.15	76.79 ± 39.92
45	3,612.62 ± 1,728.16	448.47 ± 292.03	108.36 ± 44.30
60	6,073.24 ± 2,429.00	586.84 ± 387.33	148.79 ± 55.31
75	8,610.26 ± 3,134.50	750.38 ± 535.69	199.87 ± 84.25
90	11,568.45 ± 3,845.21	966.81 ± 697.12	267.84 ± 138.05
105	14,844.89 ± 4,373.83	1,206.28 ± 876.96	356.16 ± 203.66
120	17,925.81 ± 5,139.92	1,484.62 ± 1,091.97	464.00 ± 270.30
135	21,341.55 ± 5,466.97	1,776.24 ± 1,292.91	561.69 ± 314.66
150	24,433.74 ± 5,636.01	2,095.99 ± 1,511.81	691.77 ± 391.96
165	28,100.10 ± 5,762.70	2,468.11 ± 1,737.54	826.80 ± 478.67
180	31,596.58 ± 6,133.62	2,855.08 ± 1,977.41	978.94 ± 568.63
210	39,343.64 ± 6,969.03	3,734.39 ± 2,405.47	1,317.99 ± 729.56
240	46,057.61 ± 7,971.49	4,617.36 ± 2,898.49	1,662.18 ± 914.76
270	53,266.88 ± 9,013.19	5,570.42 ± 3,374.75	2,045.94 ± 1,106.84
300	60,548.66 ± 10,555.69	6,637.85 ± 3,787.25	2,444.61 ± 1,287.48
330	67,016.96 ± 10,759.57	7,825.81 ± 4,230.21	2,867.61 ± 1,483.23
360	74,128.17 ± 11,985.90	8,911.93 ± 4,777.61	3,313.52 ± 1,661.32

[a] the values shown are mean ± S.D. from 4 experiments

Table 20 (continued) Cumulative amount per unit area of model solutes permeated through full-thickness rat skin for 6 hours at 37 ± 1ºC

Time	Cumulative amount of solute (μg/cm^2) [a]		
(min)	Nitrobenzene	3,4-Xylenol	Chlorocresol
0	0.00 ± 0.00	0.00 ± 0.00	0.00 ± 0.00
15	24.89 ± 1.94	67.61 ± 27.23	132.93 ± 22.29
30	34.18 ± 2.17	90.54 ± 31.91	163.50 ± 25.77
45	45.58 ± 3.09	110.41 ± 38.35	180.81 ± 20.52
60	60.26 ± 7.39	138.05 ± 46.81	199.25 ± 26.21
75	75.35 ± 12.63	171.67 ± 56.16	226.80 ± 28.92
90	91.62 ± 20.30	215.95 ± 72.47	254.33 ± 39.12
105	107.94 ± 25.95	259.22 ± 89.30	279.15 ± 41.62
120	125.25 ± 32.62	310.19 ± 107.01	311.75 ± 51.40
135	146.08 ± 41.23	358.54 ± 122.28	349.72 ± 61.59
150	163.91 ± 45.88	411.72 ± 138.75	385.01 ± 67.11
165	185.41 ± 50.35	467.26 ± 157.22	428.51 ± 71.08
180	206.22 ± 56.43	527.49 ± 169.80	475.03 ± 83.43
210	252.77 ± 76.85	653.15 ± 202.06	551.24 ± 95.26
240	302.19 ± 92.54	788.24 ± 237.36	650.92 ± 119.45
270	357.64 ± 114.52	939.21 ± 286.69	774.81 ± 147.91
300	418.99 ± 137.42	1,101.76 ± 328.66	902.96 ± 182.65
330	470.85 ± 155.35	1,261.73 ± 365.99	1,036.12 ± 229.13
360	530.25 ± 177.79	1,427.30 ± 401.28	1,162.02 ± 244.97

[a] the values shown are mean ± S.D. from 4 experiments

Table 21 Cumulative amount per unit area of model solutes permeated through egg shell membrane for 6 hours at 37 ± 1ºC

Time	Cumulative amount of solute (μg/cm^2) [a]		
(min)	Acyclovir	Acetophenone	4-Methylacetophenone
0	0.00 ± 0.00	0.00 ± 0.00	0.00 ± 0.00
15	188.41 ± 11.85	1,646.41 ± 274.76	420.13 ± 111.35
30	357.22 ± 4.55	2,972.12 ± 285.08	850.68 ± 205.03
45	536.87 ± 19.48	4,184.91 ± 370.14	1,225.56 ± 262.91
60	728.33 ± 4.44	5,084.97 ± 429.66	1,574.25 ± 311.06
75	881.35 ± 21.86	6,019.05 ± 476.76	1,948.12 ± 345.88
90	1,078.46 ± 0.04	6,844.87 ± 602.24	2,303.79 ± 444.56
105	1,236.86 ± 14.51	7,778.19 ± 763.24	2,652.88 ± 442.83
120	1,411.23 ± 23.61	8,534.83 ± 806.26	2,975.70 ± 484.08
135	1,604.76 ± 50.48	9,304.81 ± 972.99	3,294.46 ± 515.82
150	1,779.71 ± 76.70	10,071.68 ± 1,054.95	3,616.71 ± 563.00
165	1,978.89 ± 103.80	10,748.25 ± 1,141.31	3,921.25 ± 596.76
180	2,140.05 ± 154.01	11,450.52 ± 1,164.64	4,200.65 ± 643.79
210	2,434.72 ± 211.34	12,852.66 ± 1,400.30	4,769.32 ± 708.33
240	2,824.15 ± 252.83	14,123.44 ± 1,544.06	5,198.34 ± 760.93
270	3,187.20 ± 292.74	15,340.51 ± 1,719.50	5,618.83 ± 841.51
300	3,550.54 ± 371.11	16,376.67 ± 1,835.71	6,023.93 ± 903.96
330	3,891.12 ± 419.60	17,352.06 ± 1,944.17	6,484.47 ± 933.12
360	4,199.99 ± 441.90	18,550.05 ± 2,231.09	6,930.29 ± 964.01

[a] the values shown are mean ± S.D. from 4 experiments

Table 21 (continued) Cumulative amount per unit area of model solutes permeated through egg shell membrane for 6 hours at 37 ± 1ºC

Time	Cumulative amount of solute (μg/cm^2) [a]		
(min)	Phenol	4-Bromophenol	4-Chlorophenol
0	0.00 ± 0.00	0.00 ± 0.00	0.00 ± 0.00
15	37,077.27 ± 2,313.27	328.86 ± 41.54	1,009.22 ± 320.35
30	73,572.72 ± 6,082.62	779.10 ± 179.99	2,254.30 ± 538.35
45	106,531.18 ± 6,929.66	1,310.46 ± 363.09	3,377.76 ± 806.56
60	141,841.63 ± 12,282.12	1,892.24 ± 542.81	4,456.21 ± 1,219.17
75	170,669.40 ± 19,506.51	2,397.21 ± 665.42	5,488.15 ± 1,693.82
90	204,113.91 ± 25,392.19	2,891.10 ± 832.15	6,369.92 ± 1,910.27
105	228,645.63 ± 31,987.72	3,362.89 ± 934.70	7,327.40 ± 2,102.44
120	256,746.63 ± 38,133.13	3,825.22 ± 1,091.85	7,998.03 ± 2,083.07
135	282,455.49 ± 43,893.84	4,338.79 ± 1,286.88	8,727.42 ± 2,072.82
150	310,223.83 ± 50,663.93	4,726.62 ± 1,308.56	9,436.79 ± 2,124.80
165	336,746.52 ± 52,834.92	5,135.19 ± 1,335.29	10,122.90 ± 2,151.00
180	363,050.63 ± 56,622.08	5,528.25 ± 1,309.52	10,813.49 ± 2,138.83
210	408,404.47 ± 66,104.11	6,257.06 ± 1,319.43	12,043.15 ± 2,204.27
240	443,498.21 ± 69,085.44	6,936.37 ± 1,315.94	13,228.02 ± 2,160.73
270	475,919.60 ± 72,516.56	7,565.89 ± 1,330.90	14,622.56 ± 2,241.71
300	504,259.62 ± 68,540.71	8,221.77 ± 1,315.89	16,113.38 ± 2,405.00
330	541,025.69 ± 71,972.05	8,899.24 ± 1,295.17	17,513.81 ± 2,757.70
360	575,153.19 ± 75,960.96	9,468.57 ± 1,300.01	18,971.05 ± 3,427.23

[a] the values shown are mean ± S.D. from 4 experiments

Table 21 (continued) Cumulative amount per unit area of model solutes permeated through egg shell membrane for 6 hours at 37 ± 1ºC

Time	Cumulative amount of solute (μg/cm^2) [a]		
(min)	Nitrobenzene	3,4-Xylenol	Chlorocresol
0	0.00 ± 0.00	0.00 ± 0.00	0.00 ± 0.00
15	469.43 ± 63.86	939.18 ± 144.93	814.37 ± 75.51
30	853.62 ± 117.48	1,974.81 ± 251.64	1,702.01 ± 228.03
45	1,237.38 ± 101.75	3,020.23 ± 291.30	2,622.37 ± 336.31
60	1,611.59 ± 116.72	3,932.93 ± 310.88	3,550.93 ± 488.41
75	1,992.38 ± 89.48	4,909.02 ± 427.84	4,442.23 ± 516.16
90	2,367.79 ± 40.83	5,821.32 ± 468.30	5,368.55 ± 548.16
105	2,706.20 ± 30.18	6,662.64 ± 625.53	6,101.67 ± 816.88
120	3,043.23 ± 18.26	7,509.16 ± 746.14	6,977.10 ± 890.08
135	3,405.46 ± 31.24	8,320.75 ± 790.76	7,759.46 ± 1,042.24
150	3,736.51 ± 82.72	9,082.19 ± 849.06	8,479.37 ± 1,303.21
165	4,087.41 ± 87.19	9,944.11 ± 894.54	9,404.05 ± 1,416.02
180	4,409.03 ± 140.09	10,773.57 ± 883.44	10,151.58 ± 1,604.22
210	5,055.17 ± 168.93	12,237.96 ± 1,038.28	11,798.69 ± 1,886.07
240	5,603.24 ± 196.23	13,661.92 ± 1,156.72	13,334.10 ± 2,023.46
270	6,198.61 ± 170.98	15,116.90 ± 1,421.70	14,423.92 ± 2,075.34
300	6,696.40 ± 186.30	16,485.77 ± 1,587.87	15,802.00 ± 2,377.91
330	7,264.70 ± 262.66	17,750.19 ± 1,742.74	17,206.50 ± 2,649.13
360	7,735.48 ± 305.82	19,079.35 ± 2,010.60	18,402.01 ± 2,797.39

[a] the values shown are mean ± S.D. from 4 experiments

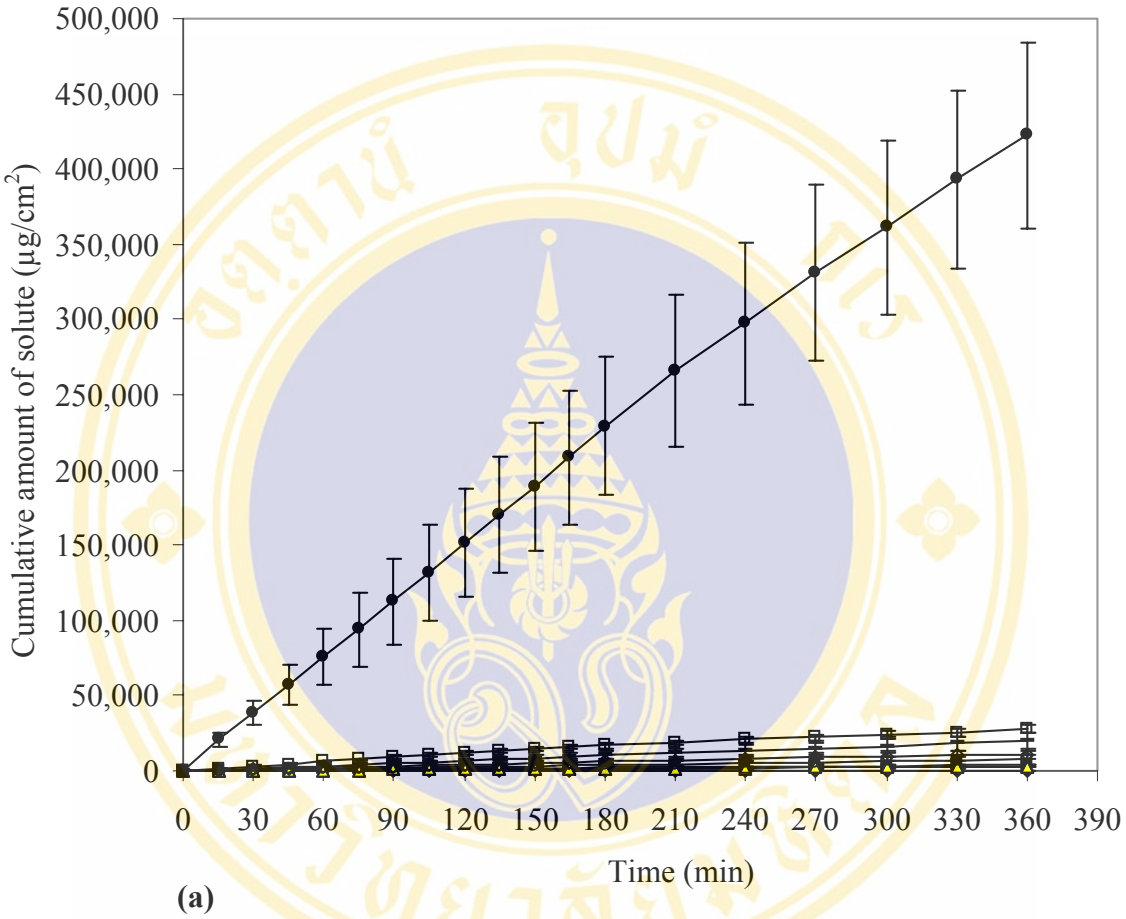

Figure 22 Cumulative amount per unit area of model solutes permeated through human epidermis for 6 hours at 37 ± 1ºC (n=4).

(◆) Acyclovir (■) Acetophenone (▲) 4-Methylacetophenone
(●) Phenol (◇) 4-Bromophenol (□) 4-Chlorophenol
(Δ) Nitrobenzene (○) 3,4-Xylenol **(-)** Chlorocresol

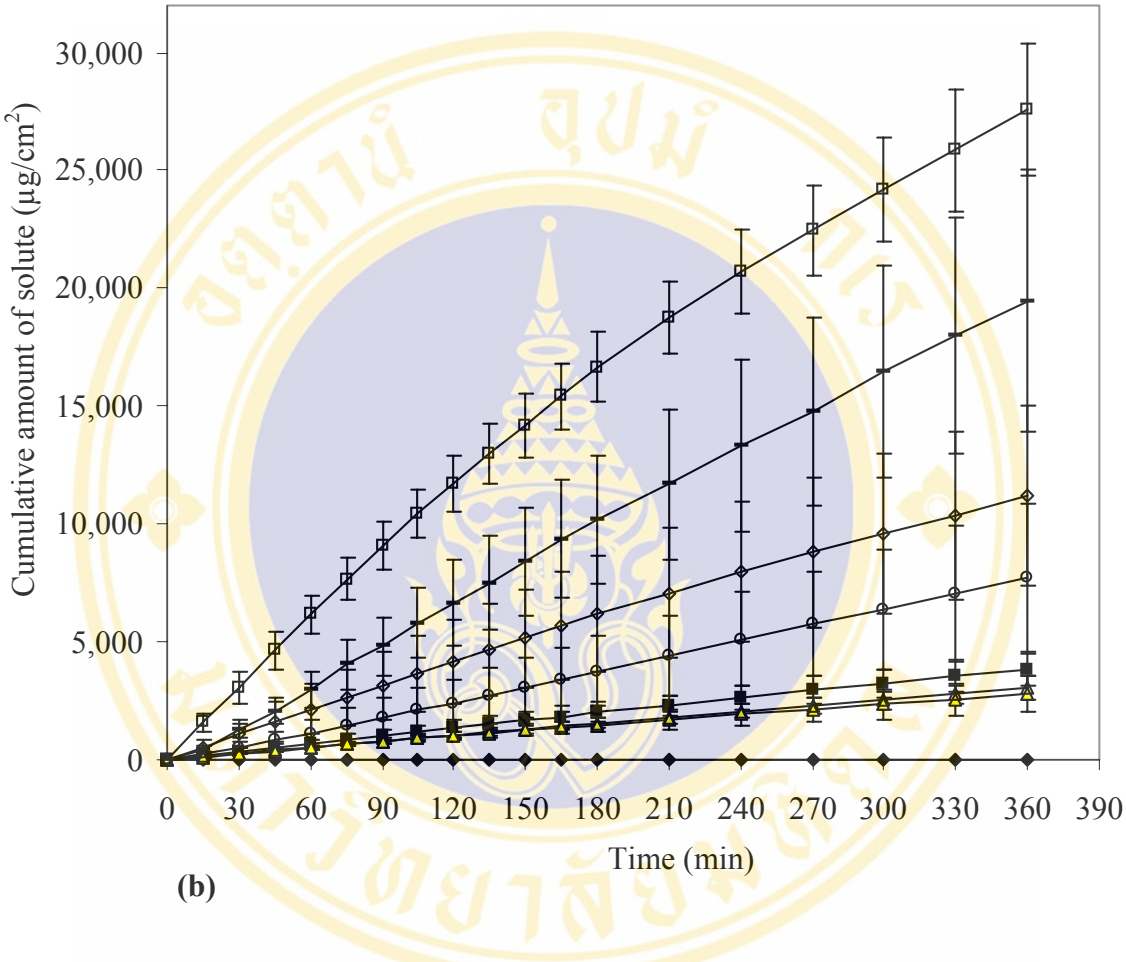

Figure 22 (continued) Cumulative amount per unit area of model solutes permeated through human epidermis for 6 hours at 37 ± 1ºC (n=4).

(◆) Acyclovir (■) Acetophenone (▲) 4-Methylacetophenone
(●) Phenol (◇) 4-Bromophenol (□) 4-Chlorophenol
(Δ) Nitrobenzene (○) 3,4-Xylenol **(-)** Chlorocresol

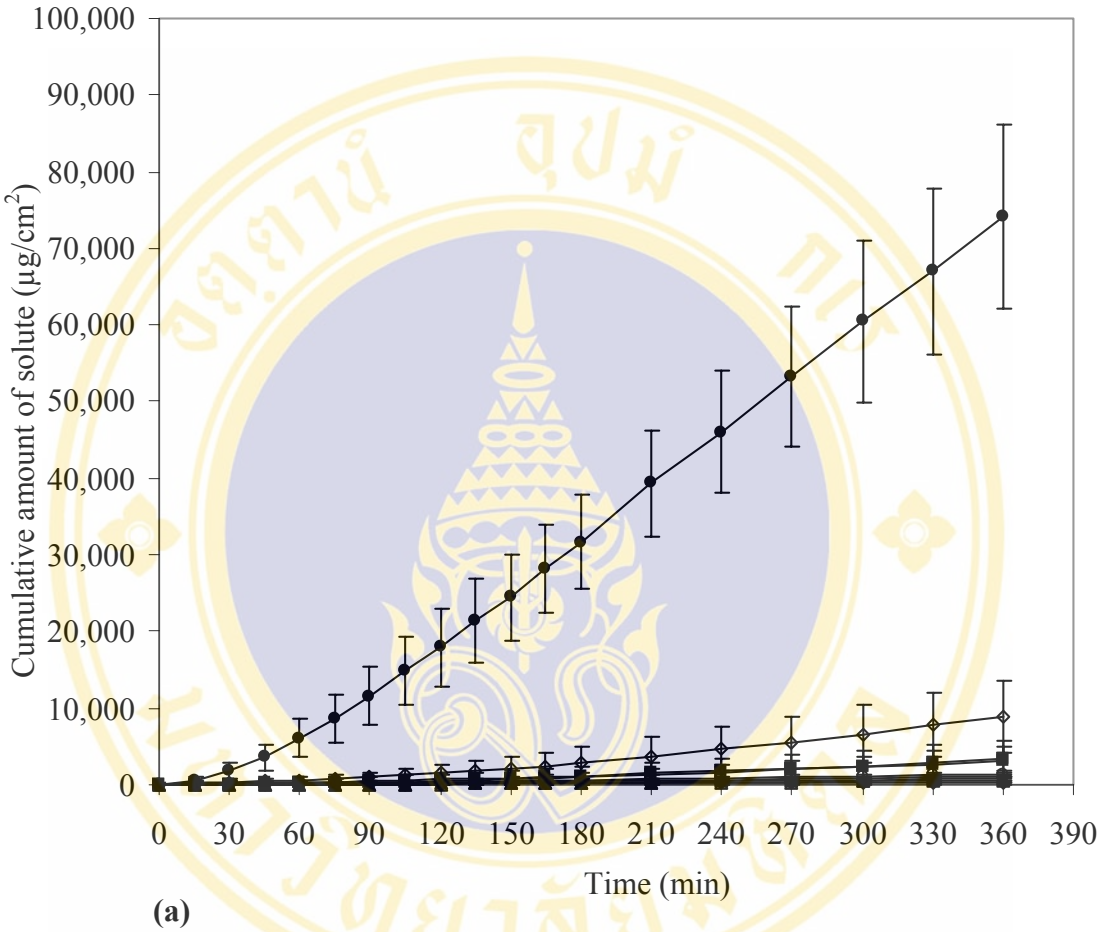

Figure 23 Cumulative amount per unit area of model solutes permeated through full-thickness rat skin for 6 hours at 37 ± 1ºC (n=4).

(◆) Acyclovir (■) Acetophenone (▲) 4-Methylacetophenone
(●) Phenol (◇) 4-Bromophenol (□) 4-Chlorophenol
(Δ) Nitrobenzene (○) 3,4-Xylenol **(-)** Chlorocresol

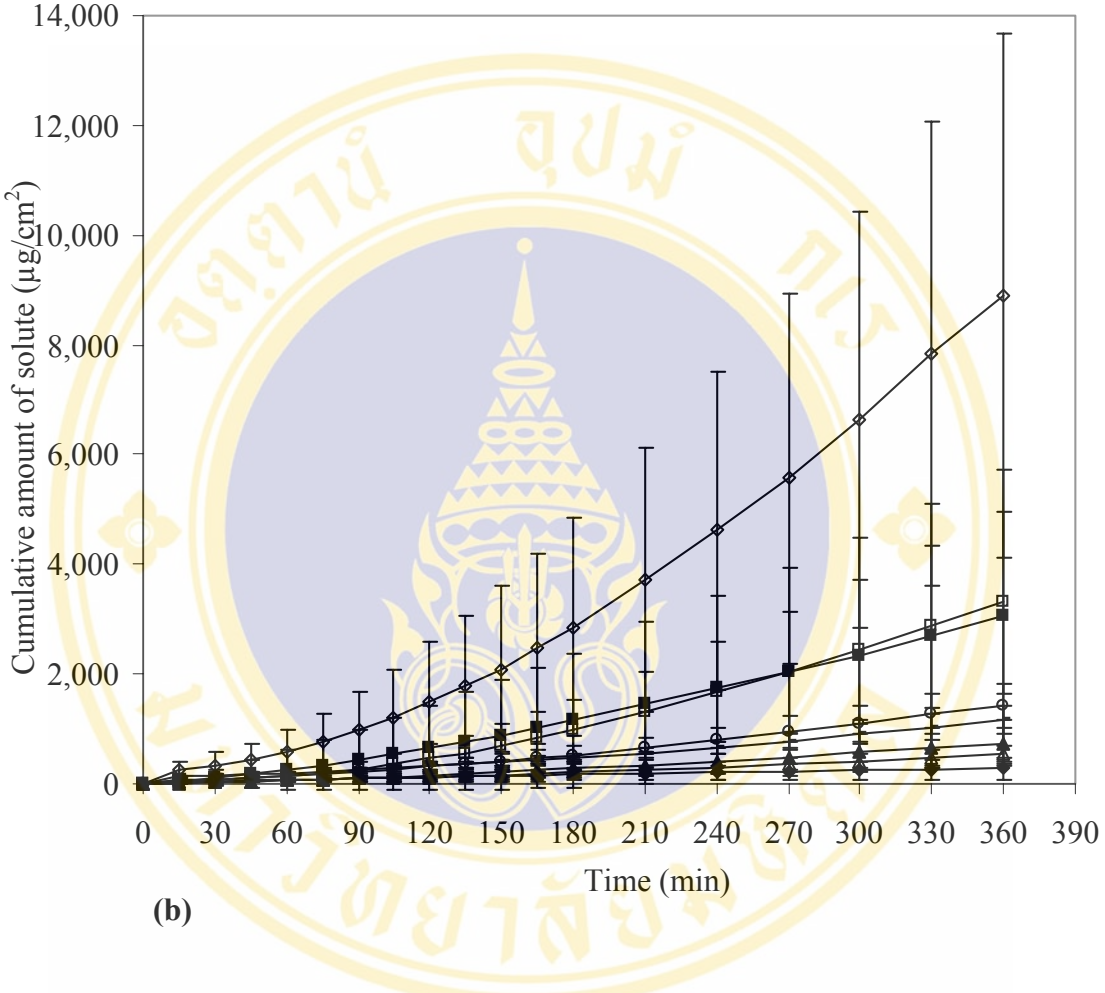

Figure 23 (continued) Cumulative amount per unit area of model solutes permeated through full-thickness rat skin for 6 hours at 37 ± 1ºC (n=4).

(◆) Acyclovir (■) Acetophenone (▲) 4-Methylacetophenone
(●) Phenol (◇) 4-Bromophenol (□) 4-Chlorophenol
(Δ) Nitrobenzene (○) 3,4-Xylenol (-) Chlorocresol

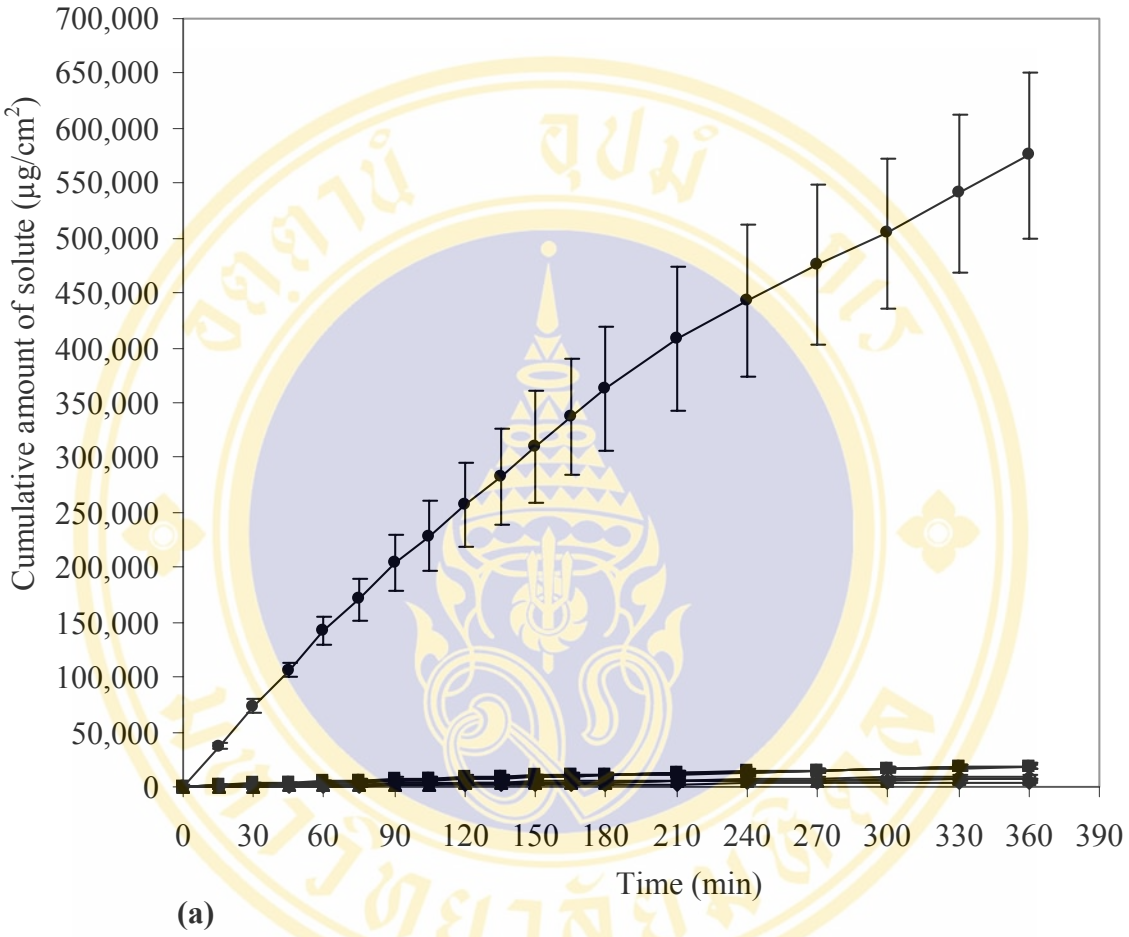

Figure 24 Cumulative amount per unit area of model solutes permeated through egg shell membrane for 6 hours at 37 ± 1ºC (n=4).

(◆) Acyclovir (■) Acetophenone (▲) 4-Methylacetophenone
(●) Phenol (◇) 4-Bromophenol (□) 4-Chlorophenol
(Δ) Nitrobenzene (○) 3,4-Xylenol (-) Chlorocresol

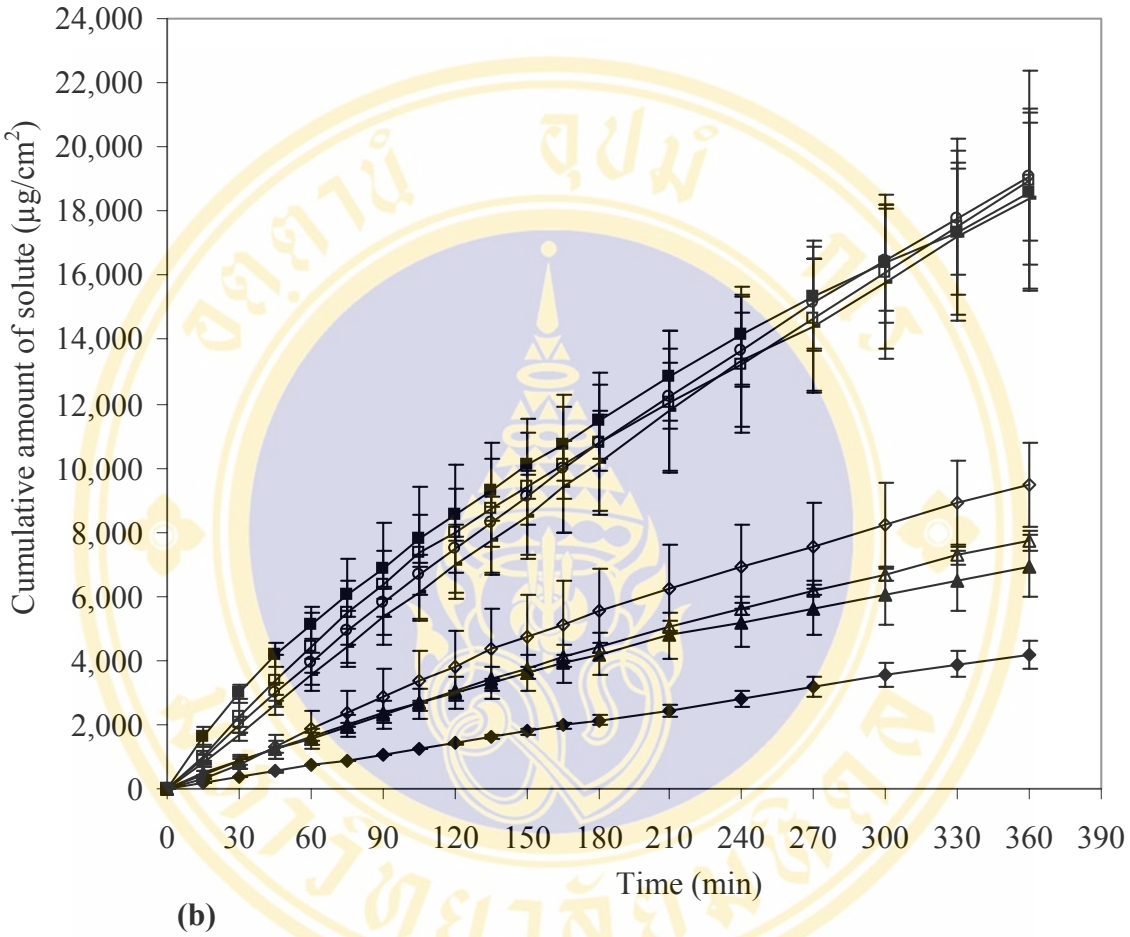

Figure 24 (continued) Cumulative amount per unit area of model solutes permeated through egg shell membrane for 6 hours at 37 ± 1ºC (n=4).

(◆) Acyclovir (■) Acetophenone (▲) 4-Methylacetophenone
(●) Phenol (◇) 4-Bromophenol (□) 4-Chlorophenol
(Δ) Nitrobenzene (○) 3,4-Xylenol (-) Chlorocresol

Table 22 Permeability of human epidermis to model solutes.

Solute	Sample	Flux (μmole/cm^2.min)	k_p x 10^3 (cm/min)	log k_p	Lag time (min)
Acyclovir	1	NC	NC	NC	NC
	2	NC	NC	NC	NC
	3	NC	NC	NC	NC
	4	NC	NC	NC	NC
	Average $\pm$ S.D.	NC	NC	NC	NC
Acetophenone	1	0.096	2.210	-2.656	-1.613
	2	0.071	1.639	-2.785	17.616
	3	0.088	2.011	-2.697	-14.807
	4	0.096	2.205	-2.657	-28.000
	Average $\pm$ S.D.	0.088 $\pm$ 0.012	2.016 $\pm$ 0.268	-2.699 $\pm$ 0.061	-6.701 $\pm$ 19.464
4-Methylacetophenone	1	0.066	4.525	-2.344	-11.176
	2	0.074	5.078	-2.294	-3.313
	3	0.038	2.655	-2.576	-53.414
	4	0.045	3.136	-2.504	-14.884
	Average $\pm$ S.D.	0.056 $\pm$ 0.017	3.849 $\pm$ 1.140	-2.430 $\pm$ 0.132	-20.697 $\pm$ 22.338
Phenol	1	11.306	14.240	-1.846	9.330
	2	15.007	18.902	-1.723	-26.151
	3	12.451	15.683	-1.805	-4.437
	4	13.306	16.759	-1.776	6.200
	Average $\pm$ S.D.	13.017 $\pm$ 1.559	16.396 $\pm$ 1.964	-1.788 $\pm$ 0.052	-3.765 $\pm$ 16.045
4-Bromophenol	1	0.157	10.917	-1.962	10.840
	2	0.209	14.592	-1.836	-30.901
	3	0.119	8.302	-2.081	4.958
	4	0.247	17.241	-1.763	-22.090
	Average $\pm$ S.D.	0.183 $\pm$ 0.057	12.763 $\pm$ 3.946	-1.911 $\pm$ 0.140	-9.298 $\pm$ 20.323

NC = could not calculate

Table 22 (continued) Permeability of human epidermis to model solutes.

Solute	Sample	Flux (μmole/cm^2.min)	$k_p \times 10^3$ (cm/min)	log k_p	Lag time (min)
4-Chlorophenol	1	0.487	11.354	-1.945	-65.994
	2	0.577	13.449	-1.871	-27.576
	3	0.640	14.916	-1.826	-20.688
	4	0.595	13.870	-1.858	-61.534
	Average $\pm$ S.D.	0.575 $\pm$ 0.064	13.397 $\pm$ 1.495	-1.875 $\pm$ 0.050	-43.948 $\pm$ 23.125
Nitrobenzene	1	0.071	4.858	-2.314	3.832
	2	0.087	6.003	-2.222	12.551
	3	0.056	3.869	-2.412	-8.143
	4	0.067	4.580	-2.339	-12.201
	Average $\pm$ S.D.	0.070 $\pm$ 0.013	4.827 $\pm$ 0.888	-2.322 $\pm$ 0.079	-0.990 $\pm$ 11.306
3,4-Xylenol	1	0.169	3.711	-2.431	-6.614
	2	0.283	6.229	-2.206	12.568
	3	0.164	3.619	-2.441	32.484
	4	0.128	2.823	-2.549	29.883
	Average $\pm$ S.D.	0.186 $\pm$ 0.067	4.095 $\pm$ 1.477	-2.407 $\pm$ 0.144	17.080 $\pm$ 18.101
Chlorocresol	1	0.238	6.441	-2.191	-15.200
	2	0.376	10.183	-1.992	7.444
	3	0.430	11.637	-1.934	-11.774
	4	0.493	13.336	-1.875	-0.947
	Average $\pm$ S.D.	0.384 $\pm$ 0.109	10.399 $\pm$ 2.937	-1.998 $\pm$ 0.137	-5.119 $\pm$ 10.346

Table 23 Permeability of full-thickness rat skin to model solutes.

Solute	Sample	Flux (μmole/cm^2.min)	k_p x 10^3 (cm/min)	log k_p	Lag time (min)
Acyclovir	1	0.005	0.425	-3.371	-59.434
	2	0.005	0.439	-3.357	-54.070
	3	0.001	0.083	-4.080	-178.899
	4	0.001	0.083	-4.081	-129.156
	Average $\pm$ S.D.	0.003 $\pm$ 0.002	0.258 $\pm$ 0.202	-3.722 $\pm$ 0.413	-105.390 $\pm$ 59.761
Acetophenone	1	0.033	0.768	-3.114	99.316
	2	0.042	0.966	-3.015	93.976
	3	0.066	1.513	-2.820	64.668
	4	0.172	3.944	-2.404	35.768
	Average $\pm$ S.D.	0.078 $\pm$ 0.064	1.798 $\pm$ 1.465	-2.838 $\pm$ 0.314	73.432 $\pm$ 29.368
4-Methylacetophe-none	1	0.011	0.765	-3.116	67.334
	2	0.006	0.425	-3.371	54.773
	3	0.024	1.660	-2.780	59.478
	4	0.026	1.828	-2.738	51.918
	Average $\pm$ S.D.	0.017 $\pm$ 0.010	1.169 $\pm$ 0.681	-3.001 $\pm$ 0.299	58.376 $\pm$ 6.737
Phenol	1	2.423	3.051	-2.515	15.439
	2	2.003	2.523	-2.598	55.659
	3	2.778	3.500	-2.456	45.135
	4	2.957	3.724	-2.429	68.515
	Average $\pm$ S.D.	2.540 $\pm$ 0.421	3.200 $\pm$ 0.531	-2.500 $\pm$ 0.075	46.187 $\pm$ 22.618
4-Bromophenol	1	0.122	8.507	-2.070	99.337
	2	0.050	3.475	-2.459	86.626
	3	0.242	16.892	-1.772	66.365
	4	0.218	15.227	-1.817	62.759
	Average $\pm$ S.D.	0.158 $\pm$ 0.089	11.025 $\pm$ 6.203	-2.030 $\pm$ 0.315	78.772 $\pm$ 17.272

Table 23 (continued) Permeability of full-thickness rat skin to model solutes.

Solute	Sample	Flux (μmole/cm^2.min)	k_p x 10^3 (cm/min)	log k_p	Lag time (min)
4-Chlorophenol	1	0.052	1.221	-2.913	88.423
	2	0.138	3.211	-2.493	81.406
	3	0.041	0.949	-3.023	81.710
	4	0.098	2.283	-2.642	88.732
	Average $\pm$ S.D.	0.082 $\pm$ 0.045	1.916 $\pm$ 1.038	-2.768 $\pm$ 0.243	85.068 $\pm$ 4.056
Nitrobenzene	1	0.018	1.246	-2.904	45.934
	2	0.012	0.795	-3.099	48.054
	3	0.010	0.698	-3.156	33.827
	4	0.009	0.601	-3.221	24.469
	Average $\pm$ S.D.	0.012 $\pm$ 0.004	0.835 $\pm$ 0.285	-3.095 $\pm$ 0.137	38.071 $\pm$ 11.023
3,4-Xylenol	1	0.037	0.808	-3.093	50.474
	2	0.039	0.857	-3.067	46.479
	3	0.020	0.449	-3.348	67.114
	4	0.038	0.846	-3.073	43.261
	Average $\pm$ S.D.	0.034 $\pm$ 0.009	0.740 $\pm$ 0.195	-3.145 $\pm$ 0.136	51.832 $\pm$ 10.607
Chlorocresol	1	0.026	0.713	-3.147	24.078
	2	0.020	0.534	-3.272	15.424
	3	0.016	0.435	-3.361	-19.234
	4	0.018	0.489	-3.311	29.390
	Average $\pm$ S.D.	0.020 $\pm$ 0.004	0.543 $\pm$ 0.120	-3.273 $\pm$ 0.091	12.415 $\pm$ 21.870

Table 24 Permeability of egg shell membrane to model solutes.

Solute	Sample	Flux (μmole/cm^2.min)	k_p x 10^3 (cm/min)	log k_p	Lag time (min)
Acyclovir	1	0.047	3.925	-2.406	-23.159
	2	0.060	5.043	-2.297	6.285
	3	0.054	4.486	-2.348	-0.829
	4	0.053	4.459	-2.351	-43.905
	Average $\pm$ S.D.	0.054 $\pm$ 0.005	4.478 $\pm$ 0.457	-2.351 $\pm$ 0.044	-15.402 $\pm$ 22.769
Acetophenone	1	0.407	9.342	-2.030	-47.713
	2	0.391	8.974	-2.047	-72.872
	3	0.423	9.720	-2.012	-71.034
	4	0.306	7.025	-2.153	-89.981
	Average $\pm$ S.D.	0.382 $\pm$ 0.052	8.765 $\pm$ 1.200	-2.061 $\pm$ 0.063	-70.400 $\pm$ 17.365
4-Methylacetophe-none	1	0.152	10.480	-1.980	-31.863
	2	0.122	8.409	-2.075	-29.668
	3	0.114	7.862	-2.104	-81.165
	4	0.156	10.743	-1.969	-56.090
	Average $\pm$ S.D.	0.136 $\pm$ 0.021	9.374 $\pm$ 1.451	-2.032 $\pm$ 0.068	-49.696 $\pm$ 24.154
Phenol	1	18.754	23.621	-1.627	-24.077
	2	12.540	15.794	-1.802	-60.286
	3	18.695	23.547	-1.628	-59.000
	4	15.537	19.570	-1.708	-69.865
	Average $\pm$ S.D.	16.381 $\pm$ 2.969	20.633 $\pm$ 3.740	-1.691 $\pm$ 0.083	-53.307 $\pm$ 20.080
4-Bromophenol	1	0.149	10.370	-1.984	-107.447
	2	0.121	8.425	-2.074	-65.858
	3	0.149	10.409	-1.983	-13.209
	4	0.155	10.804	-1.966	14.901
	Average $\pm$ S.D.	0.143 $\pm$ 0.015	10.002 $\pm$ 1.069	-2.002 $\pm$ 0.049	-42.903 $\pm$ 54.516

Table 24 (continued) Permeability of egg shell membrane to model solutes.

Solute	Sample	Flux (μmole/cm^2.min)	k_p x 10^3 (cm/min)	log k_p	Lag time (min)
4-Chlorophenol	1	0.344	8.013	-2.096	-55.335
	2	0.346	8.066	-2.093	-129.497
	3	0.294	6.849	-2.164	-83.336
	4	0.347	8.096	-2.092	-16.886
	Average $\pm$ S.D.	0.333 $\pm$ 0.026	7.756 $\pm$ 0.605	-2.111 $\pm$ 0.035	-71.263 $\pm$ 47.425
Nitrobenzene	1	0.171	11.760	-1.930	-29.750
	2	0.168	11.578	-1.936	-31.489
	3	0.188	12.944	-1.888	-14.186
	4	0.157	10.785	-1.967	-38.913
	Average $\pm$ S.D.	0.171 $\pm$ 0.013	11.767 $\pm$ 0.892	-1.930 $\pm$ 0.033	-28.585$\pm$ 10.389
3,4-Xylenol	1	0.459	10.115	-1.995	-34.952
	2	0.408	8.988	-2.046	-24.276
	3	0.376	8.289	-2.081	-43.284
	4	0.429	9.445	-2.025	-14.087
	Average $\pm$ S.D.	0.418 $\pm$ 0.035	9.209 $\pm$ 0.768	-2.037 $\pm$ 0.036	-29.150 $\pm$ 12.703
Chlorocresol	1	0.473	12.812	-1.892	-4.694
	2	0.342	9.253	-2.034	-13.641
	3	0.332	8.993	-2.046	-18.341
	4	0.354	9.573	-2.019	-4.693
	Average $\pm$ S.D.	0.375 $\pm$ 0.066	10.158 $\pm$ 1.786	-1.998 $\pm$ 0.071	-10.342 $\pm$ 6.799

all solutes could achieve steady state immediately when permeated through human epidermis and egg shell membrane. While for full-thickness rat skin, the lag time of all model solutes were in a range of about 12-85 min. This may be due to full-thickness rat skin is thicker than human epidermis and egg shell membrane. According to simple partition and diffusion theory with constant skin barrier function, lag time is expressed as $L^2/6D$, where L and D are the thickness of membrane and the effective diffusion coefficient of solute in skin barrier, respectively (1-2).

Tables 19-24 and Figure 25 reveal that most of solutes tend to permeate through egg shell membrane more than human epidermis and full-thickness rat skin. For human epidermis, the permeability coefficient of phenol permeated through this membrane was the highest followed by 4-chlorophenol, 4-bromophenol, chlorocresol, nitrobenzene, 3,4-xylenol, 4-methylacetophenone, acetophenone, and acyclovir, respectively. The amount of ayclovir permeated through this membrane was very low. Thus, flux, permeability coefficient, and lag time could not be calculated. For full-thickness rat skin, the permeability coefficient of 4-bromophenol permeated through this membrane was the highest followed by phenol, 4-chlorophenol, acetophenone, 4-methylacetophenone, nitrobenzene, 3,4-xylenol, chlorocresol, and acyclovir, respectively. For egg shell membrane, the permeability coefficient of phenol permeated through this membrane was the highest followed by nitrobenzene, chrolocresol, 4-bromophenol, 4-methylacetophenone, 3,4-xylenol, acetophenone, 4-chlorophenol, and acyclovir, respectively.

As the stratum corneum is the outer layer of the skin, providing the main barrier for chemical penetration, three possible mechanisms have been suggested for solute permeation through the skin. The first can be described as the shunt route, which provides a parallel pathway by which solutes can be absorbed by sweat ducts and hair follicles without hindrance by the stratum corneum. The second and third mechanisms are the intercellular and transcellular routes (1-3,57). These skin permeation mechanisms can be used to explain the result showing that acyclovir could permeate through rat skin more than human skin. Since, acyclovir is quite hydrophilic with log $K_{o/PB}$ of -1.74 (Table 25), it could not permeate well through the skin by intercellular and transcellular routes, both of which compose of lipid. For permeation of hydrophilic solutes or large polar molecules through the skin, the shunt route becomes more

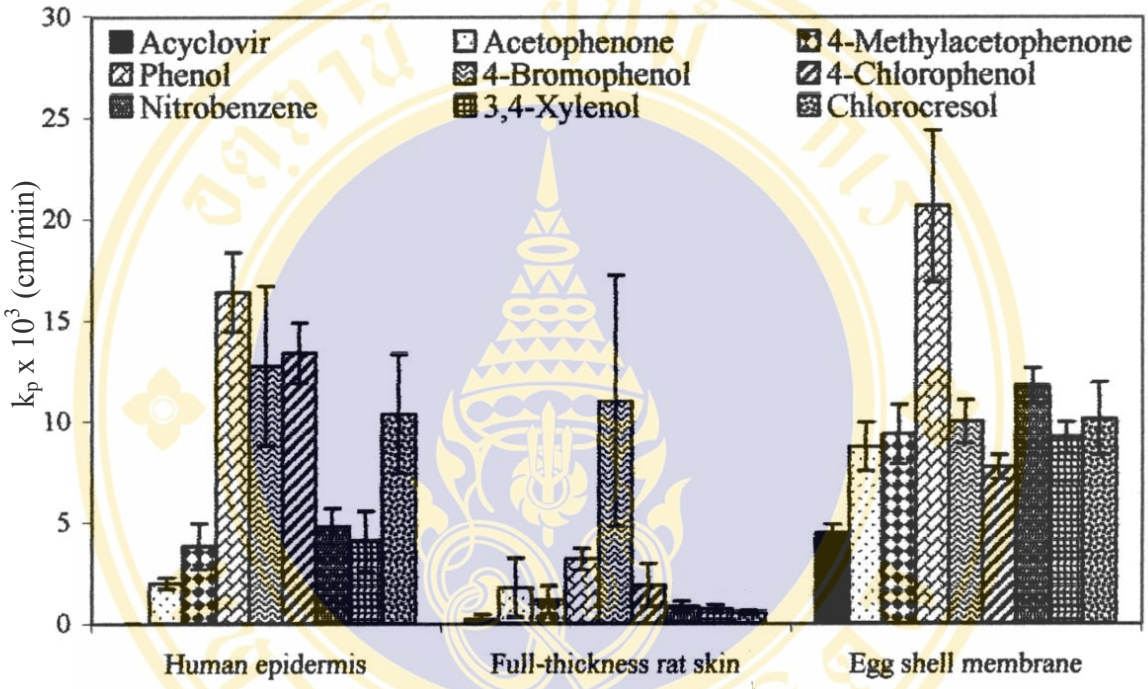

Figure 25 Comparison of permeability coefficient of three biological membranes to model solutes (n=4).

Table 25 Some physicochemical parameters[a] of model solutes

Solute	log $K_{o/w}$	MW	u	$V_I/100$	π^*	β	α
Acyclovir	-1.74[b]	225	-	-	-	-	-
Acetophenone	1.66	120.15	2.90	0.690	0.90	0.49	0.04
4-Methylacetophenone	2.28	134.18	3.22	0.788	0.86	0.50	0.00
Phenol	1.28	94.11	1.52	0.536	0.72	0.33	0.61
4-Bromophenol	2.60	173.02	2.37	0.699	0.79	0.30	0.67
4-Chlorophenol	2.42	128.56	2.28	0.626	0.72	0.23	0.67
Nitrobenzene	1.84	123.11	4.00	0.631	1.01	0.30	0.00
3,4-Xylenol	2.23	122.16	1.75	0.732	0.64	0.35	0.60
Chlorocresol	3.10	142.58	-	0.724	0.72	0.23	0.67

[a] log $K_{o/w}$ is logarithm of octanol-water partition coefficient, MW is molecule weight, u is dipole moment, $V_I/100$ is molecular volume, π^*, β, and α are solvatochromic parameters. (55)

[b] log $K_{o/PB}$ (logarithm of octanol-0.2 M phosphate buffer partition coefficient) is used instead of log $K_{o/w}$ (5)

important for permeation of these solutes (2). Additionally, the amount of hair follicles per unit area of Wistar rat skin is higher than human skin resulting in about 0.1% of total skin area available for solute permeation (2,3,57). Thus, from results of the permeation of acyclovir through human epidermis and full-thickness rat skin studies, it was reasonable to conclude that acyclovir permeated through both skin by passing through shunt route and flux of acyclovir across rat skin is higher than human skin due to the higher amount of hair follicle per unit area of rat skin. While, other model solutes have log $K_{o/w}$ higher than acyclovir and has a positive value. It is referred that they are lipophilic solutes. Form the above principle, these solutes may rather permeate through skin by passing through intercellular or transcellular routes which permits large available area for skin absorption, than shunt route.

A number of researchers have attempted to analyze the skin permeation data for finding a model capable of explaining the permeation process and predicting the penetration without recourse to morally objectionable experiments. Abraham M.H. et al, 1995 (57) analyzed the human skin permeation data. They found good correlation between logarithm of permeability coefficient (log k_p) and some of physicochemical parameters of steroids, alcohols, and phenols. Those equations are presented by following.

For alcohols, steroids (permeation data from Tayar et al, 1991 was analysed):

$$\log k_p = -5.333 - 0.622\pi^* - 0.378\alpha - 3.342\beta + 1.851V_I/100 \quad (11)$$

$n = 22 \qquad r^2 = 0.957 \qquad S.D. = 0.268 \quad F = 93.7$

For alcohols, steroids, diethylether, 2-ethoxyethanol, and butanol (permeation data from Tayar et al, 1991, and Scheuplein & Blank, 1971 was analysed):

$$\log k_p = -5.194 - 0.567\pi^* - 0.506\alpha - 3.368\beta + 1.767V_I/100 \quad (12)$$

$n = 25 \qquad r^2 = 0.956 \qquad S.D. = 0.260 \quad F = 93.7$

For Phenols (permeation data from Roberts et al, 1977 was analysed):

$$\log k_p = -4.994 - 0.341\pi^* - 1.691\alpha - 2.689\beta + 1.965V_I/100 \quad (13)$$

n = 19 $r^2 = 0.940$ S.D. = 0.160 F = 54.9

For alcohol, steroids, and phenol solutes (permeation data from equation 11-13 was analysed):

$$\log k_p = -5.048 - 0.586\pi^* - 0.633\alpha - 3.481\beta + 1.787V_I/100 \quad (14)$$

n = 46 $r^2 = 0.958$ S.D. = 0.249 F = 235.0

For all equations, they found that two main factors that influence permeability are solute hydrogen-bond basicity (β) that reduces permeability and molecular volume ($V_I/100$) which can refer to lipophilicity of solute that increase permeability. Whereas, less important factors are dipolarity (π^*) and solute hydrogen-bond acidity (α) that reduces permeability. Comparison of equation 11 and equation 13 shows that for the phenols, there is a significant term in solute acidity, while for the alcohols and steroids, there is no such term. They suggested this difference may be due to the differrence in selected solute sets and it is not necessarily due to a fundamental difference in permeation mechanism. Ghafourian T et al, 2001 (58) also found similar good correlation results by using another QSAR technique (TQSAR). They found two main factors that influence permeability of steroids and alcohols through human skin, are hydrogen-bond basicity (q_s^-) and the size of the compounds (log *TA*). Where q_s^- is the sum of atomic charges on the hydrogen bonding heteroatom which is used as the hydrogen bonding acceptor ability, and log *TA* is the logarithm of total solvent accessible surface area. The relationship between log k_p obtained in this study and physicochemical parameters of eight model solutes through human epidermis, full-thickness rat skin, and egg shell membrane, are given by equations 15-17.

For human epidermis:

$$\log k_p = -2.813(\pm 2.660) + 1.221(\pm 1.987)\pi^* + 1.053(\pm 0.970)\alpha - 0.251(\pm 1.664)\beta$$
$$-0.988(\pm 1.264)V_I/100 \quad (15)$$
$$n = 8 \qquad r^2 = 0.787 \qquad S.D. = 0.231 \qquad F = 2.8$$

For full-thickness rat skin:

$$\log k_p = -11.717(\pm 2.640) + 7.282(\pm 1.973)\pi^* + 4.050(\pm 0.963)\alpha$$
$$+ 6.305(\pm 1.652)\beta - 0.980(\pm 1.255)V_I/100 \quad (16)$$
$$n = 8 \qquad r^2 = 0.872 \qquad S.D. = 0.229 \qquad F = 5.1$$

For egg shell membrane:

$$\log k_p = -1.299(\pm 1.611) + 0.007(\pm 1.203)\pi^* + 0.072(\pm 0.587)\alpha$$
$$+ 0.442(\pm 1.008)\beta \quad -1.278(\pm 0.765)V_I/100 \quad (17)$$
$$n = 8 \qquad r^2 = 0.504 \qquad S.D. = 0.140 \qquad F = 0.8$$

From equations 15-17, it was found that poor correlation between log k_p and physicochemical parameters of model solutes were obtained. Roberts M.S. et al, 1997 (54) showed that there was an increase in permeability of human epidermis when some phenolic compounds (e.g., 4-nitrophenol, 3-nitrophenol, phenol, 4-bromophenol, 4-chlorophenol, 2-chlorophenol, 2-cresol, 3-cresol, and 4-cresol) were used at a concentration above the threshold solute concentration. They suggested that this phenomenon caused by damaging of membrane. This conclusion was supported by the findings that, for permeation of phenol through polyethylene membrane there was no increase in k_p value at higher concentration of phenol. Therefore, poor correlation obtained herein may be caused by inappropriate permeability data of phenol, 4-bromophenol, and 4-chlorophenol. When these three solutes were excluded from the data set, the regression equations are obtained as follows:

For human epidermis:

$$\log k_p = -3.470(\pm 0.440) - 0.383(\pm 0.169)\alpha - 3.206(\pm 0.517)\beta + 3.380(\pm 0.821)V_I/100 \quad (18)$$

$n = 5 \qquad r^2 = 0.985 \qquad S.D. = 0.062 \qquad F = 22.0$

For full-thickness rat skin:

$$\log k_p = -2.679(\pm 0.338) + 1.795(\pm 0.249)\beta - 1.435(\pm 0.509)V_I/100 \quad (19)$$

$n = 5 \qquad r^2 = 0.963 \qquad S.D. = 0.054 \qquad F = 26.1$

For egg shell membrane:

$$\log k_p = -1.197(\pm 0.102) - 0.468(\pm 0.083)\pi^* - 0.392(\pm 0.046)\alpha - 0.861(\pm 0.061)\beta \quad (20)$$

$n = 5 \qquad r^2 = 0.998 \qquad S.D. = 0.004 \qquad F = 210.6$

From equations 18-20, good correlation between log k_p and some physico-chemical parameters of the solutes could be obtained. For human epidermis, log k_p is influenced by three factors, i.e., solute hydrogen-bond acidity, solute hydrogen-bond basicity, and molecular volume. Increase solute hydrogen-bond basicity and solute hydrogen-bond acidity will result in decrease permeability, whereas increase molecular volume will result in increase permeability. The equation obtained herein agrees well with that of Abraham M.H. et al, 1995, although the coefficient value of each factor differs from their equation. It may due to difference in solute set, regional skin site, race, and experimental process. However, the equations obtained herein can be used to support the application of certain physicochemical parameters of solute (i.e., π^*, α, β, $V_I/100$) in the permeation process of solute through human skin. For full-thickness rat skin, it was found that increase solute hydrogen-bond basicity will result in increase permeability, whereas increase molecular volume will result in decrease permeability. For egg shell membrane, it was found that increase solute hydrogen-bond acidity, solute hydrogen-bond basicity, and dipolarity will result in decrease

permeability. From the equations obtained herein, the main factors that influence permeability of human epidermis and full-thickness rat skin are solute hydrogen-bond basicity and molecular volume. For egg shell membrane, the main factors that influence permeability are solute hydrogen-bond acidity, solute hydrogen-bond basicity, and dipolarity. Solute hydrogen-bond basicity, solute hydrogen-bond acidity, and dipolarity may indicate the hydrophilic property of solute, while solute molecular volume may indicate the hydrophobic property of solute. Therefore, the permeation of solute through these biological membranes may depend on the hydrophilic and hydrophobic nature of each solute. To study the trend of permeability property of three biological membranes (i.e., human epidermis, full-thick-ness rat skin, and egg shell membrane) to model solutes, the logarithm of ratio between solute molecular volume and solute hydrogen-bond basicity which are the main factors affecting permeability (Equations 18-20), was calculated. This value may reflect the hydrophilic-lipophilic property of solute. Table 26 shows logarithm of permeability coefficient values of model solute through three biological membranes and logarithm of ratio between molecular volume and solute hydrogen-bond basicity of model solutes (log $V_I/100/\beta$). Data from Table 26 is plotted between log k_p and log $V_I/100/\beta$ as showed in Figure 26. The relationships between log k_p and log $V_I/100/\beta$ of five model solute (i.e., acetophenone, 4-methylacetophenone, nitrobenzene, 3,4-xylenol, and chlorocresol) permeated through three biological membranes are given by equations 21-23.

For human epidermis:

$$\log k_p = 1.795(\pm 0.333)\log V_I/100/\beta - 2.894(\pm 0.107) \quad (21)$$

$n = 5$ $r^2 = 0.907$ S.D. = 0.090 F = 29.1

For full-thickness rat skin:

$$\log k_p = -1.400(\pm 0.261)\log V_I/100/\beta - 2.613(\pm 0.084) \quad (22)$$

$n = 5$ $r^2 = 0.905$ S.D. = 0.071 F = 28.7

For egg shell membrane:

$$\log k_p = 0.182(\pm 0.186)\log V_I/100/\beta - 2.063(\pm 0.060) \quad (23)$$

$n = 5$ $r^2 = 0.243$ S.D. = 0.050 F = 0.97

Table 26 Logarithm of permeability coefficient of model solutes permeated through three biological membranes and logarithm of the ratio between molecular volume and solute hydrogen-bond basicity of model solutes (n=4)

Solute	log (V_I/100/β)	log k_p		
		Human	Rat	Egg
Acetophenone	0.149	-2.696	-2.745	-2.057
4-Methylacetophenone	0.198	-2.415	-2.932	-2.028
Phenol	0.211	-1.785	-2.495	-1.685
4-Bromophenol	0.367	-1.894	-1.958	-2.000
4-Chlorophenol	0.435	-1.873	-2.718	-2.110
Nitrobenzene	0.323	-2.316	-3.078	-1.929
3,4-Xylenol	0.320	-2.388	-3.131	-2.036
Chlorocresol	0.498	-1.983	-3.265	-1.993

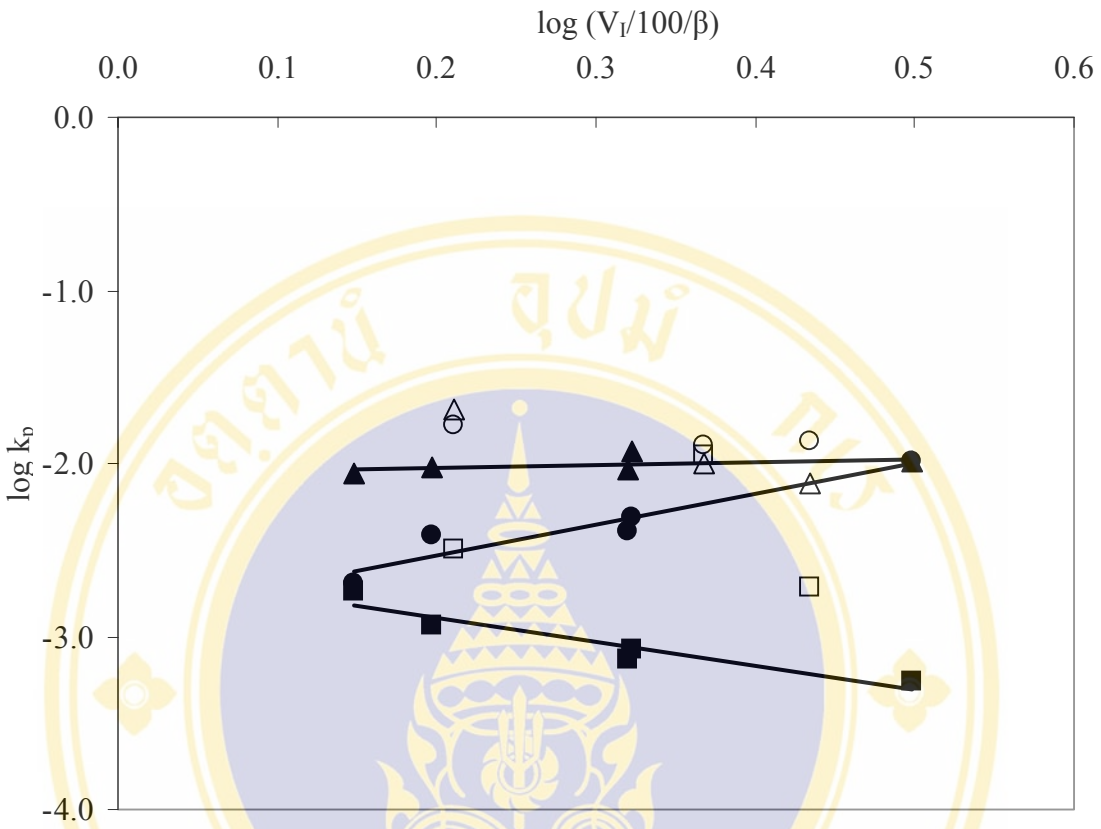

Figure 26 Comparison of permeability property of human epidermis, full-thickness rat skin, egg shell membrane (n=4).

acetophenone, 4-methylacetophenone, nitrobenzene, 3,4-xylenol, and chlorocresol permeated through human epidermis (●), acetophenone, 4-methylacetophenone, nitrobenzene, 3,4-xylenol, and chlorocresol permeated through full-thickness rat skin (■), acetophenone, 4-methylacetophenone, nitrobenzene, 3,4-xylenol, and chlorocresol permeated through egg shell membrane (▲), phenol, 4-bromophenol, 4-chlorophenol permeated through human epidermis (○), phenol, 4-bromophenol, 4-chlorophenol permeated through full-thickness rat skin (□), phenol, 4-bromophenol, 4-chlorophenol permeated through egg shell membrane (Δ)

From equations 21-23, it was found that the positive relative contribution of log $V_I/100/\beta$ value to log k_p value was obtained for permeation of five model solutes through human epidermis. In contrast, the negative relative contribution of log $V_I/100/\beta$ value to log k_p value was obtained for permeation of five model solutes through full-thickness rat skin. Poor relationship between log $V_I/100/\beta$ value and log k_p was obtained for permeation of five model solutes through egg shell membrane. This may be explained by anatomy and physiology of human skin, rat skin, and egg shell membrane. Both of full-thickness human and rat skin compose of three tissue layers, i.e., epidermis, dermis, and the underlying dermis of connective tissue and subcutaneous fat. The epidermis barrier function thus resides mainly in the stratum corneum. This has a bricks and mortar structure, analogous to a wall. The corneocytes consisting of hydrated keratin comprise the bricks. These are embedded in the mortar, which is composed of a complex lipid mixture of ceramides, fatty acids, cholesterol and cholesterol ester, formed into multiple-bilayers. The relatively aqueous environment of the dermis is higher than epidermis (stratum corneum). For the underlying dermis tissue was usually removed when skin was used *in vitro* experiment (1-3,32). Results from Figure 26 suggest that, solute with high log $V_I/100/\beta$ value could permeate through human epidermis more. It may be because solute which has relatively high lipophilic characteristic (high log $V_I/100/\beta$ value) could partition into the stratum corneum layer more than another one that has relatively hydrophilic characteristic (low log $V_I/100/\beta$ value). On the other hand, this relationship was observed conversely when solute permeated through full-thickness rat skin. It may be because the solute with high lipophilic characteristic, penetrated through the stratum corneum layer into dermis layer, which is more aqueous than stratum corneum, in which this solute was poorly soluble. This results in decrease in the permeability of the solutes. For permeation of solute through egg shell membrane, mainly consisting of mesh of keratin fibers with albuminous cementing material (59). From equation 20 and Figure 26, it is shown that molecular volume could not affect the permeability of solute through this membrane. It may be explained by structure of egg shell membrane. As this membrane does not compose of lipid and when the membrane was placed between two half diffusion cells which were filled with phosphate buffer, the pores on membrane may be filled with aqueous medium. In addition, the pore size of egg shell membrane may be up to 28

microns (59) which is larger than molecular size of model solute. Therefore, the permeation of these model solutes through this membrane will be depending mainly on solvatochromic parameters and will not be affected by molecular volume.

4. Effect of treatment and storage conditions on barrier functions of rat skin

Most of *in vitro* experiments usually used the rat skin immediately after it was cut from rat to ensure that skin permeability property is not changed. It is well recognized that there is high intrasubject and intersubject variability in animal and human skin permeability. Thus, a large number of replications for each of dosage regimen are recommended. In practical, freshly excised rat skin may be inconvenient to do, because it is need a lot of skins to obtain the reliable result. Some investigators reported that both length of time in the frozen stage and the temperature maintained throughout the storage process of hairless rat skin and excised human skin may affect iontophoretic transport of sodium ion, salicylic acid and changing of electrical resistance of human skin (32-34). This work was designed to find the optimal condition to preserve rat skin for 13-15 days without any change in skin permeability. This purpose has two reasons, i.e., economical and moral ones. Sharing organs and skin of one rat among researchers results in reducing cost and saving life of a large number of rats. Sörensen modified phosphate buffer pH 7.4, 0.9%w/v normal saline which are common isotonic solution, and 10%w/v glycerine were used as pretreated solution. 10% Glycerine was used to retard ice crystal formation which may damage skin which leads to change the barrier property of skin.

The cumulative amount of solute per unit area of acyclovir and acetophenone diffused through full-thickness rat skin of both sexes during 6 hours at 37 $\pm$ 1ºC is presented in Tables 27-30 and Figures 27-30, respectively. Full-thickness rat skins were pretreated with Sörensen modified phosphate buffer pH 7.4, 0.9%w/v normal saline, or 10%w/v glycerine and stored at -20ºC for 13-15 days before used in experiment. The calculations of flux, permeability coefficient, and lag time values of two model solutes in this experiment are presented in Tables 31-34. From Figures 27-30 and Tables 27-30, it was found that acyclovir permeated through full-thickness rat skin of both sexes without lag time, whereas acetophenone permeated through these skins with lag time of about 40-80 min. This result can be explained using the same

Table 27 Cumulative amount per unit area of acyclovir permeated through male full-thickness rat skin pretreated and stored at four conditions, for 6 hours at 37 ± 1ºC

Time	Cumulative amount of solute (µg/cm^2)[a]			
(min)	Control	SMPB pH 7.4	0.9% NSS	10% Glycerine
0	0.00 ± 0.00	0.00 ± 0.00	0.00 ± 0.00	0.00 ± 0.00
15	38.19 ± 21.36	22.63 ± 7.11	35.62 ± 20.31	25.85 ± 5.73
30	51.46 ± 28.27	31.80 ± 11.02	56.66 ± 34.65	38.12 ± 8.37
45	65.45 ± 36.72	41.76 ± 15.92	76.48 ± 49.24	49.54 ± 13.99
60	77.12 ± 44.91	53.68 ± 21.67	94.60 ± 61.82	62.39 ± 20.23
75	89.70 ± 53.27	65.90 ± 27.12	112.95 ± 76.18	74.88 ± 26.79
90	103.78 ± 64.24	77.54 ± 34.80	129.67 ± 90.08	87.02 ± 33.59
105	113.65 ± 69.81	88.82 ± 41.45	147.10 ± 104.71	100.50 ± 42.77
120	124.02 ± 77.65	100.73 ± 48.98	163.26 ± 119.31	112.35 ± 51.04
135	133.66 ± 84.61	113.92 ± 56.14	179.41 ± 133.99	121.76 ± 56.45
150	145.58 ± 94.03	127.48 ± 64.36	195.56 ± 149.42	131.68 ± 62.72
165	156.23 ± 101.99	138.55 ± 71.03	209.70 ± 162.75	144.41 ± 72.50
180	169.01 ± 113.52	148.19 ± 78.68	224.67 ± 176.85	151.23 ± 75.22
210	184.28 ± 124.02	178.35 ± 96.61	253.33 ± 204.59	179.86 ± 102.74
240	203.48 ± 139.27	202.05 ± 113.32	282.87 ± 234.24	201.75 ± 121.73
270	225.26 ± 156.21	225.87 ± 128.52	333.25 ± 242.04	222.06 ± 137.85
300	243.07 ± 170.91	250.48 ± 147.47	365.16 ± 266.43	241.60 ± 153.75
330	262.29 ± 187.58	276.47 ± 166.01	397.88 ± 291.15	261.23 ± 170.47
360	280.75 ± 203.03	299.78 ± 183.22	431.11 ± 317.81	281.18 ± 188.08

[a] the values shown are mean ± S.D. from 4 experiments

Table 28 Cumulative amount per unit area of acyclovir permeated through female full-thickness rat skin pretreated and stored at four conditions, for 6 hours at 37 ± 1ºC

Time	Cumulative amount of solute (µg/cm^2)[a]			
(min)	Control	SMPB pH 7.4	0.9% NSS	10% Glycerine
0	0.00 ± 0.00	0.00 ± 0.00	0.00 ± 0.00	0.00 ± 0.00
15	29.52 ± 5.25	36.55 ± 22.95	40.12 ± 26.45	38.76 ± 21.09
30	40.41 ± 8.58	51.01 ± 30.98	56.14 ± 37.28	53.44 ± 29.41
45	51.00 ± 13.30	61.37 ± 35.99	75.36 ± 52.05	68.82 ± 39.82
60	60.70 ± 18.45	72.98 ± 43.35	91.79 ± 64.38	83.96 ± 51.17
75	69.28 ± 22.82	83.30 ± 47.91	108.54 ± 77.42	101.34 ± 63.16
90	79.16 ± 28.94	95.16 ± 56.14	124.58 ± 89.97	116.34 ± 76.05
105	85.71 ± 31.62	103.82 ± 60.65	141.76 ± 103.78	134.04 ± 92.44
120	94.95 ± 37.51	115.07 ± 70.07	159.86 ± 119.41	150.49 ± 106.08
135	103.14 ± 42.34	126.25 ± 78.81	177.06 ± 133.44	166.74 ± 120.35
150	112.97 ± 49.34	132.89 ± 83.26	204.23 ± 158.31	182.49 ± 135.39
165	122.38 ± 56.03	141.40 ± 89.53	215.68 ± 167.61	198.97 ± 148.56
180	130.33 ± 62.02	155.19 ± 99.56	232.32 ± 182.38	215.13 ± 163.45
210	146.17 ± 75.11	170.82 ± 111.84	262.05 ± 207.92	244.13 ± 188.84
240	163.18 ± 90.12	184.11 ± 121.59	291.83 ± 235.25	274.08 ± 219.16
270	179.30 ± 104.39	200.12 ± 133.99	349.74 ± 233.70	320.88 ± 212.19
300	197.03 ± 121.13	218.60 ± 150.71	388.87 ± 258.95	355.80 ± 240.05
330	213.69 ± 135.56	236.39 ± 158.12	425.46 ± 281.44	387.01 ± 259.73
360	229.58 ± 150.33	247.82 ± 169.39	458.35 ± 304.95	418.21 ± 274.38

[a] the values shown are mean ± S.D. from 4 experiments

Table 29 Cumulative amount per unit area of acetophenone permeated through male full-thickness rat skin pretreated and stored at four conditions, for 6 hours at 37 ± 1ºC

Time	Cumulative amount of solute (μg/cm^2)[a]			
(min)	Control	SMPB pH 7.4	0.9% NSS	10% Glycerine
0	0.00 ± 0.00	0.00 ± 0.00	0.00 ± 0.00	0.00 ± 0.00
15	52.36 ± 62.27	19.68 ± 5.29	47.57 ± 24.16	26.81 ± 15.17
30	101.36 ± 146.22	42.41 ± 25.80	112.54 ± 92.51	74.95 ± 40.67
45	172.17 ± 248.47	82.73 ± 66.29	191.08 ± 169.52	147.32 ± 77.39
60	252.72 ± 353.42	136.44 ± 115.20	291.34 ± 270.31	233.25 ± 109.83
75	345.18 ± 466.47	203.22 ± 173.87	391.69 ± 366.75	325.90 ± 149.14
90	434.45 ± 561.57	277.57 ± 232.30	500.47 ± 470.55	446.45 ± 201.44
105	547.04 ± 665.49	360.37 ± 304.25	643.23 ± 573.25	576.87 ± 247.44
120	653.04 ± 771.36	452.29 ± 371.84	762.02 ± 684.43	691.62 ± 282.54
135	776.95 ± 882.30	560.79 ± 443.34	906.78 ± 821.32	815.82 ± 323.34
150	889.66 ± 989.89	680.00 ± 484.99	1,046.28 ± 943.67	944.96 ± 371.32
165	1,019.35 ± 1,100.65	779.38 ± 583.67	1,191.34 ± 1,055.53	1,088.42 ± 401.20
180	1,163.34 ± 1,221.41	889.73 ± 651.64	1,335.04 ± 1,175.26	1,212.40 ± 441.53
210	1,464.47 ± 1,471.58	1,125.64 ± 797.16	1,594.18 ± 1,324.20	1,470.14 ± 500.41
240	1,749.61 ± 1,672.68	1,359.51 ± 935.38	1,884.96 ± 1,523.74	1,750.65 ± 575.21
270	2,043.24 ± 1,908.79	1,584.41 ± 1,045.83	2,189.35 ± 1,735.27	2,036.96 ± 661.49
300	2,343.22 ± 2,127.58	1,839.65 ± 1,152.47	2,580.04 ± 2,040.64	2,345.80 ± 744.88
330	2,698.16 ± 2,405.06	2,110.61 ± 1,273.94	2,939.34 ± 2,352.16	2,637.73 ± 823.22
360	3,059.36 ± 2,648.92	2,381.79 ± 1,399.77	3,305.97 ± 2,592.28	2,979.73 ± 923.21

[a] the values shown are mean ± S.D. from 4 experiments

Table 30 Cumulative amount per unit area of acetophenone permeated through female full-thickness rat skin pretreated and stored at four conditions, for 6 hours at 37 ± 1ºC

Time	Cumulative amount of solute (μg/cm^2)[a]			
(min)	Control	SMPB pH 7.4	0.9% NSS	10% Glycerine
0	0.00 ± 0.00	0.00 ± 0.00	0.00 ± 0.00	0.00 ± 0.00
15	12.40 ± 1.99	45.34 ± 28.77	26.64 ± 15.84	27.85 ± 9.34
30	27.09 ± 3.58	110.48 ± 75.08	37.71 ± 17.01	48.09 ± 11.32
45	52.97 ± 7.95	192.27 ± 122.79	57.16 ± 21.05	79.64 ± 15.49
60	89.08 ± 14.14	292.44 ± 169.98	85.56 ± 26.32	122.42 ± 20.86
75	133.68 ± 22.28	399.64 ± 218.26	122.16 ± 36.49	172.48 ± 25.50
90	187.98 ± 35.13	461.89 ± 180.50	168.38 ± 57.52	228.83 ± 28.10
105	249.60 ± 47.64	571.24 ± 222.49	213.24 ± 64.78	288.62 ± 36.21
120	318.12 ± 61.45	700.11 ± 249.30	272.41 ± 78.72	357.25 ± 52.37
135	398.72 ± 84.07	912.29 ± 368.13	332.04 ± 93.04	433.13 ± 58.54
150	475.06 ± 97.73	1,059.07 ± 427.23	405.87 ± 110.58	518.12 ± 66.75
165	574.51 ± 118.52	1,238.47 ± 503.33	477.88 ± 130.66	602.86 ± 83.79
180	666.31 ± 139.60	1,394.02 ± 567.53	557.38 ± 156.40	691.18 ± 95.95
210	872.83 ± 170.64	1,716.24 ± 680.28	727.83 ± 193.40	890.89 ± 84.37
240	1,080.25 ± 195.85	2,059.79 ± 828.47	903.42 ± 227.75	1,106.89 ± 96.69
270	1,312.33 ± 250.26	2,405.65 ± 965.54	1,089.72 ± 276.62	1,298.84 ± 134.52
300	1,533.76 ± 237.67	2,789.78 ± 1,127.56	1,323.94 ± 326.04	1,489.34 ± 164.21
330	1,751.90 ± 277.24	3,107.66 ± 1,228.05	1,559.23 ± 367.95	1,726.98 ± 178.63
360	2,048.30 ± 347.97	3,497.88 ± 1,388.13	1,790.04 ± 425.23	1,953.80 ± 214.81

[a] the values shown are mean ± S.D. from 4 experiments

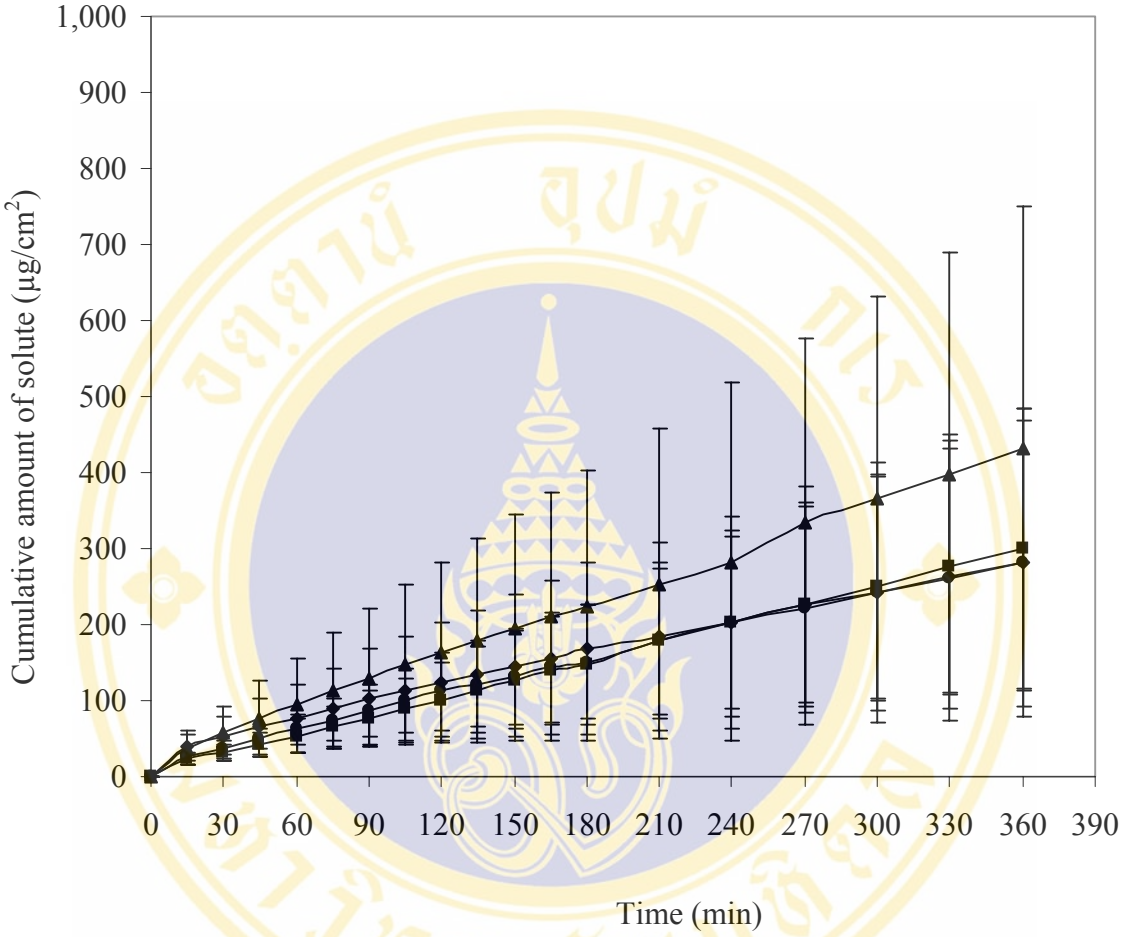

Figure 27 Cumulative amount per unit area of acyclovir permeated through male full-thickness rat skin pretreated and stored at four conditions, for 6 hours at 37 ± 1ºC (n=4).

(◆) Control group (■) SMPB pH 7.4 group

(▲) 0.9% NSS group (●) 10% Glycerine group

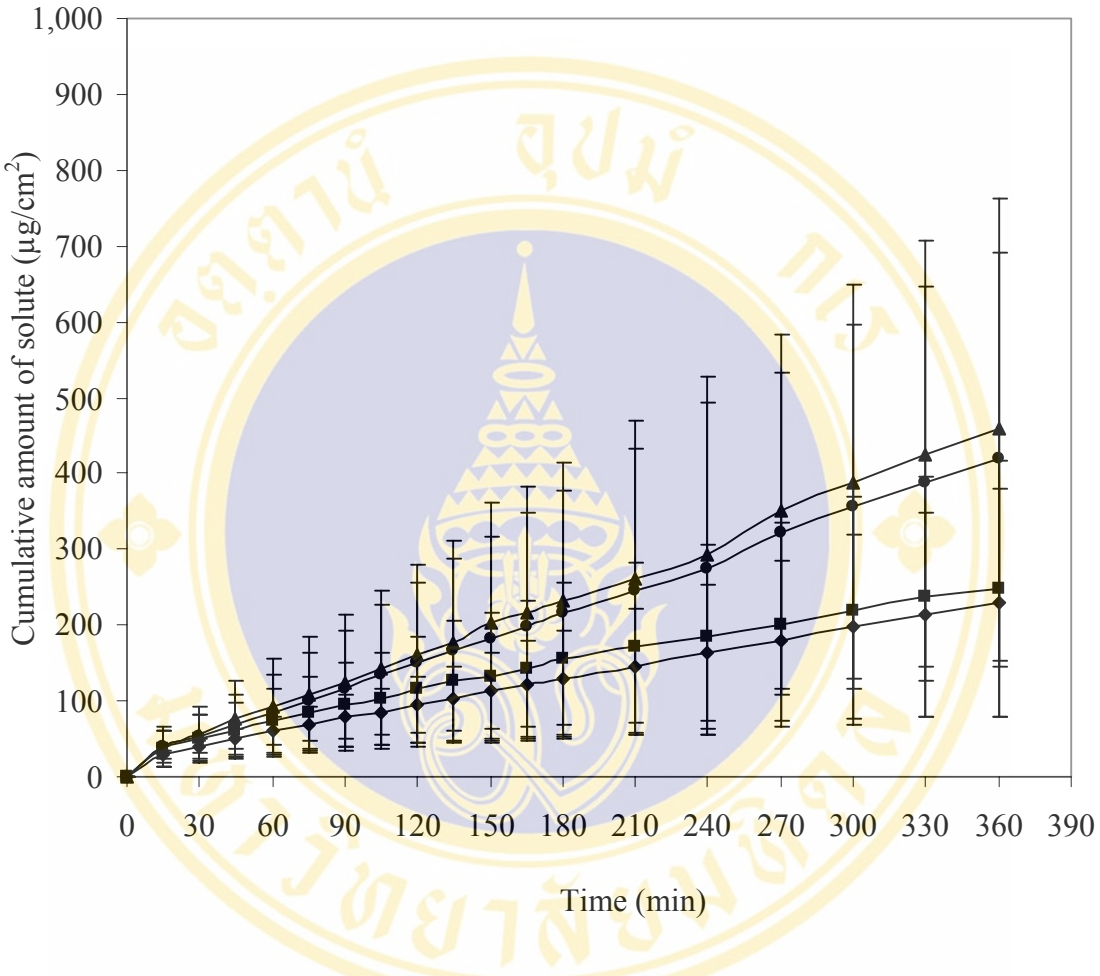

Figure 28 Cumulative amount per unit area of acyclovir permeated through female full-thickness rat skin pretreated and stored at four conditions, for 6 hours at 37 ± 1ºC (n=4).

(◆) Control group (■) SMPB pH 7.4 group

(▲) 0.9% NSS group (●) 10% Glycerine group

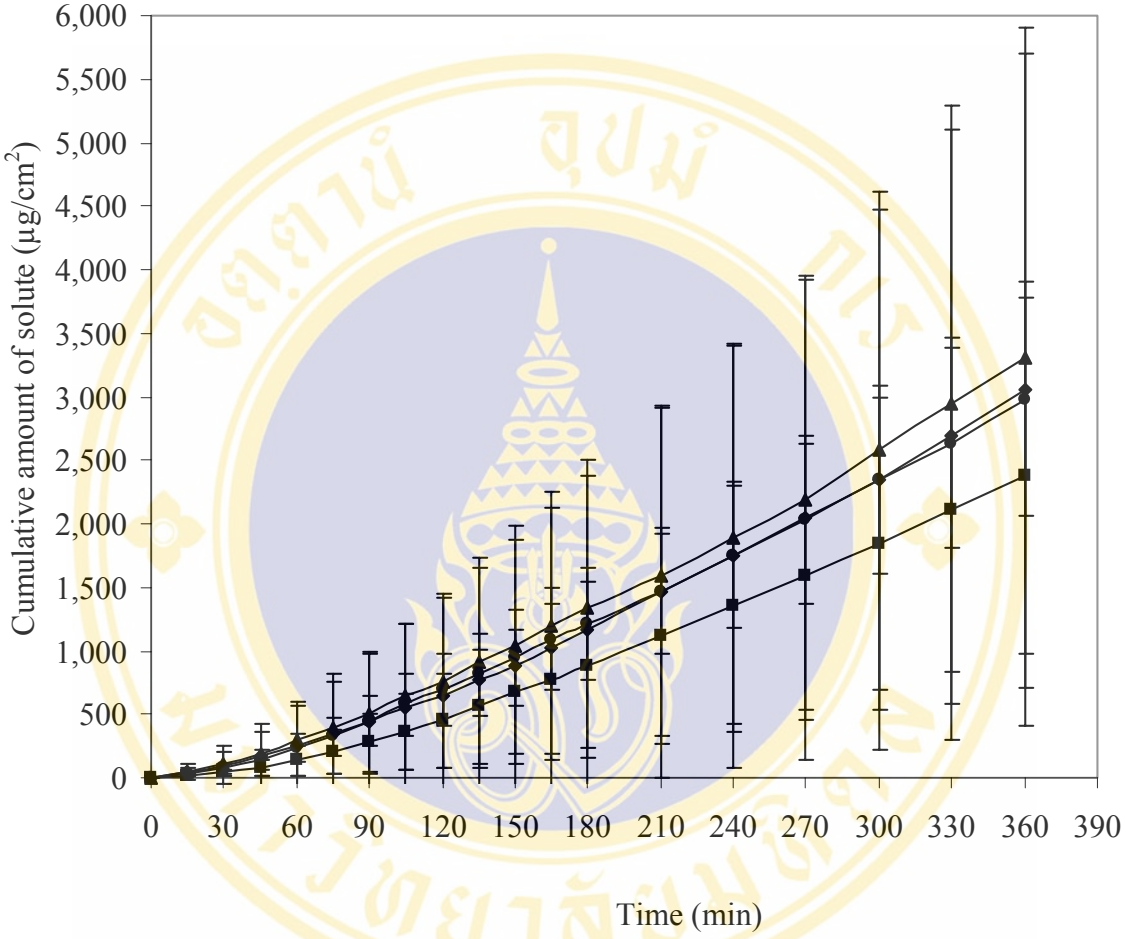

Figure 29 Cumulative amount per unit area of acetophenone permeated through male full-thickness rat skin pretreated and stored at four conditions, for 6 hours at 37 ± 1ºC (n=4).

(◆) Control group (■) SMPB pH 7.4 group

(▲) 0.9% NSS group (●) 10% Glycerine group

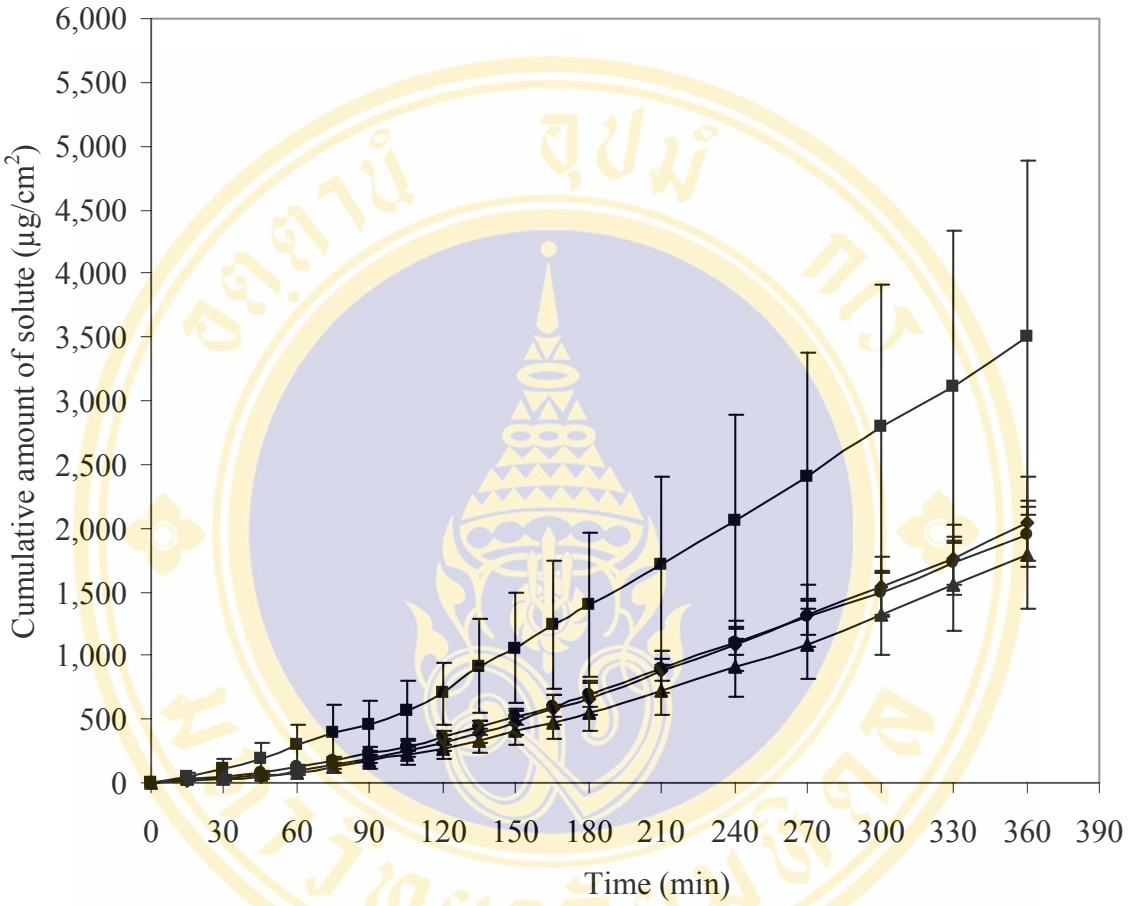

Figure 30 Cumulative amount per unit area of acetophenone permeated through female full-thickness rat skin pretreated and stored at four conditions, for 6 hours at 37 ± 1ºC (n=4).

(◆) Control group (■) SMPB pH 7.4 group

(▲) 0.9% NSS group (●) 10% Glycerine group

reason as the result in section 3 that acyclovir permeated through full-thickness rat skin more than human epidermis, although full-thickness rat skin is thicker than human epidermis. As discussed above, acyclovir is a hydrophilic solute. It could not permeate across the stratum corneum layer, because this layer consists of lipid. However it could permeate through skin by diffusing through hair follicles which are large available area of Wistar rat skin. Since, hair follicles pass deep into dermis layer, it may act as a shunt route which can help decrease time prior to steady state diffusion. This route is important for acyclovir permeating through the skin but it is not important for acetophenone. Since, acetophenone is a lipophilic solute, it would permeate through the skin by crossing the stratum corneum layer. In addition, available permeation area of the stratum corneum layer is relatively higher than hair follicles, thus, crossing through the stratum corneum of acetophenone through rat skin become the major route and the lag time could be observed. From Tables 31-34 and Figures 31-32, it was found that there was high variation in permeability coefficient of both model solutes permeated through four rat skin groups pretreated, except the result of acetophenone permeating through female rat skins of all conditions. These results showing high variation was occurring between intersubject (i.e., one rat was used in two permeation experiments). This high variation may occur due to skin preparation technique using hand razor to remove hair which might damage the stratum corneum layer leading to change of barrier property of skin. For comparison the effect of treatment and storage condition, the statistical Kruskal-Wallis test was used, because the variances of these results were different. The statistical analysis showed in Table 35 suggested that, the permeability coefficient of acyclovir or acetophenone through three rat skin groups pretreated differently did not different from the control group (p-value > 0.05). At the same time, no difference in permeability was found between male and female rat skins for both model solutes (p-value > 0.05).

5. Effect of enhancers and vehicles on percutaneous absorption of acyclovir

The cumulative amount per unit area of acyclovir permeated through human epidermis during 6 hours at 37 $\pm$ 1ºC by using 0.1%w/v acyclovir and enhancer in 50%v/v ethanol/water or Sörensen modified phosphate buffer pH 7.4 as donor solution, are shown in Table 36 and Figure 33, respectively. It was found that, the cumulative

Table 31 Effect of treatment and storage condition on barrier functions of full-thickness male rat skin using acyclovir as model solute

Treatment and storage condition	Sample	Flux ($\mu g/cm^2 \cdot min$)	$k_p \times 10^3$ (cm/min)	log k_p	Lag time (min)
Control	1	0.009	0.207	-3.685	-59.434
0ºC,	2	0.009	0.213	-3.671	-54.070
<10 hours	3	0.002	0.040	-4.393	-178.899
	4	0.002	0.040	-4.394	-129.156
	Average ± S.D.	0.005 ± 0.004	0.125 ± 0.098	-4.036 ± 0.413	-105.390 ± 59.761
SMPB pH 7.4	1	0.011	0.246	-3.610	42.565
-20ºC,	2	0.012	0.266	-3.574	2.080
13-15 days	3	0.003	0.080	-4.099	-105.126
	4	0.002	0.052	-4.282	-47.331
	Average ± S.D.	0.007 ± 0.005	0.161 ± 0.111	-3.891 ± 0.354	-26.953 ± 63.775
0.9% NSS	1	0.017	0.379	-3.421	-16.007
-20ºC,	2	0.013	0.306	-3.514	-48.484
13-15 days	3	0.001	0.027	-4.562	-312.798
	4	0.002	0.036	-4.447	-204.326
	Average ± S.D.	0.008 ± 0.008	0.187 ± 0.182	-3.986 ± 0.602	-145.404 ± 138.600
10%Glycerine	1	0.013	0.288	-3.541	18.105
-20ºC,	2	0.009	0.212	-3.674	-5.641
13-15 days	3	0.002	0.043	-4.371	-194.486
	4	0.002	0.048	-4.319	-168.674
	Average ± S.D.	0.006 ± 0.005	0.148 ± 0.122	-3.976 ± 0.430	-87.674 ± 109.375

Table 32 Effect of treatment and storage condition on barrier functions of full-thickness female rat skin using acyclovir as model solute

Treatment and storage condition	Sample	Flux ($\mu g/cm^2 \cdot min$)	$k_p \times 10^3$ (cm/min)	log k_p	Lag time (min)
Control	1	0.006	0.149	-3.826	-41.623
0ºC,	2	0.009	0.210	-3.677	4.262
<10 hours	3	0.001	0.033	-4.482	-267.439
	4	0.002	0.038	-4.420	-197.079
	Average ± S.D.	0.005 ± 0.004	0.108 ± 0.087	-4.101 ± 0.409	-125.470 ± 127.989
SMPB pH 7.4	1	0.007	0.166	-3.779	-28.882
-20ºC,	2	0.009	0.197	-3.706	-88.087
13-15 days	3	0.002	0.044	-4.354	-144.754
	4	0.001	0.030	-4.521	-285.811
	Average ± S.D.	0.005 ± 0.004	0.109 ± 0.085	-4.090 ± 0.408	-136.884 ± 109.980
0.9% NSS	1	0.016	0.366	-3.436	-20.787
-20ºC,	2	0.015	0.342	-3.466	-37.506
13-15 days	3	0.002	0.056	-4.253	-102.949
	4	0.002	0.040	-4.403	-136.643
	Average ± S.D.	0.009 ± 0.008	0.201 ± 0.177	-3.890 ± 0.510	-74.471 ± 54.543
10%Glycerine	1	0.014	0.310	-3.509	-8.438
-20ºC,	2	0.017	0.384	-3.416	-17.183
13-15 days	3	0.002	0.046	-4.338	-135.341
	4	0.002	0.040	-4.393	-183.994
	Average ± S.D.	0.008 ± 0.008	0.195 ± 0.178	-3.914 ± 0.523	-86.239 ± 87.157

Table 33 Effect of treatment and storage condition on barrier functions of full-thickness male rat skin using acetophenone as model solute

Treatment and storage condition	Sample	Flux ($\mu g/cm^2 \cdot min$)	$k_p \times 10^3$ (cm/min)	log k_p	Lag time (min)
Control	1	0.033	0.768	-3.114	84.393
0ºC,	2	0.042	0.966	-3.015	93.976
<10 hours	3	0.066	1.513	-2.820	64.668
	4	0.172	3.944	-2.404	35.768
	Average ± S.D.	0.078 ± 0.064	1.798 ± 1.465	-2.838 ± 0.314	69.702 ± 25.703
SMPB pH 7.4	1	0.029	0.672	-3.172	72.038
-20ºC,	2	0.031	0.703	-3.153	83.422
13-15 days	3	0.111	2.541	-2.595	52.925
	4	0.082	1.880	-2.726	60.901
	Average ± S.D.	0.063 ± 0.040	1.449 ± 0.920	-2.912 ± 0.295	67.322 ± 13.291
0.9% NSS	1	0.033	0.760	-3.119	66.419
-20ºC,	2	0.039	0.886	-3.052	49.423
13-15 days	3	0.085	1.959	-2.708	52.713
	4	0.151	3.475	-2.459	18.134
	Average ± S.D.	0.077 ± 0.055	1.770 ± 1.258	-2.835 ± 0.309	46.672 ± 20.400
10%Glycerine	1	0.046	1.054	-2.977	76.340
-20ºC,	2	0.064	1.477	-2.831	-0.613
13-15 days	3	0.091	2.095	-2.679	54.824
	4	0.093	2.144	-2.669	44.972
	Average ± S.D.	0.074 ± 0.023	1.693 ± 0.523	-2.789 ± 0.146	43.881 ± 32.425

Table 34 Effect of treatment and storage condition on barrier functions of full-thickness female rat skin using acetophenone as model solute

Treatment and storage condition	Sample	Flux ($\mu g/cm^2 \cdot min$)	$k_p \times 10^3$ (cm/min)	log k_p	Lag time (min)
Control	1	0.054	1.248	-2.904	76.001
0ºC,	2	0.068	1.553	-2.809	74.019
<10 hours	3	0.047	1.077	-2.968	83.300
	4	0.050	1.137	-2.944	74.717
	Average ± S.D.	0.055 ± 0.009	1.254 ± 0.212	-2.906 ± 0.070	77.009 ± 4.273
SMPB pH 7.4	1	0.121	2.777	-2.556	49.597
-20ºC,	2	0.038	0.884	-3.054	51.440
13-15 days	3	0.105	2.403	-2.619	51.260
	4	0.100	2.297	-2.639	57.012
	Average ± S.D.	0.091 ± 0.036	2.090 ± 0.830	-2.717 ± 0.227	52.327 ± 3.231
0.9% NSS	1	0.051	1.178	-2.929	64.690
-20ºC,	2	0.028	0.634	-3.198	71.227
13-15 days	3	0.049	1.128	-2.948	72.911
	4	0.054	1.231	-2.910	92.252
	Average ± S.D.	0.045 ± 0.012	1.043 ± 0.276	-2.996 ± 0.135	75.270 ± 11.864
10%Glycerine	1	0.047	1.083	-2.965	55.434
-20ºC,	2	0.057	1.304	-2.885	88.110
13-15 days	3	0.050	1.144	-2.942	65.311
	4	0.060	1.372	-2.863	67.244
	Average ± S.D.	0.053 ± 0.006	1.226 ± 0.135	-2.914 ± 0.048	69.025 ± 13.735

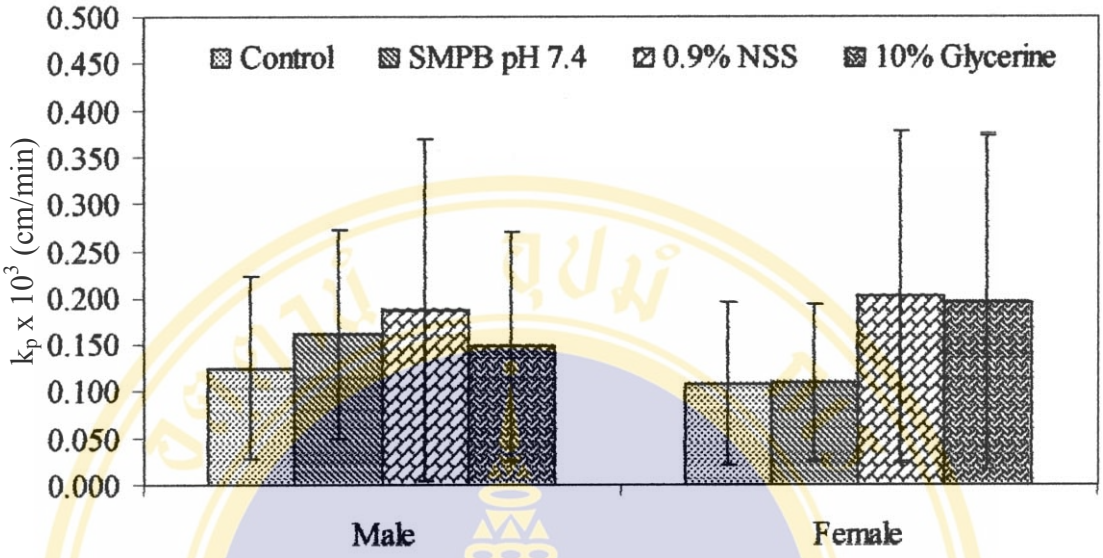

Figure 31 Comparison of permeability coefficient of acyclovir through full-thickness rat skin pretreated and stored at four conditions (n=4).

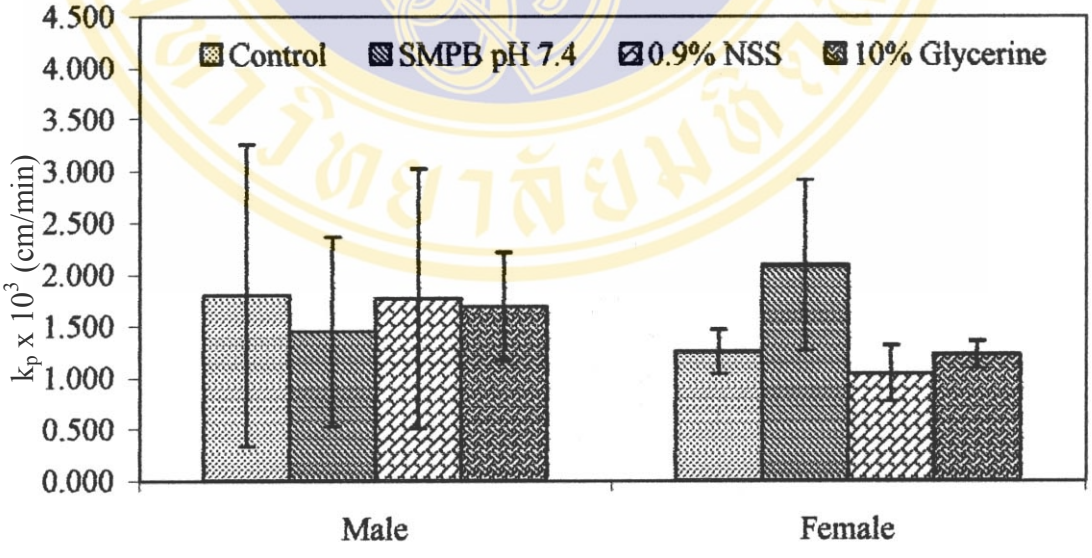

Figure 32 Comparison of permeability coefficient of acetophenone through full-thickness rat skin pretreated and stored at four conditions (n=4)

Table 35 Comparison between permeability coefficients of two model solutes through four pretreated rat skins by using Kruskal-Wallis test

Comparison	Group	*p*-value	
		Acyclovir	Acetophenone
Between sex	Control	0.384	0.773
	SMPB pH 7.4	0.248	0.248
	0.9% NSS	0.564	0.564
	10% Glycerine	0.773	0.248
Between treatment condition	Male	0.813	0.814
	Female	0.533	0.356

Table 36 Cumulative amount per unit area of acyclovir permeate through human epidermis during 6 hours at 37 ± 1ºC by using 0.1%w/v acyclovir and enhancer in 50%v/v ethanol/water as donor solution

Time	Cumulative amount of solute (μg/cm^2) [a]			
(min)	50% Ethanol	0.075% Capsaicin	0.075% Nonivamide	4% *l*-Menthol
0	0.00 ± 0.00	0.00 ± 0.00	0.00 ± 0.00	0.00 ± 0.00
15	6.70 ± 3.21	3.45 ± 1.67	5.19 ± 3.18	17.91 ± 20.15
30	6.76 ± 3.10	4.41 ± 2.30	5.60 ± 3.08	27.20 ± 29.61
45	6.92 ± 3.06	5.08 ± 2.80	6.58 ± 3.50	33.52 ± 37.98
60	8.18 ± 3.59	6.16 ± 3.61	8.00 ± 4.38	38.92 ± 48.28
75	8.19 ± 3.38	7.02 ± 4.10	8.32 ± 4.18	47.92 ± 56.17
90	8.98 ± 3.75	7.91 ± 4.50	9.07 ± 4.74	60.71 ± 62.93
105	9.50 ± 3.14	9.00 ± 4.67	11.46 ± 6.73	82.62 ± 76.21
120	9.35 ± 4.08	9.48 ± 5.44	12.90 ± 8.02	101.37 ± 92.30
135	10.79 ± 4.02	10.95 ± 5.22	12.72 ± 6.03	79.55 ± 94.31
150	11.20 ± 4.62	11.61 ± 5.45	14.28 ± 6.91	87.38 ± 98.57
165	11.17 ± 4.77	12.64 ± 5.95	14.93 ± 7.12	99.51 ± 103.16
180	11.41 ± 4.53	13.82 ± 6.36	15.56 ± 7.27	113.58 ± 100.28
210	11.71 ± 5.57	15.58 ± 6.23	16.82 ± 7.80	147.76 ± 142.86
240	12.61 ± 5.88	16.93 ± 6.16	18.22 ± 8.15	160.16 ± 148.58
270	13.37 ± 6.27	19.04 ± 5.45	19.97 ± 8.62	172.39 ± 153.07
300	14.14 ± 6.84	20.53 ± 5.81	21.39 ± 9.59	188.94 ± 163.31
330	14.93 ± 7.18	21.98 ± 5.68	23.75 ± 10.96	203.85 ± 171.36
360	15.16 ± 6.84	23.17 ± 6.51	26.12 ± 11.95	216.46 ± 172.44

[a] the values shown are mean ± S.D. from 4 experiments

Table 36 (continued) Cumulative amount per unit area of acyclovir permeate through human epidermis during 6 hours at 37 ± 1ºC by using 0.1%w/v acyclovir and enhancer in 50%v/v ethanol/water as donor solution

Time	Cumulative amount of solute (μg/cm^2) [a]		
(min)	4% Methyl salicylate	10% Tween 80	10% Tween 80[b]
0	0.00 ± 0.00	0.00 ± 0.00	0.00 ± 0.00
15	84.12 ± 4.11	5.04 ± 3.73	0.52 ± 1.04
30	109.67 ± 6.84	7.92 ± 6.70	0.63 ± 1.25
45	138.84 ± 13.19	8.84 ± 7.43	0.71 ± 1.00
60	166.81 ± 14.67	10.63 ± 7.03	0.63 ± 1.17
75	199.03 ± 18.44	10.69 ± 7.91	1.05 ± 1.21
90	230.73 ± 25.29	13.16 ± 10.02	0.83 ± 1.39
105	228.44 ± 22.19	14.44 ± 11.29	1.23 ± 1.48
120	253.87 ± 30.32	16.03 ± 11.45	0.96 ± 1.48
135	282.25 ± 38.67	17.10 ± 11.53	1.42 ± 1.71
150	312.97 ± 48.08	16.42 ± 12.92	1.23 ± 1.34
165	305.23 ± 22.18	19.09 ± 14.55	0.96 ± 1.19
180	326.06 ± 25.34	19.59 ± 14.69	0.96 ± 1.19
210	347.70 ± 27.65	21.62 ± 16.64	0.96 ± 1.19
240	350.50 ± 5.63	23.55 ± 17.06	1.28 ± 1.80
270	353.63 ± 22.84	24.96 ± 18.95	1.35 ± 1.93
300	375.03 ± 37.50	26.58 ± 19.71	1.80 ± 2.04
330	380.13 ± 22.02	29.60 ± 25.71	1.55 ± 2.16
360	389.58 ± 25.52	30.88 ± 25.57	2.28 ± 2.04

[a] the values shown are mean ± S.D. from 4 experiments

[b]10% Tween 80 is using 0.1%w/v Acyclovir and 10%w/v Tween 80 in SMPB pH 7.4

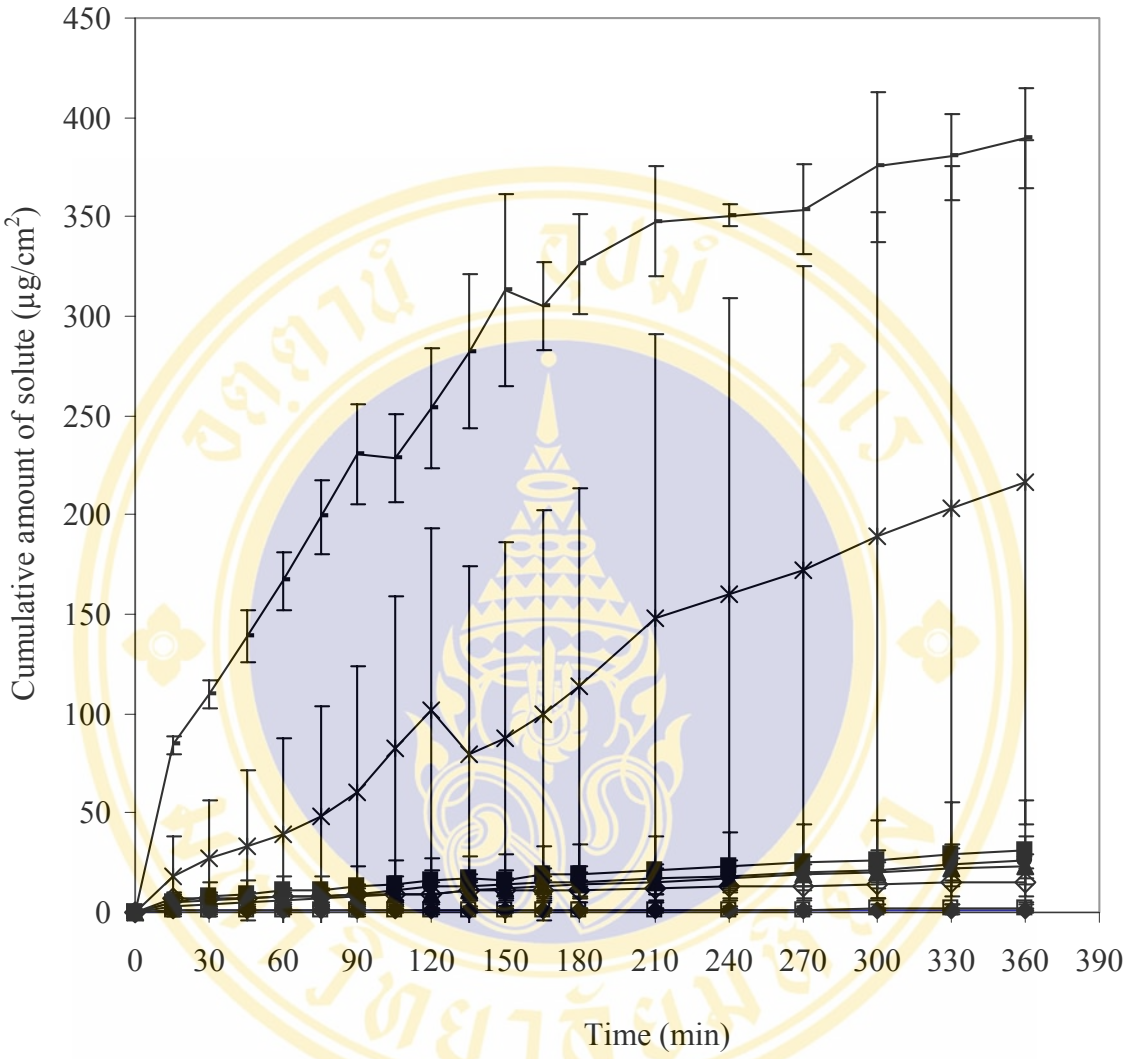

Figure 33 Effect of enhancers and vehicles on percutaneous absorption of acyclovir (n=4).

Donor solution: 0.1%w/v acyclovir in SMPB pH 7.4 (◆), 0.1%w/v acyclovir in 50%v/v ethanol/water (◇), mixture of 0.1%w/v acyclovir and 0.075%w/v capsaicin (▲), 0.075%w/v nonivamide (●), 4%w/v menthol (✶), 4%w/v methyl salicylate (-), or 10%w/v tween 80 (■) in 50%v/v ethanol/water, or 0.1%w/v acyclovir and 10%w/v tween 80 in SMPB pH 7.4 (□).

Receptor solution: SMPB pH 7.4.

amount of acyclovir permeated through human epidermis during 6 hours was increased about 19.2 times when 50%v/v ethanol/water (control 2) was used as donor solvent instead of Sörensen modified phosphate buffer pH 7.4 (control 1). When 10%w/v tween 80 was used as enhancer, it was found that cumulative amount of acyclovir permeated through human epidermis during 6 hours was about 2.9 times as much as that of control 1 when tween 80 in Sörensen modified phosphate buffer pH 7.4 was used, and 39.2 times as much as that of control 1 and 2.0 times as much as that of control 2 when 10%w/v Tween 80 in 50%v/v ethanol/water was used. When other enhancers in 50%v/v ethanol/water system was used, it was found that cumulative amount of acyclovir permeated through human epidermis during 6 hours was about 32.8 times as much as that of control 1 and 1.7 times as much as that of control 2 when 0.075%w/v capsaicin was used, about 35.1 times as much as that of control 1 and 1.8 times as much as that of control 2 when 0.075%w/v nonivamide was used, about 274.5 times as much as that of control 1 and 14.3 times as much as that of control 2 when 4%w/v *l*-menthol was used, and about 493.1 times as much as that of control 1 and 25.7 times as much as that of control 2 when 4%w/v methyl salicylate was used. Permeation enhancements of several nonpolar and ionic solutes by ethanol/water system have been extensively studied. Sathyan G et al, 1995 (60) suggested that at smaller ethanol volume fractions (<0.8), permeation enhancement due to ethanol dominates, and at large volume fraction (>0.8), dehydration effect is dominant. Kurihara-Bergstrom et al, 1990 (61,62) showed that optimal enhancement of salicylate ion permeation through human skin has been observed with ethanol volume fraction near 0.63. Hatanaka et al, 1993 (61,63) reported a marked enhancement of the permeation rate of seven lipophilic drugs through hairless mouse skin from ethanol concentration over the range 0-60%v/v although no such effect was found for hydrophilic drug (e.g., 5-fluorouracil). Berner et al, 1989 (61,64) reported that an optimal concentration range of ethanol (50-70%v/v) produced a 5-10 times increase in nitroglycerin flux across human skin. Megrab NA et al, 1995 (61) reported that human skin showed a maximum flux of oestradiol at ethanol vehicle content between 40-60%w/w and suggested that the principal mechanism of enhanced flux of ethanol is increase drug solubility in the stratum corneum layer when increasing ethanol concentration up to 20%w/w. Additionally, when increasing

ethanol concentration from 20 to 50%w/w, permeation enhancement is due to ethanol affecting the physico-chemical properties of the stratum coeneum matrix so as to reduce its barrier function resulting in increasing drug uptake. At higher ethanol concentration, the drug flux decreases because of dehydration effect. According to this report, 50%v/v ethanol/water system could enhance the permeability of acyclovir through human epidermis. For enhancing effect study of the selected enhancers, it was found that 4%w/v *l*-menthol showed superior permeability enhancement over the other four enhancers. However, it was found that two samples of human epidermis were torn at 120 minutes and 180 minutes when used *l*-menthol as enhancer. It may be due to skin irritation effect of *l*-menthol and ethanol/water system. This result was supported by Lu MF et al, 1992 (17) who observed skin irritation in rabbits treated with formulations containing 2% menthol or lauric acid in 80%v/v ethanol/water system. They suggested that the combination of a high level of ethanol and chemical enhancer was the main cause of irritation in skin and when the level of ethanol in the vehicle decrease, the skin could generally tolerate the other chemical enhancers better and at higher concentration. A number of researchers have reported the mechanism of *l*-menthol to improve the permeability of many solutes through skin. For example, Kaplun-Frischoff Y et al, 1997 (21) who investigated the effect of *l*-menthol on the stratum corneum lipid by DSC technique, found that the endotherm of the lipid was changed by reducing of peak area and lowering of lipid melting point when using 5 and 17.3% *l*-menthol. They suggested that *l*-menthol, at a concentration identical to that used in these permeation experiments, altered the stratum corneum lipids and, thus may alter the barrier resistance of the skin. Morimoto Y et al, 1993 (18) also found improvement of the permeability of morphine hydrochloride through human skin by using 5% *l*-menthol in 40% ethanol /water. They suggested that this system enhance the permeability of solute by ethanol facilitates the penetration of *l*-menthol into stratum corneum layer and *l*-menthol reduces the permeation resistance of stratum corneum layer, including permeation of solvent is increased. Another suggestion by Sugibayashi K et al, 1995 (19), they suggested that enhancing effect of 5% *l*-menthol in 40% EtOD/D_2O (ethanol-d_6/deuterium oxide) is due to delipidization from skin. They observed markedly delipidization from hairless skin and human skin into the donor compartment and their researching group also found the degree of

delipidization by various ethanol concentrations was paralleled by its enhancement effect. According to this report, the enhancement effect of 4%w/v *l*-menthol in 50%v/v ethanol/water on permeation of acyclovir through human skin may be due to a combination effect between *l*-menthol and ethanol. The UV-spectrophotometry was not specific for determination the amount of acyclovir in permeation system containing capsaicin, nonivamide, tween 80, and methyl salicylate. Because of there was interference from other chemicals. However, it may be possible that 0.075%w/v capsaicin, 0.075%w/v nonivamide, 10%w/v tween 80, and 4%w/v methyl salicylate in 50%v/v ethanol/water, had less effect on permeability of acyclovir through human skin when compared to control 2. Capsaicin, the pungent principle of red pepper, has a variety of therapeutic advantage such as antinociceptive activity. Nonivamide is one of synthetic analogues of capsaicin which has the similar chemical structure and pharmacological profiles to those of capsaicin. Both of them were reported to be a skin permeation enhancer for each other and for ketoprofen, indomethacin, and naproxen (12,14-16). Degim IT et al, 1999 (14) suggested that enhancing mechanism of capsaicin and nonivamide are similar azone, because the structures of these enhancers like azone in terms of molecular size. Therefore it is thought that both of these enhancers will insert its molecule into the lipid bilayers within the intercellular channels and create disruption in their stacking. This will reduce the diffusion resistance of the intercellular domain. The enhancing effect of tween 80, nonionic surfactant, was suggested by Shokri J et al, 2001 (65). They found that when the concentration of tween 80 was increased, the permeability of diazepam through rat skin was increased. The highest permeation rate was observed with the solution containing 1%w/w tween 80. Further the permeation rate was decreased when increased the concentration of tween 80. They suggested that the increase in flux at low enhancer concentration is normally attributed to the ability of surfactant molecules penetrate into the skin and increase its permeability. Reduction of the rate of permeation of drug is attributed to the ability of the surfactant to form micelles and is normally observed only if interaction between micelle and drug occurs. Solubilization of drug species by surfactant micelles decrease the thermodynamic activity of drug and, hence, decrease the driving force of the drug absorption. Therefore, the overall effect of a surfactant on the rate of drug permeation across a

membrane will be a combination of the influence of these two opposing effect. Additionally, Dalvi UG et al, 1981 (65) found that skin permeability was not increased by nonionic surfactants in pure aqueous media. The similar result was found by Cappel MJ and Kreuter J, 1991 (66), various concentration of tween 80 in 0.9% sodium chloride solution were found to have less effect on permeability of methanol and octanol through hairless mouse skin except 100% tween 80. Shahi V et al, 1978 (66,67) also reported that tween 80 was responsible for enhancement of hydrocortisone penetration from isopropyl alcohol/water mixture. The author hypothesized that the nature of the medium could influence the interaction between nonionic surfactant and the skin permeation. Methyl salicylate was reported to have enhancing effect on permeability of leuprolide acetate which is a nonapeptide when using 2% methyl salicylate in mixture of 80% ethanol/water and 2% Klucel (17). However, the enhancement mechanism of this enhancer has not been reported.

CHAPTER 5
CONCLUSION

The testing of transdermal delivery system should be performed *in vivo*. This is often impossible, especially in the development stages when the toxicity or irritancy of new drugs, excipients or devices may not be documented. Therefore, *in vitro* experimental procedures have become important in this field. Laboratory test systems require a membrane to mimic the barrier function of the human stratum corneum. Many different types of membrane, both biological and synthetic membranes such as rat skin, pig skin, cobra skin, excised human skin, egg shell membrane and silicone membrane have been investigated. The permeability of biological membranes, i.e., human epidermis, full-thickness rat skin and egg shell membrane, to model solutes, i.e., acyclovir, acetophenone, 4-methylacetophenone, nitrobenzene, 3,4-xylenol, chlorocresol, phenol, 4-bromophenol, and 4-chlorophenol, were studied. It was found that steady state could be achieved immediately for all model solutes permeating through human epidermis and egg shell membrane. While, for full-thickness rat skin, the lag time of all model solutes were in a range of 12-85 minutes. It may be because full-thickness rat skin is thicker than human epidermis and egg shell membrane. This can be explained by simple partition and diffusion theory. The permeation process through these biological membranes were studied by considering the relationship between logarithm of permeability coefficient (log k_p) and some physicochemical parameters of the model solutes. It was found that good correlation between log k_p and physicochemical parameters could be obtained when permeability data of phenol, 4-bromophenol, and 4-chlorophenol were excluded. Robert M.S. et al, 1997 found that there was an increase in permeability coefficient of some phenolic compounds permeated through human epidermis when used at high concentration. They suggested that this phenomenon caused by damaging of membrane. Therefore, it appears that the permeability data of phenol, 4-bromophenol, and 4-chlorophenol should not be used according to different permeation mechanism at the concentration used in this study. For human epidermis, it was found that increase in solute hydrogen-bond

basicity and solute hydrogen-bond acidicity will result in decrease in permeability, whereas increase in molecular volume will result in increase in permeability. For full-thickness rat skin, it was found that increase in solute hydrogen-bond basicity will result in increase in permeability, whereas increase in molecular volume will result in decrease in permeability. For egg shell membrane, it was found that increase in solute hydrogen-bond acidity, solute hydrogen-bond basicity, and dipolarity will result in decrease in permeability. To study the trend of permeability property of three biological membranes to model solutes, the logarithm of ratio between solute molecular volume and solute hydrogen-bond basicity which are the main factors affecting permeability was calculated. This value may reflect the hydrophilic-lipophilic property of solute. It was found that the positively relative contribution of log $V_I/100/\beta$ value to log k_p value was obtained for permeation of five model solutes, i.e., acetophenone, 4-methylacetophenone, nitrobenzene, 3,4-xylenol, and chlorocresol, through human epidermis, whereas the negatively relative contribution of log $V_I/100/\beta$ value to log k_p value was obtained for permeation of five model solutes through full-thickness rat skin. Poor relationship between log $V_I/100/\beta$ value and log k_p was obtained for permeation of five model solutes through egg shell membrane. These results suggest that, solute with high log $V_I/100/\beta$ value could permeate through human epidermis more. It may be because relatively high lipophilic solute (high log $V_I/100/\beta$ value) could partition into the stratum corneum layer, which composes of lipid, more than hydrophilic solute (low log $V_I/100/\beta$ value). On the other hand, this relationship was observed conversely when solute permeated through full-thickness rat skin. It may be because the solute with high lipophilic characteristic, penetrated through the stratum corneum layer into dermis layer, which is more aqueous than stratum corneum, in which this solute was poorly soluble. This results in decrease in the permeability of the solutes. For permeation of solute through egg shell membrane, mainly consisting of mesh of keratin fibers with albuminous cementing material. As this membrane does not compose of lipid and the pore size of egg shell membrane may be up to 28 microns which is larger than molecular size of model solutes. Therefore, permeation of these model solutes through this membrane will be depending mainly on solvatochromic parameters and will not be affected by molecular volume.

Most of *in vitro* experiments usually used the rat skin, although permeability of some solutes should be concerned when compared with human skin. The rat skin was used immediately after it was cut from rat to ensure that skin permeability property is not changed. In practical, freshly excised rat skin may be inconvenient to be used. Additionally, a lot of skin samples are required in order to obtain reliable result. The purpose of this study has two reasons, i.e., economical and moral ones. Sharing organs and skin of one rat among researchers results in reducing cost and saving life of a large number of rats. The barrier functions of full-thickness rat skin of both sexes were studied by using acyclovir and acetophenone as model solutes. Sö rensen modified phosphate buffer pH 7.4, 0.9%w/v normal saline and 10%w/v glycerine were used as pretreated solution. It was found that there was high variation in permeability coefficient except for the case of acetophenone permeating through female rat skins. This high variation may occur due to skin preparation technique using hand razor to remove hair which might damage the stratum corneum layer leading to change of barrier property of skin. For comparison of the effect of treatment and storage condition, the statistical Kruskal-Wallis test was used, because the variances of these results were different. The statistical analysis showed that, the permeability coefficient of acyclovir or acetophenone through three rat skin groups pretreated differently, after storage at -20ºC for 13-15 days, did not differ from that of the control group (p-value > 0.05). At the same time, no difference in permeability was found between male and female rat skins for both model solutes (p-value > 0.05).

As acyclovir could not permeate well through human epidermis, this solute was selected to be used in the study of the effect of chemical enhancers (i.e., capsaicin, nonivamide, *l*-menthol, methyl salicylate, and tween 80) and vehicles (i.e., Sörensen modified phosphate buffer pH 7.4 and 50%v/v ethanol/water) on percutaneous absorption of acyclovir. It was found that 50% ethanol/water system could enhance the permeability of acyclovir through human epidermis. This permeation enhancement may be due to ethanol effect on the physicochemical properties of the statum corneum resulting in reduction in the barrier function of human epidermis. For enhancing effect study of the selected enhancers, it was found that 4%w/v *l*-menthol in 50%v/v ethanol/water showed superior permeability enhancement over the other four enhancers. However, it was found that two samples of human epidermis were torn at 120 minutes

and 180 minutes when *l*-menthol was used as enhancer. It may be due to skin irritation effect of *l*-menthol and ethanol/water system. Enhancing effect of *l*-menthol may be due to the combination effect between *l*-menthol and ethanol that altered the stratum corneum lipids resulting in reduction in the barrier resistance of human epidermis. For other enhancers, it was found that 0.075%w/v capsaicin, 0.075%w/v nonivamide, 10%w/v tween 80, and 4%w/v methyl salicylate in 50%v/v ethanol/water, had less effect on permeability of acyclovir through human epidermis.

REFERENCES

1. Walters KA, editor. Dermatological and transdermal formulations. New York: Marcel Dekker; 2002.
2. Barry B. Transdermal drug delivery. In: Aulton ME, editor. Pharmaceutics the science of dosage form design. 2nd ed. London: Harcourt Publishers; 2002. 499-533.
3. Barry BW. Novel mechanism and devices to enable successful transdermal drug delivery. Eur J Pharm Sci 2001; 14: 101-14.
4. McEvoy GK, editor. AHFS Drug information. Bethesda (MD): American society of health-system pharmacists; 2001. 520-30, 3326-9.
5. Dollery C, editor. Therapeutic drugs. 2nd ed. London: Harcourt; 1999. A39-44.
6. Greenberg SB, editor. Physicians' desk reference. 53rd ed. Montvale (NJ): Medical economics company; 1999. 1272-7.
7. Gonsho A, Imanidis G, Vogt P, Kern ER, Tsuge H, Su MH, et al. Controlled (trans) dermal delivery of antiviral agent (acyclovir). I: an in vivo animal model for efficacy evaluation in cutaneous HSV-1 infections. Int J Pharm 1990; 65: 183-94.
8. Lee PH, Su MH, Kern ER, Higuchi WI. Novel animal model for evaluating topical efficacy of antiviral agents: flux versus efficacy correlation in the acyclovir treatment of cutaneous herpes simplex virus type 1 (HSV-1) infections in hairless mice. Pharm Res 1992; 9(8): 979-89.
9. Lee PH, Su MH, Ghanem AH, Inamori T, Kern ER, Higuchi WI. An application of the C* concept in predicting the topicals efficacy of finite dose acyclovir in the treatment of cutaneous HSV-1 infections in hairless mice. Int J Pharm 1993; 93: 139-52.
10. Su MH, Lee PH, Ghanem AH, Kern ER, Higuchi WI. An application of transdermal antiviral delivery systems to the establishment of a novel animal model approach in the efficacy evaluation for dermatological formulations. Drug Dev Ind Pharm 1994; 20(4): 685-718.

11. Imanidis G, Song W, Lee PH, Su MH, Kern ER, Higuchi WI. Estimation of skin target site acyclovir concentrations following controlled (trans) dermal drug delivery in topical and systemic treatment of cutaneous HSV-1 infections in hairless mice. Pharm Res 1994; 11(7): 1035-41.
12. Tsai YH, Huang YB, Fang JY, Wu PC. Percutaneous absorption of capsaicin and its derivatives. Drug Dev Ind Pharm 1994; 20(4): 719-30.
13. Fang JY, Wu PC, Huang YB, Tsai YH. In vitro permeation study of capsaicin and its synthetic derivatives from ointment bases using various skin types. Int J Pharm 1995; 126: 119-28.
14. Degim IT, Uslu A, Hadgraft J, Atay T, Akay C, Cevheroglu S. The effects of azone and capsaicin on the permeation of naproxen through human skin. Int J Pharm 1999; 179: 21-5.
15. Wu PC, Chang JS, Huang YB, Chai CY, Tsai YH. Evaluation of percutaneous absorption and skin irritation of ketoprofen through rat skin: in vitro and in vivo study. Int J Pharm 2001; 222: 225-35.
16. Fang JY, Fang CL, Hong CT, Chen HY, Lin TY, Wei HM. Capsaicin and nonivamide as novel skin permeation enhancers for indomethacin. Eur J Pharm Sci 2001; 12: 195-203.
17. Lu MF, Lee D, Rao GS. Percutaneous absorption enhancement of leuprolide. Pharm Res 1992; 9(12): 1575-9.
18. Morimoto Y, Sugibayashi K, Kobayashi D, Shoji H,Yamazaki J, Kimura M. A new enhancer-coenhancer system to increase skin permeation of morphine hydrochloride in vitro. Int J Pharm 1993; 91: 9-14.
19. Sugibayashi K, Kobayashi D, Nakagaki E, Hatanaka T, Inoue N, Kusumi S, et al. Differences in enhancing effect of *l*-menthol, ethanol and their combination between hairless rat and human skin. Int J Pharm 1995; 113: 189-97.
20. Kitagawa S, Li H, Sato S. Skin permeation of parabens in excised guinea pig doesal skin, its modification by penetration enhancers and their relationship with *n*-octanol/water partition coefficients. Chem Pharm Bull 1997; 45(8): 1354-7.

21. Frischoff YK, Touitou E. Testosterone skin permeation enhancement by menthol through formation of eutectic with drug and interaction with skin lipids. J Pharm Sci 1997; 86(12): 1394-9.
22. Kunta JR, Goskonda VR, Brotherton HO, Khan MA, Reddy IK. Effect of menthol and related terpenes on the percutaneous absorption of propranolol across excised hairless mouse skin. J Pharm Sci 1997; 86(12): 1369-73.
23. Zahir A, Kunta JR, Khan MA, Reddy IK. Effect of menthol on permeability of an optically active and racemic propranolol across guinea pig skin. Drug Dev Ind Pharm 1998; 24(9): 875-8.
24. Gao S, Singh J. In vitro percutaneous absorption enhancement of a lipophilic drug tamoxifen by terpenes. J Controlled Release1998; 51: 193-9.
25. Costa P, Ferreira DC, Morgado R, Lobo JM, Design and evaluation of a lorazepam transdermal delivery system. Drug Dev Ind Pharm 1997; 23(10): 939-44.
26. Wade A, Weller PJ, editors. Handbook of pharmaceutical excipients. 2nd ed. Washington DC: The American pharmaceutical association; 375-8.
27. Dan L, Boon KH, Lan S, Ching LP, Lynn TS, editors. MIMS Thailand. n.p.: Medimedia; 2002; 31(1). 308-12.
28. Haigh JM, Smith EW. The selection and use of natural and synthetic membranes for in vitro diffusion experiments. Eur J Pharm Sci 1994; 2: 311-30.
29. Pongjanyakul T, Prakongpan S, Priprem A. Permeation studies comparing cobra skin with human skin using nicotine transdermal patches. Drug Dev Ind Pharm 2000; 26(6): 635-42.
30. Washitake M, Takashima Y, Tanaka S, Anmo T, Tanaka I. Drug permeation through egg shell membranes. Chem Pharm Bull 1980; 28(10): 2855-61.
31. Wheatley CH, editor. Concept of human anatomy & physiology. 4th ed. Dubuque (IA). Wm.C.Brown Communications; 1995. 139.
32. Kasting GB, Bowman L. DC electrical properties of frozen, excised human skin. Pharm Res 1990; 7(2): 134-43.
33. Kasting GB, Bowman L. Electrical analysis of fresh, excised human skin: comparison with frozen skin. Pharm Res 1990; 7(11): 1141-6.

34. Hadzija BW, Ruddy SB, Ballenger ES. Effect of freezing on iontophoretic transport through hairless rat skin. J Pharm Pharmacol 1992; 44: 387-90.
35. Harada K, Murakami T, Kawasaki E, Higashi Y, Yamamoto S, Yata N. In-vitro permeability to salicylic acid of human, rodent, and shed snake skin. J Pharm Pharmacol 1993; 45: 414-8.
36. Cooper ER, Merritt EW, Smith RL. Effect of fatty acids and alcohols on the penetration of acyclovir across human skin in vitro. J Pharm Sci 1985; 74(6): 688-9.
37. Okamoto H, Muta K, Hashida M, Sezaki H. Percutaneous penetration of acyclovir through excised hairless mouse and rat skin: effect of vehicle and percutaneous penetration enhancer. Pharm Res 1990; 7(1): 64-8.
38. Volpato NM, Santi P, Colombo P. Iontophoresis enhances the transport of acyclovir through nude mouse skin by electrorepulsion and electroosmosis. Pharm Res 1995; 12(11): 1623-7.
39. Volpato NM, Nicoli S, Laureri C, Colombo P, Santi P. In vitro acyclovir distribution in human skin layers after transdermal iontophoresis. J Controlled Release 1998; 50: 291-6.
40. Jalón EG, Blanco-Príeto MJ, Ygartua P, Santoyo S. Topical application of acyclovir-loaded microparticles: quantification of the drug in porcine skin layers. J Controlled Release 2001; 75: 191-7.
41. Finnin BC, Morgan TM. Transdermal penetration enhancers: applications, limitations, and potential. J Pharm Sci 1999; 88(10): 955-8.
42. Aguiar AJ, Weiner MA. Percutaneous absorption studies of chloranphenicol solutions. J Pharm Sci 1969; 58(2): 210-5.
43. Shahi V, Zatz JL. Effect of formulation factors on penetration of hydrocortisone through mouse skin. J Pharm Sci 1978; 67(6): 789-92.
44. Wade A, Weller PJ, editors. Handbook of pharmaceutical excipients. 2nd ed. Washington DC: The American pharmaceutical association; 304-5.
45. Krishnaiah YSR, Satyanarayana V, Bhaskar P. Influence of menthol and pressure-sensitive adhesives on the in vivo performance of membrane-moderated transdermal therapeutic system of nicardipine hydrochloride in human volunteers. Eur J Pharm Biopharm 2003; 55: 329-37.

46. Fujii M, Takeda Y, Yoshida M, Utoguchi N, Matsumoto M, Watanabe Y. Comparison of skin permeation enhancement by 3-*l*-menthoxypropane-1,2-diol and *l*-menthol: the permeation of indomethacin and antipyrine through Yucatan micropig skin and changes in infrared spectra and x-ray diffraction patterns of stratum corneum. Int J Pharm 2003; 258: 217-23.
47. Pillai O, Panchagnula R. Transdermal iontophoresis of insulin: V. effect of terpenes. J Controlled Release 2003; 88: 287-96.
48. Narishetty STK, Panchagnula R. Transdermal delivery of zidovudine: effect of terpenes and their mechanism of action. J Controlled Release 2004; 95 (3): 367-79.
49. Carter RB. Topical capsaivin in the treatment of cutaneous disorders. Drug Dev Res 1991; 22: 109-23.
50. Budavari S, editor. The Merck index. 20th ed. Whitehose station (NJ): Merck; 1996. 6198.
51. Joss JD, Leblond RF. Potentiation of warfarin anticoagulation associated with topical methyl salicylate. The annals of Pharmacotherapy 2000; 34: 729-33.
52. Lund W, editor. The pharmaceutical codex: principle and practice of pharmaceutics. 12th ed. London: The royal pharmaceutical society of great britain; 1994. 66-8.
53. Martin A, editor. Physical pharmacy. 4th ed. London: Lea & Febiger; 1993. 324-30.
54. Roberts MS, Anderson RA, Swarbrick J. Permeability of human epidermis to phenollic compounds. J Pharm Pharmacol 1977; 29: 677-83.
55. Lawanprasert P, Lukkanatinaporn P, Sarisuta N. Permeability of silicone membrane to model solutes. Mahidol Univ J Pharm Sci 2002; 29(1-2): 45-8.
56. Sintov AC, Shapiro L. New microemulsion vehicle facilitates percutaneous penetration in vitro and cutaneous drug bioavailability in vivo. J Controlled Release 2004, 95: 173-83.
57. Abraham MH, Chadha HS, Mitchell RC. The factors that influence skin penetration of solutes. J Pharm Pharmacol 1995; 47: 8-16.

58. Ghafourian T, Fooladi S. The effect of structural QSAR parameters on skin penetration. Int J Pharm 2001; 217: 1-11.

59. สุวรรณ เกษตรสุวรรณ, บรรณาธิการ. ไข่และเนื้อไก่. กรุงเทพมหานคร: อมรการพิมพ์; 2529. 10-31.

60. Sathyan G, Ritschel WA, Hussain S. Transdermal delivery of tacrine: I. Identification of a suitable delivery vehicle. Int J Pharm 1995; 114: 75-83.

61. Megrab NA, Williams AC, Barry BW. Oestradiol permeation across human skin, silastic and snake skin membranes: the effects of ethanol/water co-solvent systems. Int J Pharm 1995; 116: 101-12.

62. Bergstrom TK, Knutson K, Denoble LJ, Goates CY. Percutaneous absorption enhancement of an ionic molecule by ethanol-water systems in human skin. Pharm Res 1990; 7(7): 762-6.

63. Hatanaka T, Shimoyama M, Sugibayashi K, Morimoto Y. Effect of vehicle on the skin permeability of drugs: polyethylene glycol 400-water and ethanol-water binary solvents. J controlled Release 1993; 23: 247-60.

64. Berner B, Mazzenga GC, Otte JH, Steffens RJ. Ethanol:water mutually enhanced transdermal therapeutic system: II. Skin permeation of ethanol and nitroglycerin. J Pharm Sci 1989; 78: 402-7.

65. Shokri J, Nokhodchi A, Dashbolaghi A, Zadeh DH, Ghafourian T, Jalali MB. The effect of surfactants on the skin penetration of diazepam. Int J Pharm 2001; 228: 99-107.

66. Cappel MJ, Kreuter J. Effect of nonionic surfactants on transdermal drug delivery: I. Polysorbates. Int J Pharm 1991; 69: 143-53.

67. Shahi V, Zatz JL. Effect of formulation factors on penetration of hydrocortisone through mouse skin. J Pharm Sci 1978; 67(6): 789-92.

68. Chemical Abstracts Service. (2004). *p*-Methylacetophenone. In Scifinder Scholar [On line]. Available: American Chemical Society [2004, June 7].

APPENDIX

Properties of solutes used

Acetophenone

1. Nomenclature

Chemical name: Acetophenone, 1-Phenylethanone, Phenyl methyl ketone, Acetylbenzene, Hypnone (50)

2. Formula and molecular weight:

C_8H_8O molecular weight 120.15 (50)

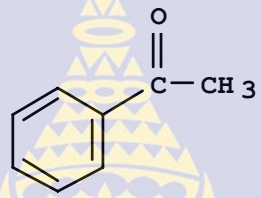

3. Appearance, color, odor, and taste:

Liquid, forms laminar crystals at low temperature (50)

4. Physical properties:

4.1 Melting point: 20.5ºC

4.2 Boiling point: 202ºC

4.3 Solubility: Slightly soluble in water, freely in alcohol, chloroform, ether, fatty oils, glycerol, soluble in concentrated sulfuric acid with orange color (50)

5. Use:

It is used in perfumery to impart and orange-blossom-like odor; catalyst for the polymerization of olefins; in organic syntheses, especially as photosensitizer (50).

4-Methylacetophenone

1. Nomenclature

Chemical name:

4-Methylacetophenone, 1-(4-Methylphenyl)-1-ethanone; 1-(4-Methylphenyl)ethanone; 1-(4-Tolyl)ethanone; 1-Acetyl-4-methylbenzene; 1-p-Tolylethanone; 4'-Methylacetophenone; 4-Acetyltoluene; 4-Methylphenyl methyl ketone; Melilotal; Methyl 4-methylphenyl ketone; Methyl p-tolyl ketone; p-Acetyltoluene; p-Methylacetophenone; p-Tolyl methyl ketone (68)

2. Formula and molecular weight:

$C_9H_{10}O$ molecular weight 134.18 (68)

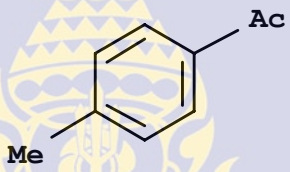

3. Appearance, color, odor, and taste:

Liquid

4. Physical properties:

4.1 Melting point: -

4.2 Boiling point: 221-223ºC

4.3 Solubility: Slightly soluble in solution pH 1, 4, 7, 8, 10 (68)

Phenol

1. Nomenclature

Chemical name:

Phenol; Carbolic acid; Phenic acid; Phenylic acid; Phenyl hydroxide; Hydroxybenzene; Oxybenzene (50)

2. Formula and molecular weight:

C_6H_6O molecular weight 94.11 (50)

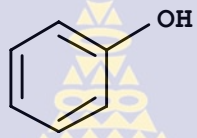

3. Appearance, color, odor, and taste:

Colorless, acicular crystals or white, crystalline mass, sickeningly sweet and acrid with a sharp and burning taste (50)

4. Physical properties:

4.1 Melting point: -

4.2 Boiling point: 182ºC

4.3 Solubility: It is liquefied by mixing with ~8% water. One gram dissolves in ~15 mL water, 12 mL benzene; very soluble in alcohol, chloroform, ether, glycerol, corbon disulfide, petrolatum, volatide and fixed oils, aqueous alkali hydroxide, almost insoluble in petroleum ether (50).

5. Use:

As a general disinfectant, either in solution or mixed with slaked lime, etc., for toilets, stables, cesspools, floors, drains, etc.; for the manufacture of colorless of light-colored artificial resins, many medical and industrial organic compounds and dyes; as a reagent in chemical analysis; pharmaceutical aid (preservative); aqueous solution as topical anesthetic; topical antiseptic; topical antipruritic (50).

4-Bromophenol

1. Nomenclature

Chemical name:

4-Bromophenol (50)

2. Formula and molecular weight:

C_6H_5BrO molecular weight 173.01 (50)

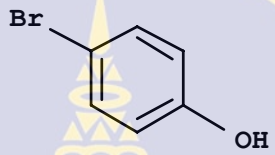

3. Appearance, color, odor, and taste:

Tetragonal bipyramidal crystals from chloroform or ether (50)

4. Physical properties:

4.1 Melting point: 64ºC

4.2 Boiling point: 238ºC

4.3 Solubility: Soluble in ~7 parts water; freely soluble in alcohol, chloroform, ether, glacial acetic acid (50)

5. Use:

Disinfectant (50)

4-Chlorophenol

1. Nomenclature

Chemical name:

4-Chlorophenol (50)

2. Formula and molecular weight:

C_6H_5ClO molecular weight 128.56 (50)

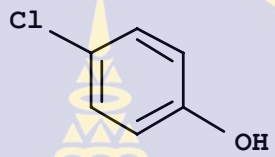

3. Appearance, color, odor, and taste:

Crystals with characteristic phenolic odor

4. Physical properties:

4.1 Melting point: 43.2-43.7ºC

4.2 Boiling point: 220ºC

4.3 Solubility: Sparingly soluble in water, liquid petroleum; very soluble in alcohol, glycerin, ether, chloroform, fixed and volatile oils (50)

5. Use:

Antiseptic (50)

Nitrobenzene

1. Nomenclature

Chemical name:

Nitrobenzene; Nitrobenzol (50)

2. Formula and molecular weight:

$C_6H_5NO_2$ molecular weight 123.11 (50)

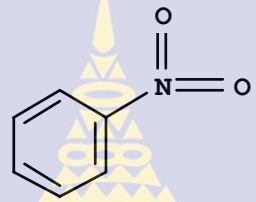

3. Appearance, color, odor, and taste:

Colorless to pale yellow, oily liquid; odor of volatile oil almond (50)

4. Physical properties:

4.1 Melting point: +6ºC

4.2 Boiling point: 210-211ºC

4.3 Solubility: Soluble in ~500 parts water; freely soluble in alcohol, benzene, ether, oils (50)

5. Use:

For manufacture of aniline; in soaps, shoe polishes; for refining lubricating oils; manufacture pyroxylin compounds (50)

3,4-Xylenol

1. Nomenclature

Chemical name:

3,4-Xylenol; 3,4-Dimethylphenol (50)

2. Formula and molecular weight:

$C_8H_{10}O$ molecular weight 122.16 (50)

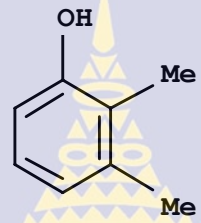

3. Appearance, color, odor, and taste:

Needles from water (50)

4. Physical properties:

4.1 Melting point: 62.5ºC

4.2 Boiling point: 225ºC

4.3 Solubility: Slightly soluble in water; freely soluble in alcohol, chloroform, ether, and benzene; soluble in sodium hydroxide solution (50)

5. Use:

For the preparation of coal tar disinfectants; manufacture of artificial resins (50)

Chlorocresol

1. Nomenclature

Chemical name:

Chlorocresol; 4-Chloro-m-cresol; 4-Chloro-3-methylphenol; 3-Methyl-4-chlorophenol; Parachlorometacresol; 6-chloro-m-cresol; 6-Chloro-3-hydroxytoluene; 2-Chloro-5-hydroxytolulene (50)

2. Formula and molecular weight:

C_7H_7ClO molecular weight 142.59 (50)

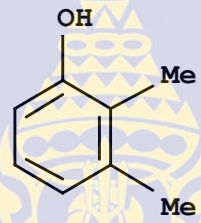

3. Appearance, color, odor, and taste:

Dismorphous crystals; odorless when very pure, but usually a phenolic odor persists (50)

4. Physical properties:

4.1 Melting point: 55.5ºC and 66ºC (ligroin)

4.2 Boiling point: 235ºC

4.3 Solubility: One gram dissolves in 260 mL water at 20ºC, more soluble in hot water; freely soluble in alcohol, benzene, chloroform, ether, acetone, petroleum ether, fixed oils, terpenes, aqueous alkaline solutions (50)

5. Use:

Antiseptic; disinfectant; more active in acid than in alkaline solutions (50)

BIOGRAPHY

NAME	Mr. Sakchai Auychaipornlert
DATE OF BIRTH	27 October 1974
PLACE OF BIRTH	Bangkok, Thailand
INSTITUTIONS ATTENDED	Mahidol University, 1993-1997: Bachelor of Science in Pharmacy Mahidol University, 2001-2003 Master of Science in Pharmacy (Pharmaceutics)
POSITION & OFFICE	April, 1998-May 2001 Chumponburi Hospital Surin, Thailand Position : Pharmacist